Carbon footprints of peatland degradation: Impacts on soil carbon leaching, aquatic CO_2 emissions and the marine carbonate system in Indonesia

Dissertation for the Doctoral Degree in Natural Sciences

(Dr. rer. nat.)

Faculty of Biology and Chemistry

University of Bremen

Submitted by

Francisca Maria Constance Wit

June 2017

Bundesministerium für Bildung und Forschung

ZMT LEIBNIZ CENTRE for Tropical Marine Research

UNIVERSITÄT BREMEN

Supervisors:

Prof. Dr. Ulrich Saint-Paul

Dr. Tim Rixen

Thesis Colloquium

Date:

29 August 2017

Reviewers:

Prof. Dr. Ulrich Saint-Paul

Prof. Dr. Boris Koch

Dr. Ronny Lauerwald

Examination board members:

Prof. Dr. Tilmann Harder (Chairperson)

Prof. Dr. Kai Bischof

Dr. Tim Rixen

Dr. Thorsten Warneke

PhD candidate Kim Vane

MSc. student Lara Stuthmann

To Rens,

for your infinite patience, love and support.

To my parents, my brother and sisters and their spouses, and my close relatives,

for your unfailing support, love and faith in me.

Summary

In Southeast Asia and Indonesia, land use change (LUC) occurs in the form of large-scale deforestation and peatland degradation for agricultural purposes, which causes terrestrial CO_2 emissions from peat soils as a consequence of oxidation, subsidence and forest fires. However, the consequences of this peatland degradation for the aquatic and marine environment and carbon cycle are less well known. In the framework of the SPICE III – CISKA subproject 1, the impact of land use change in Indonesia was determined by the quantification of the inorganic and organic carbon fluxes and CO_2 emissions from the rivers, estuaries and coastal ocean into the atmosphere as well as the marine carbonate system in order to develop sustainable mitigation strategies to reduce CO_2 emissions. The findings of this PhD study bring attention to the fact that the impacts of tropical peatland degradation in Indonesia are not limited to direct CO_2 emissions due to drainage and deforestation, but also greatly affect the carbon cycle of adjacent freshwater and marine environments through a variety of processes. By means of a mixing model it was shown that dissolved organic carbon leaching from disturbed peat soils has increased by 200% from 62 to 183 g m^{-2} yr^{-1} as a consequence of hydrological changes and secondary vegetation. Increased freshwater fluxes due to reduced evapotranspiration account for 38% of the increase in carbon leaching, whereas the labile leaf litter from secondary vegetation is responsible for the remaining 62% increase. Once the organic carbon has reached the rivers, it is either respired and emitted to the atmosphere (river outgassing) or exported to the coastal ocean (riverine carbon export). Dissolved organic carbon (DOC) and pCO_2 concentrations in the rivers increase as the share of disturbed peatland coverage in the catchment increases as a consequence of increased carbon leaching and decomposition. Based on the regression between peat coverage and CO_2 yield, the CO_2 fluxes from rivers in Indonesia have been estimated as well as in Malaysia and extrapolated to Southeast Asia, and amount to 53.9 ±12.4, 6.2±1.6 and 66.9±15.7 Tg C yr^{-1}, respectively. However, these fluxes are rather moderate due to the short residence time of the river waters and the location of peat close to the coast, which shorten the time available for decomposition. Circa 53% of the carbon that enters the freshwater system in Southeast Asia is emitted as CO_2 to the atmosphere, whereas the remaining 47% is exported to the coastal ocean. Based on total alkalinity (TA), dissolved inorganic carbon (DIC) and pCO_2 measurements in the estuaries and coastal ocean of Sumatra, it was shown that the majority of the exported carbon is respired in the estuaries. Circa 62.7% of the exported, respired CO_2 is emitted to the atmosphere, whereas 6.4% is assumed to be buried in the sediments and the

remaining 30.6% is absorbed in the water column. Here, the respired CO_2 contributes to ocean acidification and lowers the aragonite and calcite saturation states (Ω_{AR} / Ω_{CA}). This induces carbonate dissolution of sediments, but also coral reefs and other calcifying organisms and can therefore be viewed as the invisible carbon footprint, but is currently overlooked in climate mitigation strategy policies. In Indonesia, the terrestrial direct CO_2 emissions due to LUC via secondary vegetation (10.9 Tg C yr^{-1}), peat oxidation (109.9 Tg C yr^{-1}) and forest fires (82.1 Tg C yr^{-1}) amount to 192.0 Tg C yr^{-1}. Carbon loss due to indirect emissions from the rivers (53.9 Tg yr^{-1}, ref. (Wit et al. 2015)), estuaries and coastal ocean (49.4 Tg yr^{-1}), as well as the invisible carbon footprint (24.1 Tg yr^{-1}) and excluding the natural emissions from pristine peatlands (13.0 Tg C yr^{-1}) amounts to 114.3 Tg C yr^{-1}. Therefore, the total carbon loss due to LUC amounts to 306.3 Tg yr^{-1}, which represents an increase of 60% with respect to the direct terrestrial emissions currently considered in greenhouse gas mitigation policies. With respect to the development of climate change mitigation strategies as one of the overarching goals of SPICE and CISKA, the advice is to include the aquatic and marine CO_2 emissions, as well as the invisible carbon footprint in order to cover the carbon losses with respect to LUC in Indonesia. In addition, carbon leaching and fluvial carbon export should be reduced to mitigate the impact of ocean acidification and carbonate dissolution.

Zusammenfassung

In Südostasien, insbesondere Indonesien, werden seit Jahrzehnten durch Entwaldung und Entwässerung Torfwälder in landwirtschaftliche Nutzflächen umgewandelt. Hervorgerufen durch die Entwässerung und dadurch bedingte Absenkung der Torfe sowie großflächige Waldbrände kommt es zu einer massiven Freisetzung von CO_2 aus Torfen. Trotz der globalen Brisanz sind Auswirkungen der Torfdegradation auf den Kohlenstoffkreislauf aquatischer und mariner Ökosysteme bislang jedoch nur unzureichend untersucht. Im Rahmen des bilateralen Projektes SPICE III (Science for the Protection of Indonesian Coastal Ecosystems, Teilprojekt 1 CISKA) wurde daher der Einfluss von Landnutzungsänderungen auf den Kohlenstoffkreislauf indonesischer Küstenökosysteme untersucht. Die Quantifizierung anorganischer und organischer Kohlenstofflüsse, die Bestimmung von CO_2-Emissionen aus Flüssen, Ästuaren und dem Küstenozean in die Atmosphäre sowie die Untersuchung des marinen Karbonatsystems bildeten die Schwerpunkte der vorliegenden Arbeit mit dem Ziel, der Entwicklung von nachhaltigen Maßnahmen zur Reduzierung der CO_2-Emissionen in Indonesien beizutragen.

Die Ergebnisse dieser Arbeit zeigen, dass Torfdegradation nicht nur erhöhte CO_2-Emissionen aufgrund von Entwässerung und Entwaldung zur Folge hat, sondern zudem die Kohlenstoffkreisläufe der angrenzenden limnischen und marinen Ökosysteme durch eine Reihe von Prozessen beeinflusst. Basierend auf Ergebnissen eines entwickelten Mischungmodels konnte gezeigt werden, dass die Auswaschung von gelöstem organischen Kohlenstoff aus gestörten Torfen als Konsequenz hydrologischer Veränderungen und Sekundärvegetation um 200% von 62 auf 183 g m^{-2} a^{-1} angestiegen ist. Etwa 38% der erhöhten Kohlenstoffauswaschung ist auf einen erhöhten Frischwasserabfluss als Folge reduzierter Evapotranspirationsraten zurückzuführen, während der Abbau labiler Sekundärvegetation für die verbleibenden 62% der verstärkten Kohlenstoffauswaschung verantwortlich ist. Im Fluss angekommen wird der organische Kohlenstoff entweder respiriert und als CO_2 in the Atmosphäre emittiert („river outgassing“) oder als DOC in den Küstenozean exportiert („riverine carbon export“). Mit zunehmender Bedeckung mit gestörten Torfen in den Flusseinzugegebieten nehmen Auswaschung und Abbau von organischem Kohlenstoff und somit die Konzentrationen an DOC und pCO_2 in den Flüssen zu. Basierend auf der Abhängigkeit von Torfbedeckung und CO_2 Emission pro Fläche (g m^{-2} a^{-1}) konnten die CO_2-Flüsse indonesischer (53,9 ±12,4 Tg C a^{-1}) und malaysischer (6,2±1,6 Tg C a^{-1}) Flüsse abgeschätzt und für alle südostasiatischen Flüsse extrapoliert werden

(66,9±15,7 Tg C a^{-1}). Die ermittelten CO_2-Flüsse sind jedoch aufgrund geringer Verweilzeiten des Flusswassers und der küstennahen Lage der Torfe als moderat einzustufen. Etwa 53% des in das Frischwassersystem Südostasiens eingetragenen Kohlenstoffs wird als CO_2 in die Atmosphäre abgegeben. Die verbleibenden 47% werden in den Küstenozean exportiert. Messungen der Akalinität (TA), des gelösten anorganischen Kohlenstoffs (DIC) und des pCO_2 in Ästuaren und dem Küstenozean Sumatras zeigen, dass der Großteil des exportierten Kohlenstoffs in den Ästuaren respiriert wird. Etwa 63% des exportierten und respirierten CO_2 wird in die Atmosphäre abgegeben, 6,4% in Sedimenten eingelagert und 30,6% von der Wassersäule aufgenommen. Somit trägt das respirierte CO_2 zur Ozeanversauerung bei, was die Karbonatlösung von Sedimenten, Korallenriffen und anderen kalzifizierenden Organismen begünstigt und daher als „unsichtbarer Kohlenstoff-Fußabdruck (invisible carbon footprint)“ verstanden werden kann, der jedoch bisher keinerlei Berücksichtigung in Strategiepapieren zum Klimaschutz findet.

Die direkten terrestrischen CO_2 Emissionen, zurückzuführen auf Landnutzungsänderungen in Indonesien, betragen 192 Tg C a^{-1}. Dabei liegen die Emissionen durch Sekundärvegetation bei 10,9 Tg C a^{-1}, durch Torfoxidation bei 109,9 Tg C a^{-1} und durch Waldbrände bei 82,1 Tg C a^{-1}. Kohlenstoffverluste durch indirekte Emissionen über Flüsse betragen 53,9 Tg C a^{-1} und über Ästure und den Küstenozean 49,4 Tg C a^{-1}. Zusammen mit den Freisetzungen durch den unsichtbaren Kohlenstoff-Fußabdruck (24,1 Tg C a^{-1}) und abzüglich der natürlichen Emissionen ungestörter Torfe (13 Tg C a^{-1}) beträgt der Kohlenstoffverlust 114,3 Tg C a^{-1}. Daraus ergibt sich ein Gesamtkohlenstoffverlust als Folge von Landnutzungsänderungen von 306,3 Tg C a^{-1}, was einer Zunahme von direkten terrestrischen CO_2 Emissionen von 60% entspricht. Im Hinblick auf die Entwicklung von Klimaschutzstrategien, einem der übergeordneten Ziele des SPICE-Projektes, wird eine Berücksichtigung der aquatischen und marinen CO_2-Emissionen und des unsichtbaren CO_2-Fussabdrucks angeraten. Zudem sollten die Auswaschung von Kohlenstoff und der Kohlenstoffexport reduziert werden, um Auswirkungen von Ozeanversauerung und Karbonatlösung abzuschwächen.

Table of Contents

Summary 7
Zusammenfassung 9
Table of Contents 11
List of Figures 14
List of Tables 15

1 Introduction 17
1.1 Motivation 17
1.2 Tropical peatlands of Southeast Asia 18
1.2.1 Formation and distribution 18
1.2.2 Peatland degradation 19
1.3 Marine carbonate system 20
1.3.1 Carbonate chemistry 20
1.3.2 Saturation states 21
1.3.3 Marine carbon processes 21

2 Scientific objectives, approach and outline 23
2.1 Project 23
2.2 Scientific aims and objectives 23
2.3 Approach 24
2.3.1 Study area and expeditions 24
2.3.2 Data and sample acquisition 25
2.4 Manuscript outline 26
2.5 Manuscript list and authors' contributions 27
2.5.1 Manuscript 1 (Chapter 3) 27
2.5.2 Manuscript 2 (Chapter 4) 27
2.5.3 Manuscript 3 (Chapter 5) 28

3 The impact of disturbed peatlands on river outgassing in Southeast Asia 29
3.1 Introduction 31
3.2 Methods 32
3.2.1 Study area 32
3.2.2 Expeditions 33
3.2.3 Sampling methods 34
3.2.4 Calibration experiment 35
3.2.5 CO_2 flux calculation 36
3.2.6 Peat coverages 37
3.2.7 River surface coverage 37
3.2.8 Uncertainty estimates 38
3.3 Results 38
3.3.1 River processes and variability 38
3.3.2 River outgassing and DOC export 42
3.3.3 CO_2 fluxes and peat coverage in Southeast Asia 43
3.3.4 Study comparison 45
3.3.5 Explanatory arguments for moderate fluxes 47
3.4 End notes 48

3.4.1 Acknowledgements ... 48
3.4.2 Author contributions ... 48

4 Carbon leaching from tropical peat soils and consequences for carbon balances ... 49
4.1 Abstract ... 51
4.2 Introduction ... 51
4.3 Methods ... 52
4.3.1 Study area and expeditions ... 52
4.3.2 DOC sampling and analysis ... 54
4.3.3 DOC age determination ... 54
4.3.4 DOC end-members, yields and exports ... 55
4.3.5 Precipitation, evapotranspiration and freshwater flux ... 55
4.3.6 River catchments and peat coverage ... 56
4.3.7 Mixing model principle ... 56
4.4 Results ... 58
4.5 Discussion ... 61
4.5.1 Acrotelm thickness ... 61
4.5.2 Leaching ... 61
4.5.3 Numerical leaching experiments for the Siak ... 62
4.5.4 Extrapolation of Siak results ... 64
4.5.5 Anthropogenic perturbations ... 66
4.5.6 Carbon budgets ... 67
4.6 Conclusion ... 68
4.7 End notes ... 69
4.7.1 Conflict of Interest Statement ... 69
4.7.2 Author Contribution Statement ... 69
4.7.3 Acknowledgments ... 69
4.8 Supplementary Material – Mixing model (written in Python) ... 69
4.8.1 Basic parameters: ... 69
4.8.2 Hydrological parameters: ... 69
4.8.3 DOC concentrations in the source waters: ... 70
4.8.4 DOC concentrations caused by mixing: ... 71
4.8.5 DOC decomposition in the Siak: ... 71

5 The invisible carbon footprint: from land use change to coral reef dissolution in Sumatra, Indonesia ... 73
Abstract ... 75
5.1 Introduction ... 75
5.2 Methods ... 76
5.2.1 Study area ... 76
5.2.2 Expeditions ... 77
5.2.3 Sampling methods ... 77
5.2.4 CO_2 flux and piston velocity calculations for estuaries and coastal ocean ... 78
5.2.5 Carbon export and end-members ... 81
5.2.6 Surface area calculations ... 81
5.2.7 Mixing lines ... 82
5.2.8 Calibration experiment ... 83
5.2.9 Uncertainty estimates ... 84

5.3 Results and discussion 84
5.3.1 Riverine carbon processes and exports 84
5.3.2 Carbon fluxes and processes in the estuaries and coastal ocean 87
5.3.3 Carbonate dissolution 89
5.3.4 The invisible carbon footprint 91
5.4 End notes 93
5.4.1 Acknowledgements 93
5.4.2 Author contributions 93
5.4.3 Author information 93

6 General discussion 95
6.1 Grand picture 95
6.2 Perspectives and outlook for Indonesia 97
6.3 Global relevance 98

7 Main conclusions 101
7.1 Background 101
7.2 Manuscript 1: River outgassing 101
7.3 Manuscript 2: Carbon leaching 102
7.4 Manuscript 3: Carbon export and coastal ocean processes 102
7.5 Discussion 103
References 105
Acknowledgements 115
Declaration in lieu of oath 117

List of Figures

Figure 1.1 Peatland distribution in Southeast Asia. 18
Figure 1.2 Example of peatland degradation in Sumatra from 1990 (left) to 2008 (right) 19
Figure 1.3 Effects of processes on TA and DIC. 22
Figure 2.1 Cruise sampling stations 2009, 2012 and 2013. 25
Figure 2.2 Expedition equipment and sampling. 26
Figure 3.1. Study area and river in Indonesia and Malaysia. 32
Figure 3.2 Calibration experiment results. 35
Figure 3.3 Patterns of salinity and pCO_2 underway measurements 39
Figure 3.4 Linear correlations of CO_2 and O_2 versus DOC. 41
Figure 3.5 Correlations of DOC yield and CO_2 yield versus peat coverage. 41
Figure 4.1 Study area. 52
Figure 4.2 Schematic of the model structure with the three water types 57
Figure 4.3 DOC concentrations versus precipitation rates. 59
Figure 4.4 DOC sampling and salinity correlation. 60
Figure 4.5 Mixing model DOC end-member results 62
Figure 4.6 Mixing model mean DOC yield results 65
Figure 4.7 Leaching of organic carbon 66
Figure 4.8 Carbon fluxes in disturbed peatlands. 67
Figure 4.9 Cross-section through the Siak and Bengkalis peat domes. 68
Figure 5.1 Study area and sample stations 77
Figure 5.2 Correlation salinity and distance from shore 82
Figure 5.3 Mixing lines for DIC (a) and TA (b) 83
Figure 5.4 Calibration experiment results. 83
Figure 5.5 $\delta^{13}C_{DIC}$ values plotted against salinity. 85
Figure 5.6 Measured pCO_2 concentrations (dots) and expected pCO_2 concentrations during mixing in the estuaries (mixing lines). 87
Figure 5.7 Saturation states of a) aragonite (Ω_{AR}) and b) calcite (Ω_{CA}) versus salinity 89
Figure 5.8 Deviations of DIC and TA 90
Figure 5.9 Overview of the carbon fluxes (Tg C yr^{-1}) 91

List of Tables

Table 3.1 River surface area 38
Table 3.2 Averaged parameters per river and year 40
Table 3.3 CO_2 flux versus DOC export – river outgassing in percentage. 43
Table 3.4 CO_2 yields and fluxes 44
Table 3.5 pCO_2 concentrations, piston velocities and CO_2 yields per COSCAT area. 46
Table 3.6 Study comparison 46
Table 4.1 Rivers and expeditions, as well as riverine DOC 53
Table 4.2 Rivers and coordinates used to obtain precipitation rates 55
Table 4.3 Ground and surface water concentrations 59
Table 5.1 CO_2 outgassing fluxes for the rivers, estuaries and coastal ocean of Sumatra according to Nightingale's principle 80
Table 5.2 Precipitation, discharge and end-member concentrations 80
Table 5.3 Carbon export rates from rivers in Sumatra 86
Table 5.4 CO_2 outgassing fluxes of the rivers, estuaries and coastal ocean of Sumatra according to Wanninkhof's principle 88

I

Introduction

1.1 Motivation

Peatlands are important ecosystems as they sequester carbon through the accumulation of plant remains in their water-saturated soils and are therefore significant carbon sinks. Circa 77% of the tropical peat is located in Southeast Asia with the majority found in Indonesia (Page et al. 2011). However, land use change in the form of rapid peatland degradation for the purpose of oil palm plantations, agriculture and logging in this area has led to the vast release of carbon from the peat soils into the atmosphere through drainage and forest fires (Couwenberg et al. 2010; Miettinen & Liew 2010). Furthermore, disturbed peatlands enhance carbon leaching from their soils to the rivers (Moore et al. 2013). Many studies have aimed to quantify the direct terrestrial carbon emissions from the soils and its consequences for the environment. However, so far it has remained uncertain what the fate of the leached carbon is once it has reached the rivers, estuaries and coastal ocean, and how it affects the environment and marine carbonate system. The importance of inland waters with respect to the global carbon cycle has gained more awareness during the last decades through studies that have revealed that inland waters, which include rivers, streams, lakes, reservoirs and estuaries, actually play an integral role for carbon storage, transport and greenhouse gas emissions to the atmosphere (Cole et al. 2007). In addition, estuaries and coastal oceans in the tropics are considered carbon sources (Borges et al. 2005). Still, large uncertainties remain with respect to carbon processes in and fluxes from inland waters, estuaries and the coastal ocean in Southeast Asia due to data scarcity.

The SPICE III program associated with this study (see Chapter 2) aims to address the scientific, social and economic issues related to the management of Indonesian coastal ecosystems and their resources, in addition to the development of mitigation strategies that consider the impacts on aquatic and marine ecosystems. Under the umbrella of this program,

this study aimed to strengthen the existing scientific database and clarify these uncertainties to further complement the current understanding of the influence of peatland degradation on the carbon cycle in Indonesia.

For further background information on the tropical peatlands of Southeast Asia and the marine carbonate system, short descriptions are provided in paragraphs 1.2 and 1.3.

1.2 Tropical peatlands of Southeast Asia

1.2.1 Formation and distribution

Peatlands have soils that consist of incompletely decomposed organic remains of mostly vegetative origin, officially classified as histosols. They occur as mangrove and swamp forest peat in the humid tropics and are typically confined to poorly drained basins and depressions with shallow groundwater (Driessen et al. 2001). The waterlogged conditions inhibit aeration and therefore decomposition of dead plant material, which allows for the accumulation of this plant material into thick peat layers. Under natural conditions, tropical peatlands are therefore considered important carbon sinks as they sequester CO_2 from the atmosphere into their biomass and subsequently store carbon in their soils for over centuries and even millennia. Furthermore, peat swamp forests host a multitude of hydrological and ecological values in the sense of wildlife and flood retention (Miettinen & Liew 2010).

Approximately 4 million km^2 (3%) of Earth's land surface is covered by peatlands (Hooijer et al. 2006) of which circa 422,025 km^2 (11%) is located in tropical regions. Southeast Asia is of particular importance, as its peatlands stretch over 247,778 km^2 or 56% of the tropical peat area, and hold approximately 68.5 Pg, which forms 77% of the tropical carbon pool. The majority of this carbon pool is found in Indonesia with 57.4 Pg (83.8 %) and 9.1 Pg (13.3 %)

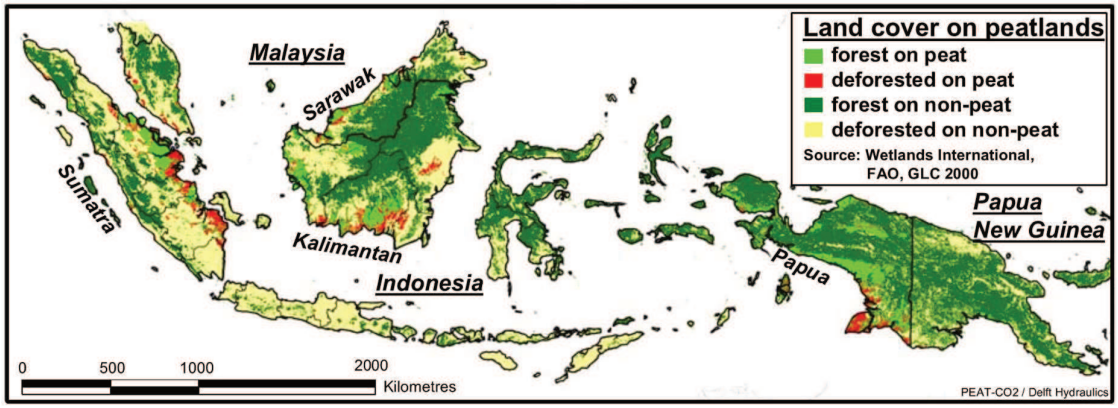

Figure 1.1 Peatland distribution in Southeast Asia. (Hooijer et al. 2006)

in Malaysia (Page et al. 2011). The bulk density of peat soils found in Southeast Asia falls within the range of 0.03 – 0.64 g cm^{-3} with a carbon content between 44.6 – 62.0 % (Page et al. 2010). Peat soils in Indonesia have an average bulk density of 0.127 g cm^{-3} with a carbon content of 51.3%, which amounts to 65.3 kg m^{-3} (Warren et al. 2012). The peatlands in Southeast Asia, which is this study is considered to be comprised of Indonesia, Malaysia, Papua New Guinea and Brunei, are mainly located along the coastlines (Figure 1.1).

1.2.2 Peatland degradation

Since the 1970's, the peatlands in Southeast Asia and particularly in Indonesia have been undergoing severe degradation in the form of deforestation and drainage for the purpose of logging, small holders and industrial plantations, especially oil palm plantations (Sorensen 1993). In the period 1990 – 2008, the extent of peat swamp forest cover in Southeast Asia has declined from 11.6 to 5.1 Mha (75% to 42%), with circa 10% of pristine peat swamp forest left (Miettinen & Liew 2010), which has since then further declined to 6% (Miettinen et al. 2016) (Figure 1.2). Drainage, induced by digging ditches, lowers the water table, which allows for aeration and thus decomposition of the organic content in the peat soils, also referred to as oxidation (Hooijer et al. 2006). CO_2 emissions from disturbed peatlands due to

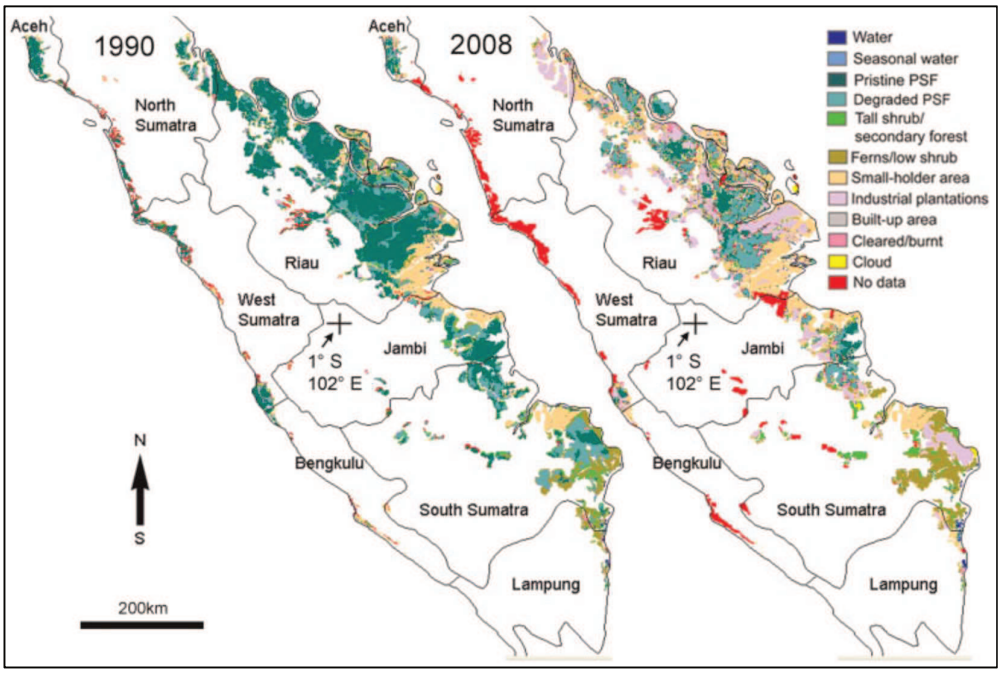

Figure 1.2 Example of peatland degradation in Sumatra from 1990 (left) to 2008 (right) (Miettinen & Liew 2010).

peat oxidation have been estimated to be 165±68 Tg yr^{-1} in Southeast Asia (Hooijer et al. 2010). In addition, drainage induces soil compaction as water is extracted from the peat with subsidence as a result. This process of water extraction is responsible for 40% of the observed soil subsidence, whereas oxidation can be accounted for 60% (Wösten et al. 1997) and gradually increases to 75 – 92% over time as water is drained completely (Hooijer, Page, Jauhiainen, W. A. Lee, et al. 2012). In contrast to pristine peatlands, which are water-saturated and therefore better protected against fires, drained disturbed peatlands are more vulnerable to fires (Turetsky et al. 2015). In Southeast Asia forest fires account for 128 ±51 Tg yr^{-1} (van der Werf et al. 2008)

1.3 Marine carbonate system

1.3.1 Carbonate chemistry

Since the onset of the industrial era, more than 500 Pg of carbon has been emitted as CO_2 through cement production, burning of fossil fuels and land use change (Andersson 2013), of which circa 30% has been taken up by the ocean (P. Ciais et al. 2013). Once in the water column, it becomes part of the marine carbonate system, which is comprised primarily of CO_2, HCO_3^-, CO_3^{2-}, H^+ and OH^-. The sum of the dissolved carbon compounds is referred to as dissolved inorganic carbon and denoted as ΣCO_2 or DIC (Zeebe & Wolf-Gladrow 2001). The marine carbonate system acts as a natural buffer, where the absorbed CO_2 reacts with H_2O and forms carbonic acid (H_2CO_3). It then disintegrates into bicarbonate (HCO_3^-) and the spare hydrogen ion (H^+) reacts with a carbonate ion to form another bicarbonate molecule according to (1.1):

$$CO_2 + H_2O + CO_3^2 \rightarrow 2\ HCO_3^- \qquad (1.1)$$

Typically, the ratio of the DIC species $[CO_2]$:$[HCO_3^-]$:$[CO_3^{2-}]$ in seawater are distributed as 0.5:86.5:13.0 %, which ensures a pH of circa 8.1. The capacity to absorb and thereby buffer the CO_2 to maintain a steady pH is measured by the total alkalinity (TA), which, in a more simplified and practical approach, is the sum of the charges of the carbonate alkalinity ($[HCO_3^-] + 2\ [CO_3^{2-}]$), borate alkalinity $[B(O)_4^-]$ and water alkalinity ($[OH^-] - [H^+]$). The higher the alkalinity, the more compounds are available to bind this H+ and maintain a steady pH.

1.3.2 Saturation states

The availability of $[CO_3^{2-}]$ in the ocean, is measured by the saturation state (Ω) according to:

$$\Omega = [Ca^{2+}]\,[CO_3^{2-}] / K^*_{sp} \qquad (1.2)$$

where K^*_{sp} is the stoichiometric solubility product for a given $CaCO_3$ mineral form (Andersson 2013). Marine organisms primarily use two major forms of $CaCO_3$, namely aragonite (corals and many mollusks) and calcite (coccolithophores, foraminifera and some mollusks). Typically, net precipitation takes place at $\Omega > 1$, whereas at $\Omega < 1$ net dissolution occurs.(S. C. Doney 2010). Whereas in a steady-state the removal of $CaCO_3^{2-}$ into the sediments is balanced by the supply of calcium carbonate to the ocean, currently more $CaCO_3$ is accumulating in the sediments than is supplied to the oceans (Iglesias-Rodríguez et al. 2002). This reduced supply causes a deficiency in $[CO_3^{2-}]$, thereby lowering Ω and leaving a surplus of $[H^+]$, which leads to ocean acidification. The absorbed anthropogenic CO_2 and subsequent [H+] is thought to be primarily neutralized by the reaction with $CaCO_3$ in marine sediments (Archer et al. 1998). However, it also dissolves the carbonate constructions of calcifying organisms leading to reduced calcification rates and poor cementation of coral reefs (Langdon & Atkinson 2005; Manzello et al. 2008), which is why ocean acidification is such an environmental and ecological issue.

1.3.3 Marine carbon processes

The ratio of change in concentrations of TA and DIC gives an indication of the processes in the ocean (Figure 1.3, (Zeebe & Wolf-Gladrow 2001)). An increase in TA and DIC concentrations of 2:1 indicates $CaCO_3$ dissolution, as the dissolved $[CO_3^{2-}]$ contributes 2 to the charge of the seawater and thereby TA and adds 1 to the [DIC]. Visa versa, $CaCO_3$ formation extracts CO_3^{2-} from the water, reducing the charge (TA) and lowering the DIC in the same 2:1 ratio. As CO_2 [aq] has no charge, its invasion or evasion does not affect TA but only the DIC concentration. In addition to CO_2, respiration and photosynthesis produces and takes up nutrients, respectively, the latter of which is responsible for the slight change in TA during these processes.

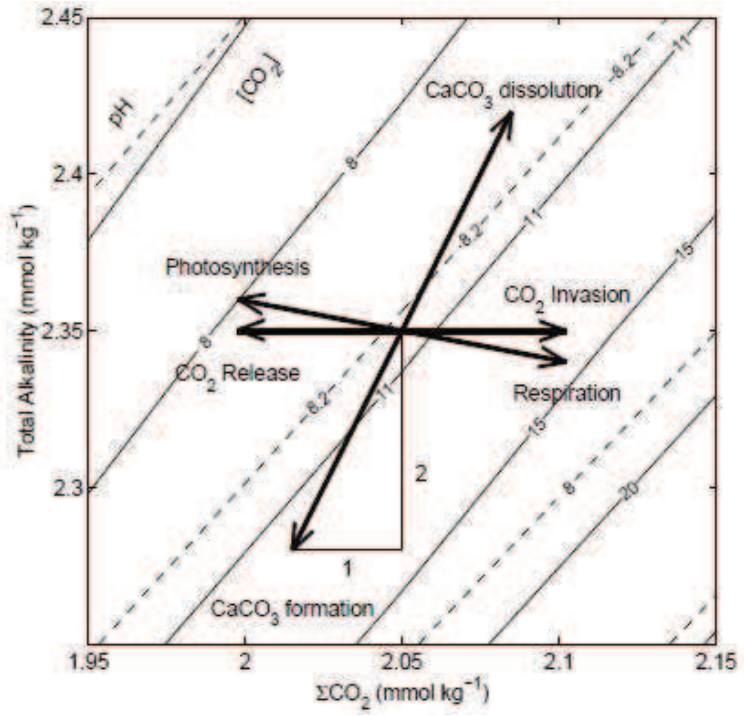

Figure 1.3 Effects of processes on TA and DIC. (Zeebe & Wolf-Gladrow 2001)

II

Scientific objectives, approach and outline

2.1 Project

This study is part of the co-operative project 'Carbon sequestration in the Indonesian Seas and its global significance: Generation of scientific knowledge for formulating strategies for adaptation to climate change' (CISKA) within the 'Science for the Protection of Indonesian Coastal Marine Ecosystems' (SPICE III) program between Germany and Indonesia, funded by the German Federal Ministry of Education and Research (BMBF, Bonn Grant No. 03F0642-ZMT). It concerns subproject 1 entitled 'Impact of river discharges on the marine carbonate system and the resulting CO_2 emissions into the atmosphere'.

2.2 Scientific aims and objectives

The overarching goal of the CISKA project was to estimate budgets for the inorganic and organic carbon cycle and CO_2 emissions from Indonesian waters caused by declining ecosystems in order to develop sustainable mitigation strategies to reduce CO_2 emissions.

The aim of subproject 1 was to quantify the riverine carbon inputs into the coastal ocean and its impact on the marine carbonate system, as well as to quantify the CO_2 emissions from the rivers, estuaries and coastal ocean into the atmosphere. In order to do so, the following objectives were formulated:

- Quantify riverine input of dissolved and particulate organic and inorganic carbon (DOC, POC, DIC, PIC) as well as total alkalinity (TA) into the ocean.
- Estimate CO_2 emissions from the rivers, estuaries and coastal ocean.
- Determine components of the oceanic carbonate system, including the aragonite (Ω_{AR}) and calcite (Ω_{CA}) saturation states.

2.3 Approach

2.3.1 Study area and expeditions

The Indonesian peatlands are located in the coastal plains of the islands of Sumatera, Borneo, and Ian Jaya (Hooijer et al. 2006). To achieve the scientific aims and objectives of this study, two cruise expeditions were carried out along the coast of Sumatra and its rivers in October 2012 and April 2013. Originally, a third cruise was planned in the Spermonde Archipelago, but unfortunately could not be carried out by the participants of this subproject due to bureaucratic difficulties. To complement the data measurements, data from the cruise in October 2009 obtained in the framework of the previous project (SPICE II) were used.

The investigated rivers in Sumatra, Indonesia, are the Musi, Batanghari, Indragiri, Kampar, Siak and Rokan. All six rivers originate from the Barisan Mountains with a short steep descent and continue to flow towards the Malacca Strait. Towards the river mouths, the rivers cut through peatland areas which scatter the low-lying areas along the northern coast and are subject to leaching of organic matter (Baum 2008). The Siak river is particularly well investigated and is a typical black-water river (Baum et al. 2007); its brown color is derived from dissolved organic matter leached from adjacent disturbed peatlands, which cover 21.9% of its catchment area. The Rokan, Kampar, Indragiri, Batanghari and Musi have a peat coverage of 30.2%, 22.4%, 11.9%, 5.0% and 3.5%, respectively (FAO/UNESCO 2004). The thickness of the Sumatran peatlands varies between 2 to 10 m (Hooijer et al. 2006).

Indonesia is subject to the Malaysian-Australian monsoon as a result of the meridional variation of the intertropical convergence zone (ITCZ). During the wet season from October to April, northern air currents laden with moisture from Asia bring heavy rains to the southeastern parts, whereas southern dry air currents from Australia dominate during the dry season from May to September (Gentilli et al. 2014). Precipitation in Pekanbaru, central Sumatra, ranges from 123 mm in July to 312 mm in November, with an annual sum of 2696 mm (Schwarz 2014).

In October 2009, 72 sampling stations were made and focused mainly on the Siak river and continued along the coast, passing the other rivers to the Musi. In October 2012, the expedition stretched from the Banten bay in northeast Java to the Batanghari river with a total of 32 sampling stations. In April 2013 the expedition started in the Musi river going northwest along the other rivers and back via the outer coastal regions, covering a total of 57 sampling stations. Figure 2.1 shows the cruise trajectories and sampling stations for these three expeditions.

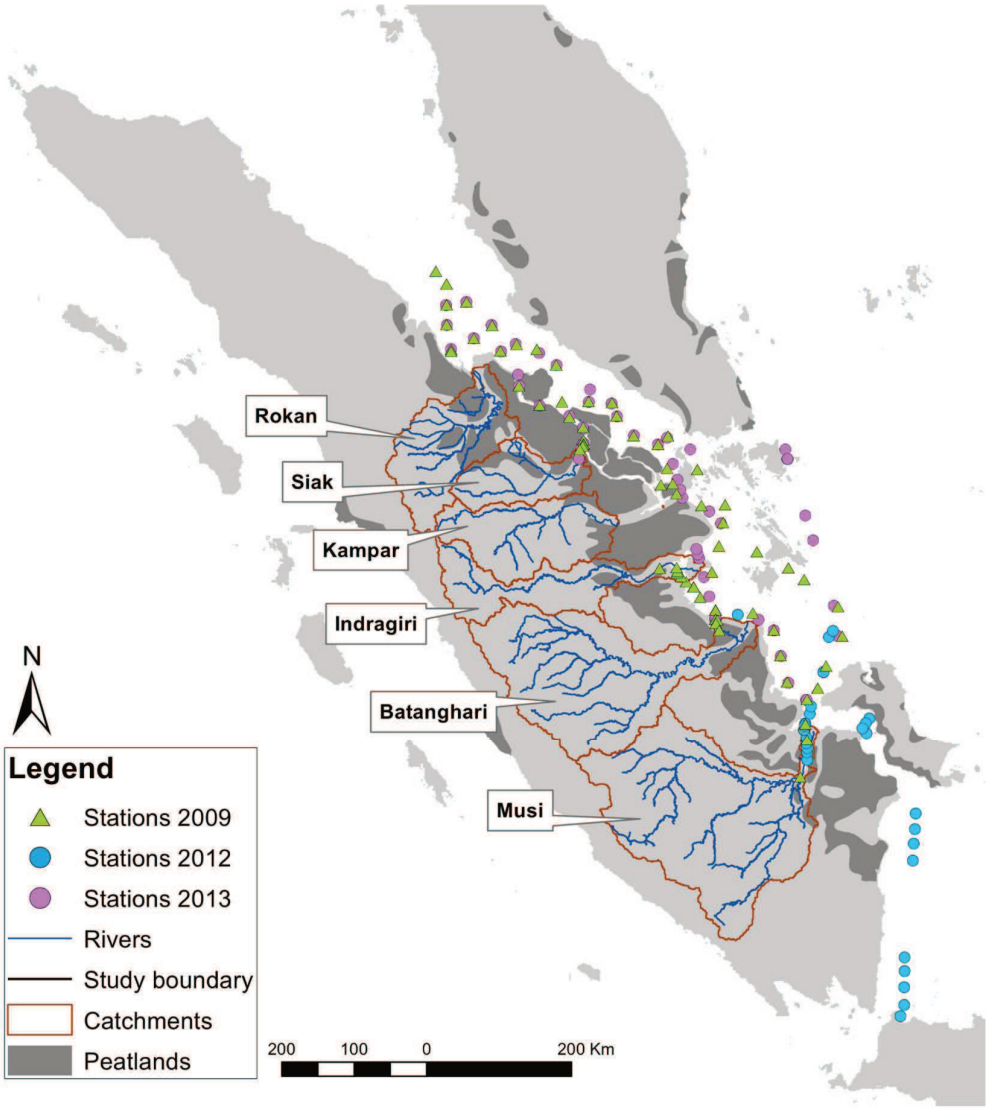

Figure 2.1 Cruise sampling stations 2009, 2012 and 2013.

2.3.2 Data and sample acquisition

During the expeditions, salinity, temperature, pH, oxygen and pCO_2 were measured continuously by means of underway instruments. All sensors were arranged in a flow-through-system and supplied with surface water from a depth of approximately 1 m. In addition, water samples were taken at each station for DOC, nutrients, $\delta^{13}C_{DIC}$ and total alkalinity using a Niskin bottle at 1 m depth (Figure 2.2a-d). For the quantification of POC and PIC, unpublished data of the previous SPICE I and II programs have been used.

Further method information with regard to specific device details, laboratory analyses and calibration are extensively described in the method sections of the chapters 3 to 5.

Figure 2.2 Expedition equipment and sampling. a) Niskin bottle; b) Expedition ship Matahari Ku; c) Water samples; d) Ferry box.

2.4 Manuscript outline

During the course of this PhD study, cutting-edge results were obtained with respect to the following topics: processes and quantities of carbon leaching from disturbed peat soils by means of a mixing model, as well as river outgassing of CO_2 in Southeast Asia, which contradicts conventional assumptions. Furthermore, riverine carbon exports and coastal CO_2 emissions were quantified as well as the contemporary marine carbonate system, which revealed potentially perilous conditions for the coral reefs. These results are discussed in detail in chapters 3 to 5, where the main topic of chapter 3 is river outgassing of CO_2, chapter 4 is concerned with soil carbon leaching and chapter 5 focuses on CO_2 emissions and subsurface processes in the estuaries and coastal ocean. A general discussion is provided in chapter 6 in which the results are connected to provide an overall picture of the situation, including current perspectives for Indonesia and the global relevance of the findings. An overview on the main conclusions is listed in chapter 7.

For readability, the manuscripts have been formatted to provide a consequent layout throughout the dissertation chapters. Therefore, their layout may differ from the published versions with respect to for instance the order of paragraphs and distribution of graphs, but their contents are identical.

2.5 Manuscript list and authors' contributions

This paragraph gives a declaration of the contribution of the PhD candidate in each manuscript, provided by a short description, as well as expressed in percentages of the total work load.

2.5.1 Manuscript 1 (Chapter 3)

Title: The impact of disturbed peatlands on river outgassing in Southeast Asia.

Authors: Francisca Wit, Denise Müller, Antje Baum, Thorsten Warneke, Widodo Setiyo Pranowo, Mority Müller, Tim Rixen.

Status: Published in *Nature Communications*, December 2015.

Contribution: 1st author. F.W. has carried out the fieldwork and laboratory analyses in Indonesia in October 2012 and 2013, performed the data analyses for Indonesia and all (extrapolation) calculations and was the leading author, including graph and table design.

Concept and design	50 %
Data acquisition	95 % (90% in 2012 and 100% 2013)
Data analysis and interpretation	80 %
Preparation of figures and tables	100 %
Drafting of the manuscript	80 %

2.5.2 Manuscript 2 (Chapter 4)

Title: Carbon leaching from tropical peat soils and consequences for carbon balances.

Authors: Tim Rixen, Antje Baum, Francisca Wit, Joko Samiaji.

Status: Published in *Frontiers in Earth Science*, July 2016.

Contribution: 3rd author. F.W. has carried out the fieldwork and laboratory analyses in Indonesia in October 2012 and 2013, and conducted online measurements. F.W. was involved in the study design and has participated in the discussions, as well as contributed to the writing and designed the schematization figure.

Concept and design	20 %
Data acquisition	95 % (90% in 2012 and 100% 2013)
Data analysis and interpretation	100 % (samples) / 15 % (mixing model)
Preparation of figures and tables	25 %
Drafting of the manuscript	30 %

2.5.3 Manuscript 3 (Chapter 5)

Title: The invisible carbon footprint: from land use change to coral reef dissolution in Sumatra, Indonesia.

Authors: Francisca Wit, Tim Rixen, Antje Baum, Widodo Setiyo Pranowo, Andreas A. Hutahaean.

Status: Submitted at *Nature Climate Change*, June 2017.

Contribution: 1st author. F.W. has carried out the fieldwork and laboratory analyses in October 2012 and 2013, performed data analyses and calculations and was the leading author, including graph and table design.

Concept and design	75 %
Data acquisition	95% (90% in 2012 and 100% 2013)
Data analysis and interpretation	95 %
Preparation of figures and tables	100 %
Drafting of the manuscript	100 %

III

The impact of disturbed peatlands on river outgassing in Southeast Asia

Francisca Wit[1,*], Denise Müller[1,2], Antje Baum[1], Thorsten Warneke[2], Widodo Setiyo Pranowo[3], Moritz Müller[4] and Tim Rixen[1,5]

1) *Francisca Wit (*Corresponding author), Leibniz Center for Tropical Marine Ecology (ZMT), Fahrenheitstrasse 6, 28359 Bremen, Germany (francisca.wit@leibniz-zmt.de)*
2) *Institute for Environmental Physics, University of Bremen, Otto-Hahn-Allee 1, 28359 Bremen, Germany*
3) *Research & Development Center for Marine & Coastal Resources (P3SDLP), Gedung II BALITBANGKP, Jalan Pasir Putih II, Ancol Timur, Jakarta, 14430, Indonesia*
4) *Swinburne University of Technology, Sarawak Campus, Jalan Simpang Tiga, 93350 Kuching, Sarawak, Malaysia*
5) *Institute of Geology, University of Hamburg, Bundesstrasse 55, 20146 Hamburg, Germany*

Keywords: River outgassing, CO_2, Indonesia, Malaysia, Southeast Asia, peatlands

Published in *Nature Communications*

Citation: Wit, F., Müller, D., Baum, A., Warneke, T., Pranowo, W.S., Müller, M. and Rixen, T., 2015. The impact of disturbed peatlands on river outgassing in Southeast Asia. *Nature Communications*, 6:10155, doi: 10.1038/ncomms10155.

Abstract

River outgassing has proven to be an integral part of the carbon cycle. In Southeast Asia, river outgassing quantities are uncertain due to lack of measured data. Here we investigate six rivers in Indonesia and Malaysia, during five expeditions. CO_2 fluxes from Southeast Asian rivers amount to 66.9±15.7 Tg C yr^{-1}, of which Indonesia releases 53.9±12.4 Tg C yr^{-1}. Malaysian rivers emit 6.2±1.6 Tg C yr^{-1}. These moderate values show that Southeast Asia is not the river outgassing hotspot as would be expected from the carbon enriched peat soils. This is due to the relatively short residence time of dissolved organic carbon (DOC) in the river, as the peatlands, being the primary source of DOC, are located near the coast. Limitation of bacterial production, due to low pH, oxygen depletion or the refractory nature of DOC, potentially also contributes to moderate CO_2 fluxes as this decelerates decomposition.

3.1 Introduction

The importance of inland waters in the global carbon cycle has gained more awareness since the last decade through studies which have revealed that inland waters (rivers, streams, lakes, reservoirs and estuaries) are not a passive conduit but play an integral role both for carbon storage and greenhouse gas emissions to the atmosphere (Regnier et al. 2013; Battin et al. 2009; Cole et al. 2007; Tranvik et al. 2009). These studies estimate, in line with the 5th Assessment IPCC Report (P. Ciais et al. 2013), that on a global scale approximately 45-60% (0.9 to 1.4 Pg C yr^{-1}) of carbon entering the freshwater system is decomposed and emitted back to the atmosphere as CO_2. Another 0.2 to 0.6 Pg C yr^{-1} is buried in freshwater sediments and about 0.9 Pg C ^{1} reaches the coastal ocean. However, an estimate of inland water outgassing by Raymond et al. (Raymond et al. 2013) revealed an emission of 2.1 Pg C yr^{-1}, of which 1.8 Pg C yr^{-1} from streams and rivers, which is significantly larger than previous estimates. On the other hand, a more recent study by Lauerwald et al. (Lauerwald et al. 2015) estimates a global river outgassing of 0.65 Pg C yr^{-1}, however, they have excluded stream orders lower than 2. These variable findings challenge our current understanding of the global carbon cycle and in particular that of the terrestrial biosphere as a sink for anthropogenic CO_2. Still, large uncertainties remain in outgassing fluxes due to scarcity of data, which we aim to resolve for Southeast Asia. Indonesia and Malaysia are areas of particular interest due to their peatlands, which together store 66.5 Pg C (Page et al. 2011). It has been shown recently that the fluvial organic carbon flux increases once these tropical peatlands are disturbed (Moore

et al. 2013). However, it remains unclear to what extent this influences the CO_2 emissions from these aquatic systems.

In this study, river outgassing fluxes are quantified for Southeast Asia by using measurements from four rivers in Sumatra, Indonesia, and two rivers in Sarawak, Malaysia (Figure 3.1). CO_2 fluxes and yields for all rivers are determined and related to peat coverage, which uncovers a positive relationship. Based on this correlation, CO_2 fluxes for Southeast Asia are calculated, which reveal moderate fluxes and show that Southeast Asia is not a hotspot for river outgassing.

3.2 Methods

3.2.1 Study area

Southeast Asian peatlands cover 27.1 million hectares and are located in the coastal plains of the islands of Sumatera, Borneo, and Ian Jaya (Hooijer et al. 2006). Tropical peatlands are particularly vulnerable to anthropogenic stressors, such as deforestation and drainage, which are used to convert peat swamp forests into cropland. Today, a large fraction of this peat is already found under oil palm plantations (Miettinen et al. 2012) and only 10% remains undisturbed (Miettinen & Liew 2010). The investigated rivers in Sumatra, Indonesia, are the

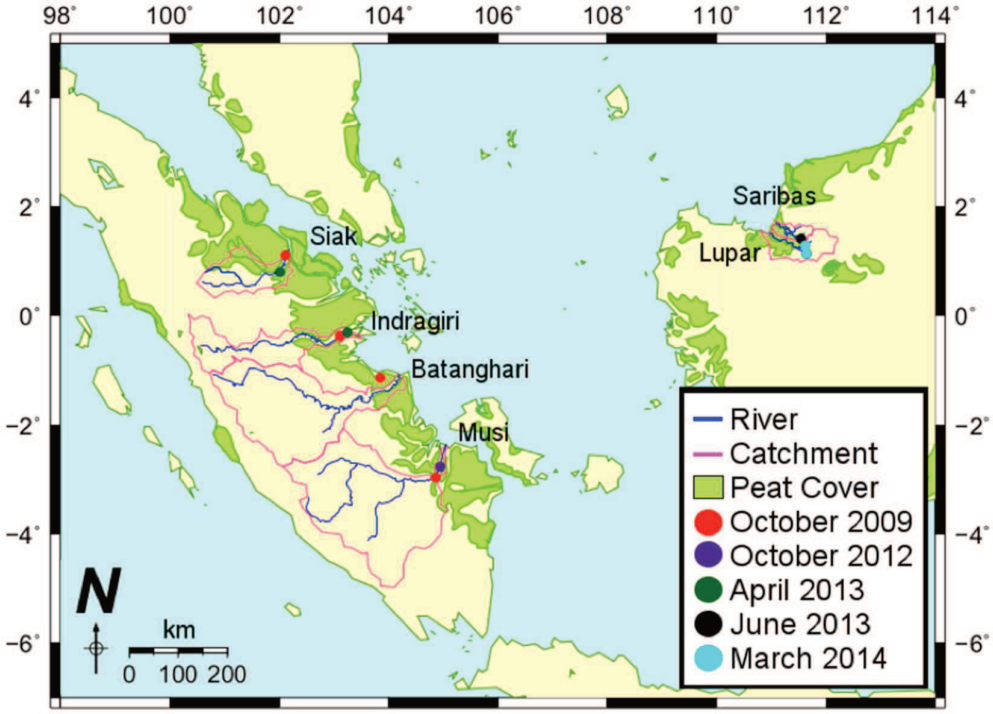

Figure 3.1. Study area and river in Indonesia and Malaysia. The data points indicate the zero-salinity locations in each river, from which the parameter values were averaged.

Musi, Batanghari, Indragiri and Siak. All four rivers originate from the Barisan Mountains with a short steep descent and continue to flow towards the Malacca Strait. Towards the river mouths, the rivers cut through peatland areas which scatter the low-lying areas along the northern coast and are subject to leaching of organic matter (Baum 2008). The Siak is a typical black-water river (Baum et al. 2007); its brown color is derived from dissolved organic matter leached from adjacent disturbed peatlands, which cover 21.9% of its catchment area. The Indragiri, Batanghari and Musi have a peat coverage of 11.9%, 5.0% and 3.5%, respectively (FAO/UNESCO 2004). The thickness of the Sumatran peatlands varies between 2 to 10 m (Hooijer et al. 2006). Malaysia has approximately 2 million hectares of peatlands. Sarawak on the island of Borneo holds the largest share of Malaysia's peatlands, most of which used to be forested (Joosten et al. 2012). The two rivers Lupar and Saribas in Sarawak enclose a peninsula with protected peat swamp forest that has a peat thickness of up to 10 m (Melling et al. 2007). The estimated peat coverage for the Lupar basin is 30.5% and 35.5% for the Saribas catchment (Nachtergaele et al. 2009).

Southeast Asia is subject to the Malaysian-Australian monsoon as a result of the meridional variation of the intertropical convergence zone (ITCZ). During the wet season from October to April, northern air currents laden with moisture from Asia bring heavy rains to the southeastern parts, whereas southern dry air currents from Australia dominate during the dry season from May to September (Gentilli et al. 2014). Precipitation in Pekanbaru, central Sumatra, ranges from 123 mm in July to 312 mm in November, with an annual sum of 2696 mm (Schwarz 2014). Rainfall in Kuching, Sarawak, Malaysia, is even higher and ranges from 196 mm in June to 675 mm in January (Schneider et al. 2011) with an annual sum of 4616 mm.

3.2.2 Expeditions

In this study, data is considered from a total of five expeditions, three of which took place in Sumatra (October 2009, October 2012 and April 2013), and two in Sarawak (June 2013 and March 2014). In October 2009, 72 sampling stations were made and focused mainly on the Siak river and continued along the coast, passing the other rivers to the Musi. In October 2012, the expedition stretched from the Musi river to the Batanghari river with a total of 32 sampling stations. In April 2013 the expedition started in the Musi river going northwest along the other rivers and back via the outer coastal regions, covering a total of 57 sampling stations. In Sarawak, 21 sampling stations were made along the Lupar and Saribas rivers and

their estuaries in June 2013 and 26 stations in March 2014. The locations of the river sampling stations at salinity zero are shown on the map in Figure 3.1.

3.2.3 Sampling methods

In Sumatra, pH, salinity, temperature, dissolved oxygen and pCO_2 were measured continuously by means of underway instruments. All sensors were arranged in a flow through system and supplied with surface water from an approximate depth of 1 m. Salinity was measured using a Seabird SBE 45 Micro TSG sensor. Temperature and pH were measured with a Meinsberg EGA 140 SMEK with integrated temperature sensor. Oxygen measurements were conducted with an Aanderaa Optode 3835. pCO_2 was measured with two devices: the Li-Cor 7000 pCO_2 analyzer (October 2009 and October 2012) and the Contros HydroC CO_2 Flow Through sensor (October 2012 and April 2013). Prior to the expeditions both devices were calibrated, of which the Contros at 100, 448 and 800 ppm. The Li-Cor 7000 analyzer was calibrated with certificated NOAA reference gases (#CB08923 with 359.83 ppm, #CA06265 with 1021.94 ppm and another certified calibration gas with 8000 ppm CO_2).

In addition to the continuous measurements, water samples were collected at each station using a Niskin bottle at an approximate depth of 1.5 m. DOC samples were filtered (0.45 µm), stored in 60 ml HDPC bottles and acidified with phosphoric acid (20%) to a pH-value of 2. After a total storage time during and after the expeditions of maximum three weeks, DOC samples were analyzed upon arrival in the laboratory in Bremen, Germany, with a Dohrmann DC-190 Total Organic Carbon Analyzer. The samples were combusted at 680 °C within a quartz column, filled with Al_2O_3-balls covered with platinum. The released CO_2 was purified, dried and measured by a non-dispersive infrared detection system. The relative standard deviation for the method was ±2%.

In Sarawak, pCO_2 was measured with an in-situ FTIR analyzer (Griffith et al. 2012), using a Weiss equilibrator (Johnson 1999). In the headwater region, which was not accessible by boat, a Li-820 CO_2 analyzer was used, together with headspace equilibration in a 10 L water bottle (June 2013) and a 600 ml conical flask (March 2014). The FTIR and the Li-820 were calibrated with the same set of secondary standards, ranging from 380 to 10000 ppm CO_2. Samples were taken for DOC following the same procedure as described above. Dissolved oxygen, pH and conductivity were measured using a WTW Multi 3420 with an FDO 925 oxygen sensor, a SenTix 940 IDS pH sensor and a TetraCon 925 conductivity sensor. Salinity was calculated from conductivity using the equations by Bennet (Bennett 1976). Floating

chamber measurements were performed in order to determine the CO_2 flux. The chamber had a volume of 8.7 L and a surface area of 0.05 m^2. The CO_2 flux was determined from the increase of the CO_2 mixing ratio over time, which was monitored with the Li-820.

3.2.4 Calibration experiment

In order to calibrate the Contros river measurements, a CO_2 calibration experiment was conducted during which different concentrations of CO_2 gas were delivered using a gas mixing system. Prior to the calibration with water measurements, the gas concentrations delivered by the gas mixing system were controlled by the mixing system regulator, the Li-Cor 7000, the Li-820 and the cavity ring-down spectrometer (Picarro G2201-i) in a range from circa 500 to 6000 ppm (Figure 3.2a). The gas was then used to calibrate freshwater in a range of 1500 – 5500 ppm that was pumped into the Li-Cor 7000 equilibrator and the Contros sensor. The measured pCO_2 concentrations were correlated and the regression equation (Figure 3.2b) was used to calibrate the Contros river data measured during the expedition in 2013.

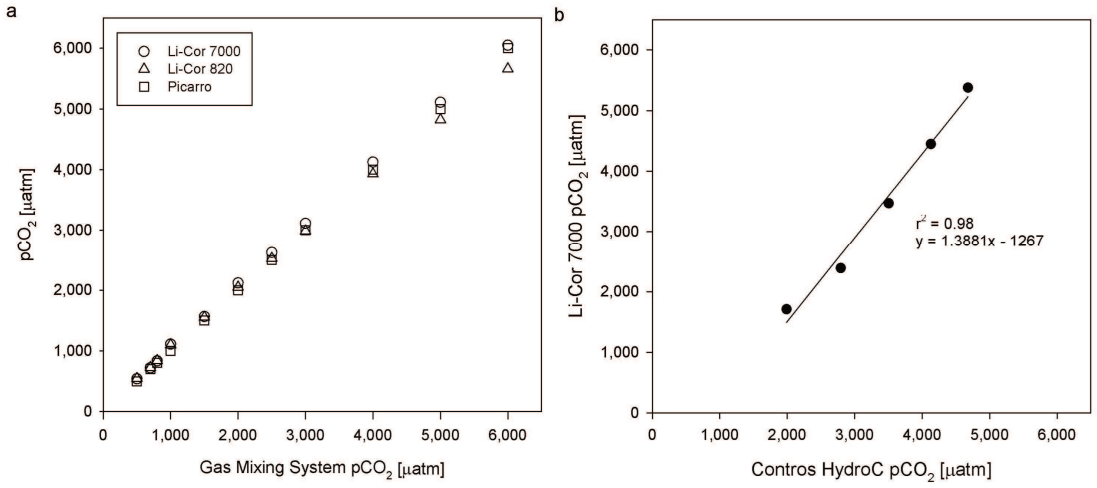

Figure 3.2 Calibration experiment results. a) Gas control with the Li-Cor 7000, Li-820 and Picarro. b) The data points for the Li-Cor 7000 and Contros HydroC can be fitted with a linear regression with $r^2 = 0.98$. The Contros HydroC data was corrected according to this fit.

3.2.5 CO_2 flux calculation

CO_2 fluxes (F) were calculated from pCO_2 using:

$$F = K_{CO2} * K_0 * \Delta pCO_2 \quad (1)$$

where K_{CO2} is the CO_2 piston velocity (cm h^{-1}), K_0 the solubility coefficient of CO_2 in seawater (Weiss 1974) and ΔpCO_2 (µatm) is the sea-air pCO_2 difference.

Usually, the piston velocity is poorly constrained and spatially and temporally highly variable. Raymond and Cole (Raymond & Cole 2001) have pointed out that flux estimates can easily be altered by considerable amounts depending on the choice of the piston velocity. Meanwhile, the ways to determine the piston velocity are multifarious. Relationships with wind speed, hydraulic characteristics (Raymond et al. 2012), in-situ measurements using floating chambers (Striegl et al. 2012; Alin et al. 2011) or dual tracer techniques (Ho et al. 2011) are commonly used. Empirical models neglect small-scale fluctuations and allow for estimates on larger scales. These models relate environmental parameters to the piston velocity. In coastal systems and the ocean, this is mostly wind speed (Wanninkhof 1992). In rivers, stream velocity, stream slope, depth, discharge and bedrock roughness have been identified as the main drivers of in-stream turbulence and consequently the piston velocity (Raymond et al. 2012). In this study, floating chambers were used to determine piston velocities. The performance of floating chambers is a matter of debate, where both over- and underestimations occur due to artificial turbulence and shielding of wind, respectively, are suggested. On the other hand, sometimes, a relatively good agreement between floating chamber measurements and other techniques is reported (Huotari et al. 2013). The floating chamber measurements conducted on the Lupar and Saribas river are described in detail in Müller et al. (Müller et al. 2015). There, we also discuss potential biases. The piston velocities of the Lupar and Saribas rivers were determined with 9 floating chamber measurements and are averaged at 26.5±9.3 cm h^{-1} and 17.0±13.6 cm h^{-1}, respectively, after normalization to a CO_2 Schmidt number of 360 (30 °C) (Raymond et al. 2012). For the Siak river, Rixen et al. (Rixen et al. 2008) derived a similar piston velocity of 22.0 cm h^{-1} using an oxygen balance model. Given that these rivers have piston velocities of a similar range, despite having different catchment sizes (Milliman & Farnsworth 2011) and slopes, we believe that they provide a good representation of the piston velocities in the Indragiri, Batanghari and Musi, Therefore, their average of 21.8±4.7 cm h^{-1} is used to calculate the fluxes in these three rivers, whereas the river-specific piston velocities were applied accordingly in the other rivers.

3.2.6 Peat coverages

Catchment area was calculated using a relief model of the Earth's surface in ArcGIS 9.3 with the ArcHydro extension. Digital Elevation Data (DEM) such as the SRTM90mDEM can be obtained from the web site of the Consortium for Spatial Information (CGIAR-CSI) of the Consultative Group for International Agricultural Research (CGIAR, http://www.cgiar-csi.org) (Reuter et al. 2009). The SRTM90mDEM has a spatial resolution of 90 m at the equator and was originally produced in the framework of the NASA Shuttle Radar Topographic Mission (SRTM). Peat coverage (%) for each catchment was estimated using a combination of the FAO Soil Map of the World (FAO/UNESCO 2004) and the catchment area derived from the ArcGIS DEM model.

The peat coverage for Malaysia, Indonesia and Southeast Asia was derived from Hooijer et al. (Hooijer et al. 2006), who based their peat coverage percentages for these areas on field surveys provided by Wetlands International and the FAO Digital Soil Map of the World (FAO/UNESCO 2004), as well as Miettinen et al. (Miettinen et al. 2012), who used satellite images from as recent as 2010. However, data of Miettinen et al. (Miettinen et al. 2012) only covers Malaysia, Sumatra and Kalimantan, whereas that of Hooijer et al. (Hooijer et al. 2006) covers entire Southeast Asia. Therefore, peat coverage for Malaysia, Indonesia and Southeast Asia is based on the combination of Hooijer et al. (Hooijer et al. 2006) and Miettinen et al. (Miettinen et al. 2012), wherein the most recent data was integrated where possible.

3.2.7 River surface coverage

For all six rivers a surface area estimation has been conducted based on the length and width of their primary course and main tributaries (Table 3.1). Length was estimated using HydroSheds stream lines and Google Earth was used to estimate width along multiple sections in the primary course and main tributaries for each river. River area (%) was calculated based on the share of river surface area with respect to the catchment area. River coverages for Malaysia, Indonesia and Southeast Asia are derived from the average pCO_2, piston velocity and CO_2 yield found for these locations.

Table 3.1 River surface area

River	*Length [km]*	*Width [m]*	*Catchment area [km²]*	*River area [km²]*	*River coverage [%]*
Musi	780	312	56,931	243	0.43
Batanghari	678	374	44,890	269	0.60
Indragiri	366	475	17,968	174	0.97
Siak	447	182	10,423	81	0.78
Lupar*	246	758	6,541	186	0.12
Saribas*	176	444	2,149	78	0.26
*Location***					
Malaysia	-	-	327,291	2291	0.70
Indonesia	-	-	1,919,317	15354	0.80
SE-Asia	-	-	2,652,370	20688	0.78

* For the CO_2 calculations of Lupar and Saribas, only the catchment area upstream from the measurement point was considered, as the measurement data is representative for the upstream river characteristics and not the peatland area further downstream. The river coverage of the entire catchment area of the Lupar is 2.85% and that of the Saribas 3.64%.

** River coverages for Malaysia, Indonesia and Southeast Asia are derived from the average pCO_2, piston velocity and CO_2 yield found for these locations.

3.2.8 Uncertainty estimates

The errors associated with the averaged parameter per expedition are presented as the standard deviation. The errors of the averaged parameter per river are calculated as the standard error where possible; otherwise the error is presented as the deviation of the two averages from the mean. Throughout the calculations of the CO_2 yield and fluxes, the standard errors as derived from the averages were integrated. Therefore, the errors of the CO_2 yields and fluxes are representative for the best and worst case scenarios, named as the best/worst case deviation.

3.3 Results

3.3.1 River processes and variability

In estuaries, salinities higher than zero can be measured 18 to 50 km downstream with increasing salinities towards the coastal ocean (Figure 3.3a), whereas pCO_2 concentrations show an opposite pattern with increasing concentrations going upstream (Figure 3.3c). Indeed, in the estuaries salinity is inversely correlated with CO_2 concentrations (Figure 3.3b) as a consequence of mixing between river and oceanic waters and the associated decrease of pH in rivers. In order to calculate mean river parameter values, estuaries were excluded to avoid the influence from ocean waters and only data points with salinity 0-0.1 in the respective rivers were taken into consideration (Figure 3.3d, Table 3.2).

Figure 3.3d shows the variability of the pCO_2 data in the Sumatran rivers in 2009 and 2013. The highest pCO_2 concentrations were measured in the Siak river, which also reveals the

highest DOC and the lowest O_2 concentrations (Table 3.2, Figure 3.4). This agrees with results derived from numerical model and DOC decomposition experiments, which show that DOC leaching from peat soils and the decomposition of its labile fraction are the main factors controlling DOC and O_2 concentrations in the Siak (Rixen et al. 2008). The resulting input of dissolved inorganic carbon and the already low pH, caused by the organic acids from peat, shift the carbonate system ($CO_2 \Leftrightarrow HCO_3^- \Leftrightarrow CO_3^{2-}$) towards CO_2 and explain the high CO_2 concentrations in the Siak. Increasing pCO_2 concentrations associated with increasing DOC concentrations denote that DOC leaching and decomposition are prime factors controlling pCO_2 concentrations also in all other studied rivers (Figure 3.4).

Contrary to the Siak, which is a typical black-water river where its dark brown color reduces light penetration to a few centimeters, non-black-water rivers have a higher light availability. Accordingly, photosynthesis plays a role and therefore these rivers have a pronounced day and night cycle, as seen in the Musi river during our expedition in 2013. As we entered this

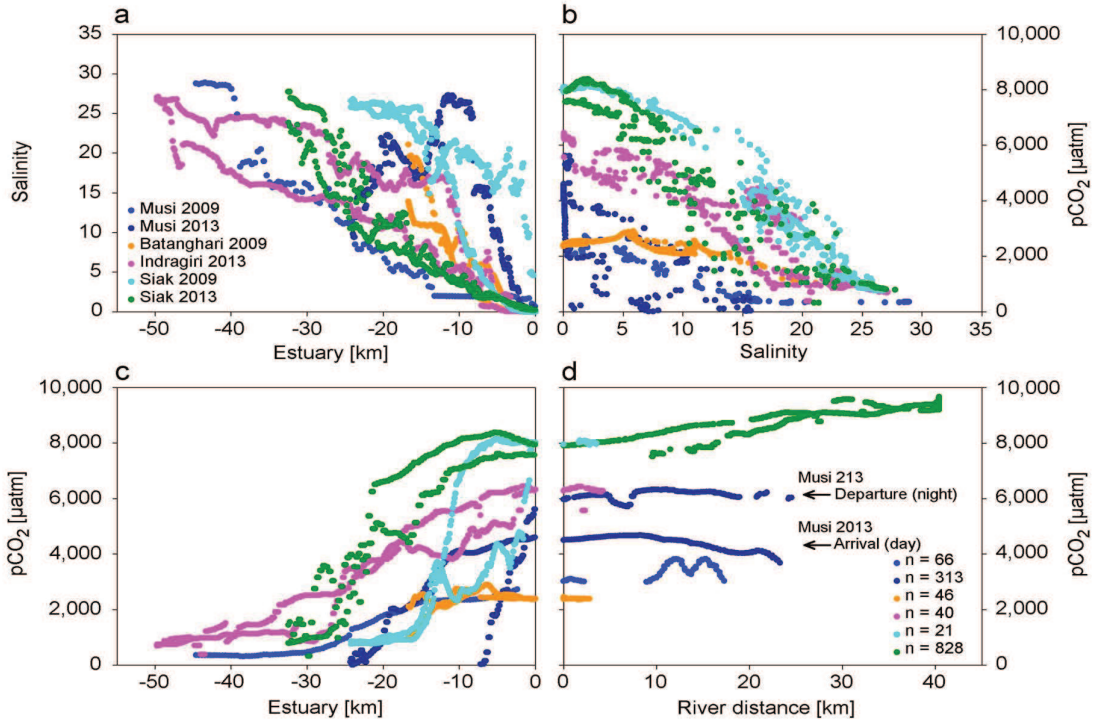

Figure 3.3 Patterns of salinity and pCO_2 underway measurements on the way in and out of the estuaries and rivers in 2009 and 2013. Estuaries start at 0 km, which is the border with the river at salinity 0, with increasing (negative) distance towards the coastal ocean. Measurements in the rivers start at 0 km at salinity <0.1 with increasing distance upstream. a) Decrease of salinity across estuary towards river. b) Inverse relationship of pCO_2 versus salinity (>0.1). c) Increase of pCO_2 across estuary towards river. d) pCO_2 data points at zero salinity (0-0.1) against river distance, with number of data points in the lower right corner.

Table 3.2 Averaged parameters per river and year. The spread of the data per individual year is determined by the standard deviation. The spread of the averages is based on the standard error if possible, otherwise as the largest deviation from the mean.

River	*Time*	*pCO_2 (µatm)*	*DOC (µmol l^{-1})*	*O_2 (µmol l^{-1})*	*Temp. (°C)*	*pH (-)*	*Precip.* (mm)*
Musi	Oct '09	3388±294	223.3±4.5	158.4±24.9	30.8±0.11	-	197±50
	Oct '12	-	264.5±5.3	137.1±48.3	31.4±0.09	6.86±0.25	249±63
	Apr '13	5244±892	-	152.8±55.9	29.7±0.57	-	238±61
	Average	**4316±928**	**243.9±20.6**	**149.4±6.4**	**30.6±0.50**	**6.86±0.25**	**228±34**
Bata.	Oct '09	2400±18	363.0±2.7	162.8±1.3	29.8±0.08	7.07±0.01	180±46
	Oct '12	-	286.9±2.8	-	29.5±0.05	-	293±75
	Apr '13	-	314.2±5.1	-	30.8±0.05	-	252±64
	Average	**2400±18**	**321.4±22.6**	**162.8±1.3**	**29.8±0.39**	**7.07±0.01**	**242±72**
Indr.	Oct '09	5275±0	774±5.1	128.4±0	29.8±0.00	-	227±58
	Apr '13	6278±206	651.1±4.5	69.4±4.0	32.3±0.13	6.30±0.05	332±85
	Average	**5777±527**	**712.6±61.5**	**98.9±29.5**	**31.1±1.25**	**6.30±0.05**	**280±93**
Siak	Mar '04**	-	1866± -	-	-	-	-
	Sep '04**	-	2195± -	-	-	-	-
	Aug '05**	-	2247± -	-	-	-	-
	Mar '06**	-	1613± -	-	-	-	-
	Nov '06**	-	1793± -	-	-	-	-
	Oct '09	8027±40	2453.0±49.1	17.1±1.2	29.8±0.00	4.78±0.03	318±81
	Apr '13	9083±567	636.1±3.9	35.3±18.3	30.1±0.57	5.48±0.20	206±67
	Average	**8555±528**	**1829.0±245.6**	**26.2±9.1**	**30.0±0.15**	**5.13±0.48**	**262±79**
Lupar	Jun '13	1527±38	88.5±1.8	161.3±0.8	29.0±0.05	6.70± -	88±22
	Mar '14	1021±357	207.9±1.1	180.1±0.9	28.4±0.05	7.10±0.34	167±43
	Average	**1274±148**	**148.2±59.7**	**170.7±9.4**	**28.7±0.30**	**6.90±0.28**	**128±70**
Sari.	Jun '13	1159±29	312.2±1.3	121.2±0.6	29.2±0.05	7.30± -	88±22
		1159±29	**312.2±1.3**	**121.2±0.6**	**29.2±0.05**	**7.30± -**	**88±22**

*Precipitation and standard deviations derived from Deutsche Wetterdienst (DWD)(Anon 2015) and Schneider (Schneider et al. 2015), respectively.

** DOC values derived from Rixen et al. (Rixen et al. 2008)

river during the day, the pCO_2 concentrations were lower than during the departure, which took place during the night when photosynthesis and CO_2 uptake could not take place, but decomposition and CO_2 production prevailed. In total, the observed variability of pCO_2 in the Musi was ±21.5%, which was reduced to ±6.2% in the Siak due to a reduced impact of photosynthesis in peat-draining rivers. The Musi also shows an interannual variability with lower pCO_2 concentrations in 2009 as compared to 2013 due to lower precipitation rates and lower DOC leaching. Although this supports our former finding that DOC leaching is a prime factor controlling pCO_2 concentrations, there are also exceptions, which point to other processes, as indicated by the high pCO_2 but low DOC concentrations in the Siak in 2013.

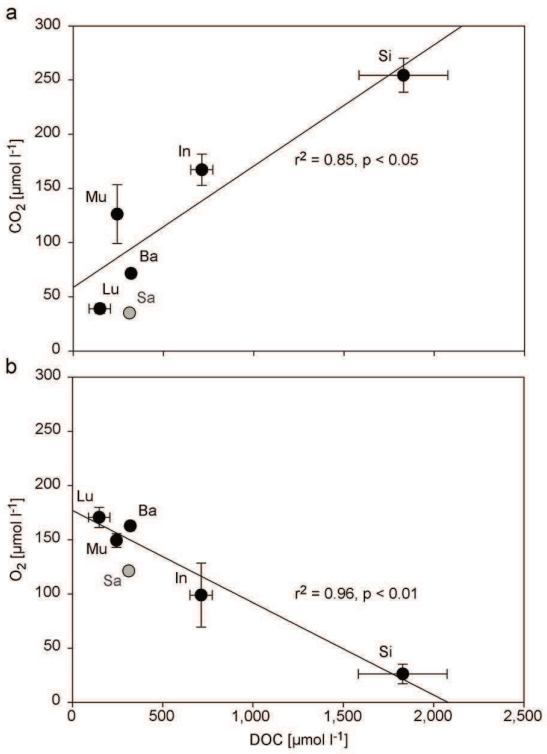

Figure 3.4 Linear correlations of CO_2 and O_2 versus DOC. a) Correlation of CO_2 versus DOC. b) Correlation of O_2 versus DOC. All values are in µmol l^{-1}. The data points represent annual averages in the Musi, Batanghari, Indragiri and Siak rivers in Sumatra (Indonesia) and the Lupar and Saribas rivers in Sarawak (Malaysia). The Saribas, having only one (seasonal) data point, was excluded from the correlation and is shown in grey. Error bars mean ±s.d..

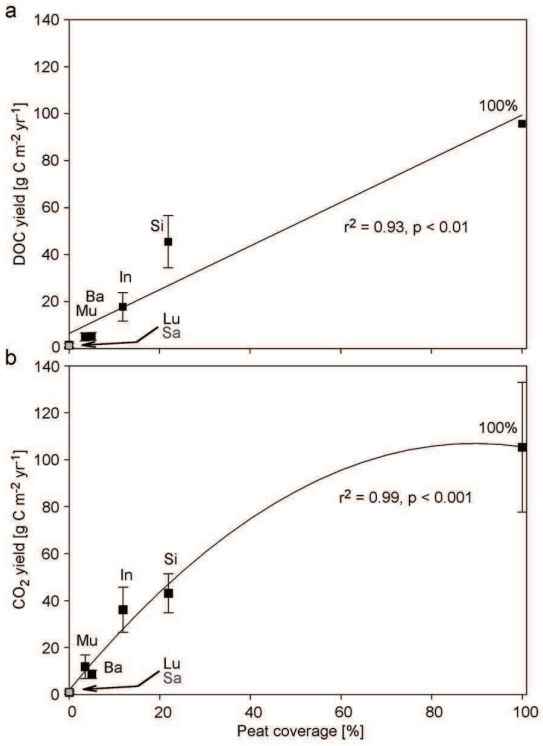

Figure 3.5 Correlations of DOC yield and CO_2 yield versus peat coverage. a) Correlation of DOC yield versus peat coverage. b) Correlation of CO_2 yield versus peat coverage. The yields are shown in g C m^{-2} yr^{-1} and the peat coverage in %. The peat coverage is expressed in percentage for each of the river catchments. The data points represent annual estimates at salinity S=0 in the rivers Musi, Batanghari, Indragiri and Siak in Sumatra, Indonesia. The salinity S=0 stations in the Lupar and Saribas rivers were located further upstream and outside of the peatland area. Consequently, their DOC concentrations and CO_2 yields are representative for areas with 0% peat coverage. The Saribas, having only a seasonal data point, was excluded from this correlation, but is shown in grey. Note that the CO_2 yield is expressed in grams of carbon per m^2 of catchment area per year, not river area. Error bars represent the best and worst case scenario as a result of incorporating the s.d. of the DOC, pCO_2, piston velocity and temperature into the DOC and CO_2 yield calculation.

Contrary to non-peat-draining rivers, enhanced discharge lowers DOC concentrations in rivers draining undisturbed peat. This reverse behavior is caused by the high water saturation of peat due to which enhanced precipitation leads to flooding and the resulting surface runoff increases discharge, which dilutes the DOC concentrations in the peat-draining rivers (Clark et al. 2008; Moore & Jackson 1989; Schiff et al. 1998). However, the peatlands in the Siak catchment as well as elsewhere in Indonesia are largely drained. When precipitation is relatively low, the ground water table could fall below the peat and the DOC concentrations in the river would be reduced (Moore & Jackson 1989). This might explain the exceptionally low DOC concentration in April 2013, which can be associated with low precipitation rates (Table 3.2). However, despite the low DOC concentration, pCO_2 concentrations remained high pointing to an additional carbon source. This could have been a decaying plankton bloom favored by the enhanced light availability due to the lower DOC concentrations. A similar situation might also explain the Lupar in 2013, where low DOC concentrations are associated with low precipitation rates, but relatively high pCO_2 concentrations still occur. This indicates that the dampening effects of reduced carbon input from soil leaching on the pCO_2 concentrations could be counterbalanced by input of CO_2 from presumably plankton blooms, which reduces the temporal variability of pCO_2 in the rivers during time characterized by extremely low DOC leaching.

3.3.2 River outgassing and DOC export

Quantification of both river outgassing and riverine DOC export sheds light on their flux ratio and consequently the share of river outgassing with respect to the carbon entering the freshwater system. CO_2 emissions were calculated for all investigated rivers using equation 1 (see Methods) with their respective piston velocities and respective ΔpCO_2, which were based on their averaged pCO_2 values (Table 3.2) and an atmospheric CO_2 concentration of 390 µatm. Subsequently, these fluxes were multiplied by their respective river surface area (see Methods and Table 3.1) to calculate the flux per river. Riverine DOC exports were calculated by multiplying the DOC concentrations with the discharges, which were based on the averaged monthly precipitations (Table 3.2) and assuming an evapotranspiration of 38% (Moore et al. 2013). The resultant net water-air CO_2 fluxes and riverine DOC exports are presented in Table 3.3. Note that both CO_2 and DOC fluxes are shown in g 10^9 mth^{-1}. These results suggest that on average 53.3±6.5% of the organic carbon leached from soils is decomposed in the river and emitted as CO_2 into the atmosphere. This percentage is based on

Table 3.3 CO_2 flux versus DOC export – river outgassing in percentage. The error of the ΔpCO_2 is the standard error, the K_{co2} has the largest error from the mean, the discharge has the standard deviation and the DOC flux, CO_2 flux and outgassing errors are based on the best/worst case deviation, with the average having a standard error.

River	ΔpCO_2 [µatm]	K_{CO2} [cm h^{-1}]	River area [km^2]	Discharge [m^3 s^{-1}]	DOC flux [Gg mth^{-1}]	CO_2 flux [Gg mth^{-1}]	Outgassing [%]
Musi	3926±928	21.8±4.7	243	3054±254	23.6±4.0	55.8±23.3	70.3±6.0
Batanghari	2010±18	21.8±4.7	269	2556±422	26.0±6.1	32.5±6.7	55.6±0.7
Indragiri	5387±527	21.8±4.7	174	1184±313	26.7±9.4	54.2±14.2	67.0±2.0
Siak	8165±528	22.0±4.7	87	684±76	39.6±9.7	37.5±7.5	48.6±1.1
Lupar	884±148	26.5±9.3	186	197±86	0.92±0.8	0.83±0.0	47.4±21.0
Saribas	769±29	17.0±13.6	78	44±11	0.44±0.1	0.19±0.0	30.6±5.6
Average							**53.3±6.5**

monthly averages from six rivers, has a relatively small standard error and is similar to the 45-60% that was reported as the global average in the IPCC report, as mentioned before. Therefore, we may assume that this percentage is also a representative value for river outgassing in Southeast Asia.

3.3.3 CO_2 fluxes and peat coverage in Southeast Asia

As the data of this study is limited to a peat coverage of 21.9%, the lateral DOC exports of 95.7 g C m^{-2} yr^{-1} for disturbed peat and 61.7 g C m^{-2} yr^{-1} for pristine peat, as determined in rivers on Borneo by Moore et al. (Moore et al. 2013), were used to extend the dataset to 100% peat coverage. Based on the fact that carbon leaching equals the sum of CO_2 outgassing and riverine DOC export, this DOC export yield for 100% peat coverage was then converted to CO_2 yield by assuming a river outgassing of 53.3±6.5 % as found in the Southeast Asian rivers. This results in CO_2 yield for 100% peat coverage of 109.2 g C m^{-2} yr^{-1} (disturbed) and 70.5 g C m^{-2} yr^{-1} (pristine). Knowing that 90% of Southeast Asian peatlands are disturbed and 10% pristine (Miettinen & Liew 2010), the CO_2 yield for 100% peat coverage amounts to 105.3±27.6 g C m^{-2} yr^{-1}. This ratio for disturbed and pristine is naturally accounted for in the in situ river measurements, assuming an even distribution.

The lateral DOC export of 95.7 g C m^{-2} yr^{-1} and the net ecosystem C loss of disturbed peatlands of 433 g C m^{-2} yr^{-1} derived from eddy covariance measurements (Hirano et al. 2007) together amount to 529 g C m^{-2} yr^{-1}. Including the river outgassing flux of 109.2 g C m^{-2} yr^{-1}, which accounts for a 20% increase, raises the net ecosystem C loss to a total of 638 g C m^{-2} yr^{-1} (net C source).

The extent of peat coverage in the investigated rivers differs in each catchment and correlates with the DOC and CO_2 yield, emphasizing the importance of peat as DOC and CO_2 source (Figure 3.5). The correlation found between peat coverage and CO_2 yield shows that the

correlation initially appears linear, but levels off after a peat coverage of 25%, which indicates that the rate of pCO_2 production declines with increasing peat coverage. This may be attributed to a limitation of bacterial production as a consequence of the low pH caused by the acidic organic environment (Borges et al. 2015) or oxygen depletion (this study, (Rixen et al. 2008; Borges et al. 2015)). Based on the peat coverages and respective CO_2 yields, the annual CO_2 fluxes were interpolated for Indonesia, Malaysia and Southeast Asia (Table 3.4) using the regression.

As a whole, Southeast Asia releases 66.9±15.7 Tg C yr^{-1} through river outgassing, of which the majority is emitted by Indonesia with 53.9±12.4 Tg C yr^{-1}. This is due to the fact that Indonesia holds 83% of Southeast Asian peatlands in addition to a large land surface area. River outgassing in Malaysia amounts to 6.2±1.6 Tg C yr^{-1}. Although no CH_4 measurements were taken in the river, CH_4 fluxes are not considered to play a significant role in river carbon emissions. This is supported by CH_4 fluxes from the Saribas and Lupar estuaries, which emit 27±24 t CH_4-C yr^{-1} and 84±24 t CH_4-C yr^{-1}, respectively, and are a minute fraction of the estuary CO_2 fluxes 0.09±0.08 and 0.31±0.09 Tg C yr^{-1} (Müller 2015). CH_4 fluxes from peat soils are with 0.02 g C m^{-2} yr^{-1} also much lower than those of peat soil CO_2 fluxes 250 g C m^{-2} yr^{-1} (Couwenberg et al. 2010). Considering that the data is collected during the transitional stages during the year with respect to precipitation, the mean values represent a suitable

Table 3.4 CO_2 yields and fluxes. The errors of the CO_2 yield and flux represent the best/worst case deviation.

Location	*Peat coverage (%)*	*Catchment area (km^2)*	*CO_2 yield (g C m^{-2} yr^{-1})*	*CO_2 flux (Tg C yr^{-1})*	*Peat impact (%)*
Musi	3.5	56,931	11.8±5.0	0.67±0.28	83.5
Batanghari	5.0	44,890	8.6±1.8	0.39±0.08	77.7
Indragiri	11.9	17,968	36.1±9.7	0.65±0.17	95.1
Siak	21.9	10,423	43.1±8.3	0.45±0.09	96.3
Lupar*	30.5	6,541	61.5±13.0	0.30±0.04	97.7
Saribas*	35.5	2,149	69.0±14.6	0.11±0.01	98.1
Malaysia	**7.6**	**327,291**	**19.1**±4.8	**6.2**±1.6	90.1
Indonesia	**11.9**	**1,919,317**	**28.1**±6.5	**53.9**±12.4	93.7
SE Asia**	**10.5**	**2,652,370**	**25.2**±5.9	**66.9**±15.7	92.8

*The Lupar and Saribas stations were located upstream from the peatland area; their data are therefore typical for a peat coverage of 0%. With the Lupar pCO_2 measurements at 0% peat coverage, the correlation between annual CO_2 yield and peat coverage was derived (Figure 3.5b). The Saribas, having only one (seasonal) data point, was excluded from this correlation, but is shown in grey in Figure 3.5b. The correlation was then used to estimate the CO_2 yields and fluxes of the Lupar and Saribas with respect to their peat coverages of 30.5 and 35.5, respectively, in their catchments.

**Southeast Asia is defined here as Malaysia, Indonesia, Brunei and Papua New Guinea(Hooijer et al. 2006). Their peat coverages and catchment areas are derived from Hooijer et al. (Hooijer et al. 2006) and Miettinen (Miettinen et al. 2012). Peat coverage and catchment areas of the rivers were derived using an ArcGIS relief model and FAO Soil map of the world (see Methods).

yearly average. Although extreme events such as droughts or heavy rainfall have not been measured, their influence will not alter the estimated CO_2 fluxes significantly. As discussed earlier, the effect of increased discharge due to high water saturated peatlands dilutes the DOC concentration, which dampens the effect of enhanced discharge (Clark et al. 2008; Clark et al. 2007; Worrall et al. 2006). Therefore, a decrease is expected in DOC and hence pCO_2 concentrations during extreme events in peatland areas. In non-peat areas, enhanced precipitation will increase DOC leaching and hence, DOC and pCO_2 concentrations in the river waters. However, as seen in Table 3.4, the impact of peat on the CO_2 fluxes, wherein the impact is defined as the share of CO_2 emissions from peatlands expressed in percentage, is much larger than that of non-peat areas. The regression indicates that non-peat areas have a CO_2 yield of 2.0 g C m^{-2} yr^{-1} and only contribute 7.1% (4.8 Tg yr^{-1}) to the CO_2 fluxes in Southeast Asia, as opposed to 92.8% (62.1 Tg yr^{-1}) from peatlands (Table 3.4). Assuming a case of heavy rainfall, wherein the CO_2 yield would double to 4.0 g C m^{-2} yr^{-1}, would increase the CO_2 flux from non-peat areas to 9.6 Tg yr^{-1}, but would not significantly increase the total annual CO_2 fluxes for Southeast Asia. Additionally, the effect of the large peat impact and that CO_2 fluxes from peatlands will decrease due to dilution from increased discharge, will outweigh the increased CO_2 flux of non-peat areas, thereby maintaining a steady or even decreased CO_2 flux during extreme rainfall. Therefore, our annual CO_2 flux estimates can be assumed to be representative for Southeast Asia, wherein fluctuations due to extreme events are accounted for in the error range.

3.3.4 Study comparison

For data comparison, the CO_2 flux and piston velocity estimates of Raymond et al. (Raymond et al. 2013) were used, who have calculated global inland water CO_2 effluxes by means of a global set of calculated piston velocities, pCO_2 values (Hartmann et al. 2011) and COSCAT areas (Coastal Segmentation and related CATchments). These COSCAT areas are characterized by their coastal segment limits and length and by catchment characteristics, such as runoff direction and physiographic units (Meybeck et al. 2006). Raymond et al. (Raymond et al. 2013) assigned an average piston velocity and an average pCO_2 value to each of these COSCATs from which they estimated the CO_2 yield per m^2 land per year. Several of these COSCAT areas, ten of which are relevant for our study area, overlap Southeast Asia and are summarized in Table 3.5. Based on the COSCATs in Table 3.5 the pCO_2, K_{CO2} and CO_2 yield were averaged for Malaysia (row 1 – 3), Indonesia (row 2 – 8) and Southeast Asia

Table 3.5 pCO_2 concentrations, piston velocities and CO_2 yields per COSCAT area.

Row Nr.	*Country covered by COSCAT*	*COSCAT Code*	*pCO_2 (µatm)*	*K (cm h^{-1})*	*CO_2 yield (g C m^{-2} yr^{-1})*
1	Malaysia/Brunei	1328	11760	39.58	148.10
2	Malaysia/Indonesia	1329	11772	36.67	122.90
3	Malaysia/Indonesia	1335	7404	65.83	174.00
4	Indonesia	1330	11265	40.83	111.00
5	Indonesia	1333	458	58.33	0.20
6	Indonesia	1334	10497	87.08	124.40
7	Indonesia/Papua New Guinea	1416	292	66.25	-1.70
8	Indonesia/Papua New Guinea	1401	372	143.33	-3.00
9	Papua New Guinea	1402	435	31.67	1.00
10	Papua New Guinea	1403	1269	64.17	7.30

(row 1 – 10), after which the corresponding CO_2 flux was calculated and compared to our data (Table 3.6). In addition, an indirect comparison was made based on recent estimates by Lauerwald et al. (Lauerwald et al. 2015) (Table 3.6). Although no data is available for Southeast Asia, they do provide estimates of pCO_2 concentrations and piston velocities for the tropical zone (<25°), which we used to predict their CO_2 fluxes in Southeast Asia (Table 3.6), assuming a river surface coverage as determined in our study (Table 3.1). The comparison of Raymond et al. (Raymond et al. 2013) with our data reveals that the CO_2 flux estimates for Indonesia and Southeast Asia by Raymond et al. (Raymond et al. 2013) are almost three times higher than those found in this study with 144.7 Tg C yr^{-1} and 181.5 Tg C yr^{-1}, respectively. The Malaysian estimate peaks almost eight-fold with 48.8 Tg C yr^{-1}. These overestimations were already anticipated by Raymond et al. (Raymond et al. 2013) and are explained by the small number of calculated CO_2 values they had available in these

Table 3.6 Study comparison of averaged pCO_2 concentrations, piston velocities, CO_2 yields and estimated CO_2 fluxes. Studies include that of Raymond et al.(Raymond et al. 2013), Lauerwald et al. (Lauerwald et al. 2015) and this study. Errors indicate the standard error ((Raymond et al. 2013)), largest deviation from the mean ((Lauerwald et al. 2015)) and best/worst case deviation (this study).

Location	*Study*	*pCO_2 (µatm)*	*K (cm h^{-1})*	*CO_2 yield (g C m^{-2} yr^{-1})*	*CO_2 flux (Tg C yr^{-1})*
Malaysia	(Raymond et al. 2013)	10312±1781	47.4±11.4	148.33±18.1	48.8±5.9
	*(Lauerwald et al. 2015)	3188±575	24.6±2.9	15.1±4.9	4.9±1.6
	**This study	4369± 393	21.8±11.5	19.6±4.0	6.2±1.6
Indonesia	(Raymond et al. 2013)	6009±4554	59.9±11.3	75.4±30.5	144.7±54.5
	*(Lauerwald et al. 2015)	3188±575	24.6±2.9	17.3±5.6	33.1±10.7
	**This study	5535±498	21.9±4.71	26.6±4.6	53.8±12.4
SE-Asia	(Raymond et al. 2013)	5552±3943	63.4±19.6	68.4±24.4	181.5±64.8
	*(Lauerwald et al. 2015)	3188±575	24.6±2.9	14.4±5.4	44.6±14.4
	**This study	5155±464	21.8±7.0	24.5±4.4	66.8±15.7

* CO_2 yield and fluxes for Lauerwald et al. (Lauerwald et al. 2015) are estimated based on the river surface areas defined in our study (Table 2).

** Errors for pCO_2 are based on the average standard error of 9% as found for the studied rivers.

COSCATs. Moreover, compared to our findings, their piston velocities appear to be largely overestimated (Table 3.5) and are mainly responsible for the resulting CO_2 flux overestimations of Raymond et al. (Raymond et al. 2013). As for Lauerwald et al. (Lauerwald et al. 2015), their data for the tropical zone (<25°) include piston velocities similar to ours, but show pCO_2 concentrations that are 21%, 40% and 35% lower in Malaysia, Indonesia and Southeast Asia, respectively, and result in lower CO_2 emissions.

3.3.5 Explanatory arguments for moderate fluxes

The overall statement of this study conveys that SE-Asia is in fact not such a river CO_2 outgassing hotspot as one could assume due to the carbon enriched peat soils (Table 3.4). Even temperate zones, with a CO_2 yield of 18.5 g C m^{-2} yr^{-1} (based on an average CO_2 yield of 2370 g C m^{-2} yr^{-1} (Butman & Raymond 2011) of river surface area, converted to m^2 catchment area with a river coverage of 0.78% as estimated for SE-Asia) are close to the CO_2 yield of 25.2 g C m^{-2} yr^{-1} of SE-Asia. CO_2 yields from other tropical river systems, such as the Amazon are much larger with 120±30 g C m^{-2} yr^{-1} (Richey et al. 2002) , and show that CO_2 outgassing from SE-Asian rivers is rather moderate. The main reason for these moderate fluxes is the relatively short residence time (Rixen et al. 2008) of DOC in the river water due to the location of the peatlands near the coast, which are the main source of DOC. Limitation of bacterial production, as a consequence of the low pH caused by the acidic organic environment (Borges et al. 2015), oxygen depletion (this study, (Rixen et al. 2008; Borges et al. 2015)), or the refractory nature of DOC (Alkhatib et al. 2007; Rixen et al. 2008; Castillo et al. 2003), potentially also contributes to the moderate CO_2 fluxes as this decelerates decomposition, especially with increasing peat coverage.

In conclusion, this study shows that river outgassing fluxes in SE-Asia are in fact moderate and, in line with the 5th Assessment IPCC report, suggest that approximately 53.3±6.5% of carbon entering the freshwater system is decomposed and emitted back to the atmosphere as CO_2. Globally there are three tropical regions, of which Africa (Borges et al. 2015) and Amazonia (Richey et al. 2002) are significantly important contributors to the river outgassing budget. However, due to the fact that the main source of DOC is located near the coast, which further shortens the residence time of DOC in rivers, Southeast Asia is a moderate emitter and global river outgassing estimates can therefore be scaled down. In future assessments, it needs to be considered that rivers function in a different way with respect to discharge, depending on residence time of DOC in the river and the soil type as it strongly affects the DOC leaching and consequently respiration and CO_2 emission.

3.4 End notes

3.4.1 Acknowledgements

We would like to thank all scientists and students from the University of Pekanbaru for the fieldwork assistance and the captain and crew of the Matahari-ku ship for their support. We also want to thank the scientists and students from the University of Kuching. Maps were drawn using the Generic Mapping Tools (Wessel & Smith 1998) and calculations were executed with Python software, version 2.7 (van Rossum 2007). We are also grateful to the Federal German Ministry of Education, Science, Research and Technology (BMBF, Bonn grant number 03F0642–ZMT).

Furthermore, we would like to thank the Sarawak Biodiversity Center for permission to conduct research in Sarawak waters (Permit No. SBC-RA-0097-MM). We are grateful to Moritz Müller for his contribution to this manuscript. We thank Nastassia Denis and all scientists and students from Swinburne University and the University of Malaysia Sarawak who were involved in the sampling campaigns in Malaysia, as well as Lukas Chin and the crewmembers of the SeaWonder for their support. Dr. Aazani Mujahid (University of Malaysia Sarawak) is acknowledged for her comprehensive organizational support. The expeditions to Malaysia were funded by the University of Bremen through the "exploratory project". Moritz Müller

3.4.2 Author contributions

T.R. and W.S.P. designed the study. D.M., T.W. and M.M. performed the Sarawak field data collection and D.M. performed the analysis. A.B. performed the Sumatra field data collection and analysis in 2009 and F.W. in 2012 and 2013. F.W. led the writing of the paper. All authors discussed results and commented on the manuscript.

IV

Carbon leaching from tropical peat soils and consequences for carbon balances

Tim Rixen[1,2]*, Antje Baum[1], Francisca Wit[1], Joko Samiaji[3]

1) *Leibniz Center for Tropical Marine Ecology, Fahrenheitstraße 6, 28359 Bremen, Germany*
2) *Institute of Geology, University of Hamburg, Bundesstraße 55, 20148 Hamburg, Germany*
3) *Faculty of Fishery and Marine Science, University of Riau, Jl. Simpang Panam Km 12.5, 28293 Pekanbaru, Riau, Indonesia*

Keywords: tropical peat soil, degradation, secondary forest, carbon loss, Sumatra, Indonesia

Published in *Frontiers in Earth Science*

Citation: Rixen T, Baum A, Wit F and Samiaji J (2016) Carbon Leaching from Tropical Peat Soils and Consequences for Carbon Balances. *Front. Earth Sci.* 4:74. doi: 10.3389/feart.2016.00074

4.1 Abstract

Drainage and deforestation turned Southeast (SE) Asian peat soils into a globally important CO_2 source, because both processes accelerate peat decomposition. Carbon losses through soil leaching have so far not been quantified and the underlying processes have hardly been studied. In this study, we use results derived from nine expeditions to six Sumatran rivers and a mixing model to determine leaching processes in tropical peat soils, which are heavily disturbed by drainage and deforestation. Here we show that a reduced evapotranspiration and the resulting increased freshwater discharge in addition to the supply of labile leaf litter produced by re-growing secondary forests increase leaching of carbon by ~200%. Enhanced freshwater fluxes and leaching of labile leaf litter from secondary vegetation appear to contribute 38% and 62% to the total increase, respectively. Decomposition of leached labile DOC can lead to hypoxic conditions in rivers draining disturbed peatlands. Leaching of the more refractory DOC from peat is an irrecoverable loss of soil that threatens the stability of peat-fringed coasts in SE Asia.

4.2 Introduction

Pristine peat swamp forests are rare with only circa 10% left on the islands of Borneo and Sumatra (Miettinen and Liew, 2010). The remaining disturbed peat soils are drained, covered by plantations, shrubs and secondary forests, and are characterized by a heavily altered hydrological cycle. As seen in a river catchment on Borneo, deforestation decreases evapotranspiration and thereby increases freshwater fluxes as well as the riverine export of DOC (Moore et al., 2013). Depending on the soil types in their catchments, DOC concentrations in rivers differ in their response to changes in freshwater fluxes, which are mostly linked to precipitation. In rivers draining organo-mineral soils, enhanced freshwater fluxes raise DOC concentrations, whereas DOC concentrations in high-latitude rivers draining peat soils do not respond to changing precipitation rates until flooding occurs at which point the surface runoff dilutes the DOC concentration in the river (Clark et al., 2008; Moore and Jackson, 1989).

Processes controlling carbon leaching from tropical peat soils have so far not been studied. Approximately half of all tropical peat soils are located in Indonesia ($0.207\ 10^{12}$ m^2) and mostly in the coastal plains of the islands of Irian Jaya, Borneo, and Sumatra (Page et al., 2011). This study uses data obtained during nine expeditions to the Siak and five other major

rivers draining peatlands in Central Sumatra in combination with a mixing model with three experiments, each representing certain environmental conditions, in order to quantify carbon leaching from Indonesian peat soils and to simulate the processes responsible for the carbon leaching (Figure 4.1, Table 4.1).

4.3 Methods

4.3.1 Study area and expeditions

The investigated rivers were the Rokan, Siak, Kampar, Indragiri, Batang Hari and Musi (Figure 4.1). All rivers originate in the Barisan mountains, pass through the Northeastern lowlands and discharge into the Malacca Strait. On their way to the ocean all rivers cut through peat soils, which are located in the coastal flat plains and cover 3.5% to 30.2% of their catchments (Table 4.1). The Siak river, which was investigated most intensively over the years, originates at the confluence of its two headstreams, S. Tapung Kanan and S. Tapung Kiri (Figure 4.1b). Its main tributary is the Mandau river. The S. Tapung Kiri drains non-peatlands, whereas the S. Tagung Kanan, the Mandau, and the Siak cut through peatlands covering in total 21.9% of the Siak catchment (Table 4.1). Expeditions one to five to the Siak

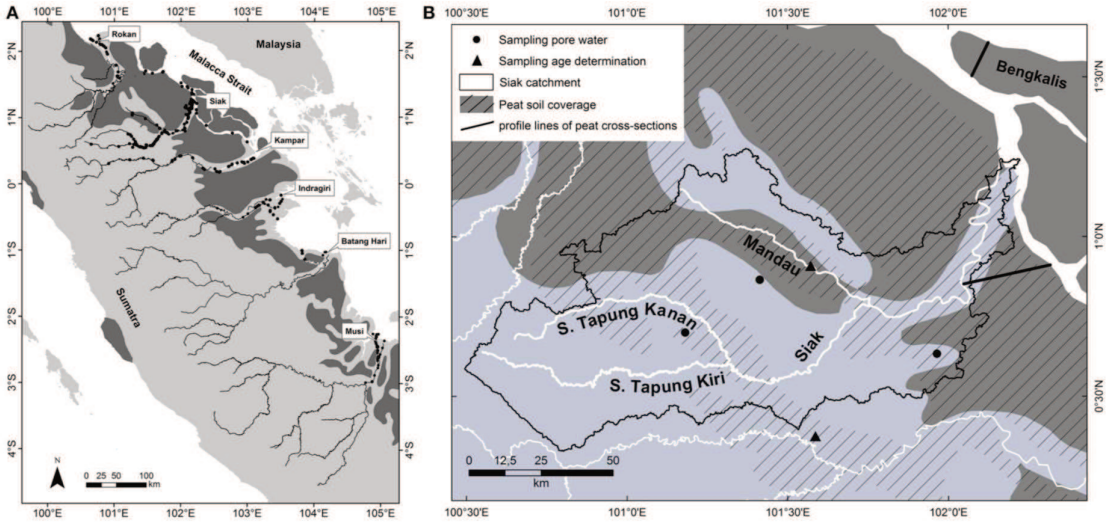

Figure 4.1 Study area. a) Major rivers including sampling sites (black circles) and peatlands (dark grey) in central Sumatra according to the digital soil map of the world (FAO, 2003). b) A scale-up showing the Siak catchment in more detail. Black circles indicate the sites at which pore water samples were taken. Triangles mark the sites were water (DOC) and soil (peat) samples for radiocarbon age determinations were taken. The black lines are profile lines of cross-sections through the Siak and Bengkalis peat domes as shown in **Figure 4.9**. The striped areas show the peatland distribution according to reference (Laumonier, 1997) which deviates from those of the FAO (dark grey). The map and scale-up were created using ArcGIS 9.3.1 software by Esri.

Table 4.1 Rivers and expeditions, as well as riverine DOC end-member concentrations, monthly precipitation rates (Schneider et al., 2014) averaged for the catchment area of the respective rivers (Table 4.2), and the DOC yields calculated according to equation 1. Results obtained for each river during all expeditions were presented as "mean expedition". Additionally, DOC yields were calculated by using the mean riverine DOC end-member concentration and the precipitation rates averaged for the entire period of observations between 1987 and 2013. The "mean precipitation" is the average of all precipitation rates determined within the catchments of all six rivers.

River	*Expedition*		*DOC conc.*	*Precipitation*	*DOC yield*
	Month	*Year*	*[µM]*	*[mm]*	*[g C m^{-2} $year^{-1}$]*
Siak	9	2004	2187± 040	250±42	49±15
Siak	8	2005	2159±136	426±55	82±24
Siak	3	2006	1633± 055	216±48	32±11
Siak	11	2006	1849± 022	244±67	40±15
Siak	3	2008	2205± 056	409±43	81±22
Siak	10	2009	2632±164	317±42	75±22
Siak	4	2013	633± 088	205±38	12±04
Peat coverage	*mean (expedition)*		1900±593	295±50	53±25
21.9%	*1986-2013*			232±88	39±22
Rokan	4	2006	833± 50	300±04	22±06
Rokan	3	2008	728± 54	438±15	29±07
Peat coverage	*mean (expedition)*		781± 53	369±69	25±08
30.2%	*1986-2013*			250±96	17±08
Kampar	4	2006	1236± 51	290±57	32±10
Kampar	11	2008	1325± 39	281±37	33±09
Peat coverage	*mean (expedition)*		1280±44	285±5	33±08
22.4%	*1986-2013*			248±97	28±13
Indragiri	3	2008	846±159	366±47	28±09
Indragiri	10	2009	774± 71	272±83	19±08
Peat coverage	*mean (expedition)*		810± 36	319±47	23±07
11.9%	*1986-2013*			209±82	15±07
Batang Hari	10	2009	377± 10	214±58	7±03
Batang Hari	10	2012	241±01	249±54	5±02
Batang Hari	4	2013	*314±00	190±42	5±02
Peat coverage	*mean (expedition)*		311± 055	218±25	6±02
5%	*1986-2013*			199±74	6±03
Musi	11	2008	423±21	436±075	17±05
Musi	10	2012	*264±00	249±046	6±02
Peat coverage	*mean (expedition)*		344±80	343±093	11±05
3.5%	*1986-2013*			223±105	7±04
			Mean precipitation rate	227±019	

* Samples were taken at a salinity of approximately zero; no samples were taken in the estuary

were land-based during which smaller speedboats were used, whereas we chartered ocean-going vessels for expeditions seven and nine.

4.3.2 DOC sampling and analysis

In the rivers DOC samples were taken using a Niskin bottle at a water-depth of approximately 1 m. After sampling, DOC samples were immediately acidified with phosphoric acid to a pH≤2 and stored cool and dark until analysis. DOC samples were analyzed by means of high temperature catalytic oxidation using a Dohrmann DC-190 and a Shimadzu TOC-V_{CPH} total Organic Carbon Analyzer. Before injection into the furnace, the samples were decarbonated by purging with oxygen. The evolving CO_2 was purified, dried and detected by a non-dispersive infrared detection system.

Groundwater samples for the determination of DOC concentrations were taken with a pore-water-lance during the expedition in March 2008. On top of the 4 mm thick pipe a syringe was attached to extract pore water from the soil. The obtained samples were preserved and analyzed as the river samples.

4.3.3 DOC age determination

The age determination of peat and water samples was conducted at the Leibniz Laboratory for Radiometric Dating and Isotope Research in Kiel, Germany, in 2007. Organic fragments of the peat sample were inspected and collected under a light microscope and pre-treated based on an acid-alkali-acid cleaning with diluted hydrochloric (1%) and sodium hydroxide (1%). The extracted organic material (humin acid fraction) was precipitated, washed and dried. The river water was pre-treated for dating by filtering and freeze-drying the sample. River water and peat samples were combusted in evacuated, flame sealed quartz tubes containing copper oxide at 900°C. The evolved CO_2 was reduced to graphite with H_2 on an iron catalyst. The resulting graphite-iron powder was pressed into aluminum target holders for the ion sputter source with the help of a pneumatic press. The ^{14}C concentration of the sample is calculated by comparing the $^{14}C/^{12}C$ ratio of each sample, determined by AMS, with those of an international standard (NIST Oxalic Acid standard 2 - OxII). Radiocarbon concentrations are reported in percent Modern Carbon (pMC) with ±1-σ measurement uncertainty. 100 pMC is defined as the radiocarbon concentration of the atmosphere in 1950 AD (Stuiver and Polach, 1977).

4.3.4 DOC end-members, yields and exports

In order to estimate DOC exports from the rivers into the ocean, DOC end-member concentrations were determined. These DOC end-member concentrations were derived from the correlation between DOC concentrations measured in the river estuary and salinity, wherein the zero salinity y-intercept defined the riverine DOC end-member concentration (Table 4.1, Figure 4.4b). As DOC respiration and its release from e.g. phytoplankton could lead to deviations from the mixing line, which affect the regression equation and thus the calculated DOC end-member concentrations, the standard deviation of the y-intercept was obtained from a least square fit in order to achieve a quantitative error estimate (Bevington and Robinon, 1992). The calculated DOC end-member concentrations were subsequently multiplied by the river discharge in order to obtain the riverine DOC exports into the ocean. The DOC export normalized to the respective catchment area is the DOC yield, which was calculated as the product of the freshwater flux (FW_{flux}) and the DOC end-member concentration (Eq. 2).

$$FW_{flux}\ [L\ m^{-2}] = (Precipitation * (1 - Evapotranspiration)) \quad (1)$$

$$DOC\ yield\ [g\ m^{-2}\ yr^{-1}] = FW_{flux} * DOC_{end\text{-}member} \quad (2)$$

4.3.5 Precipitation, evapotranspiration and freshwater flux

The 1x1 degree gridded GPCC-rainfall data (Global Precipitation Climatology Centre, Landsurface Monitoring Product 1.0) (Schneider et al., 2011) were used to calculate the precipitation rates and their standard deviations in the river catchments during our expeditions (Table 4.1, Table 4.2).

Table 4.2 Rivers and coordinates used to obtain precipitation rates from the GPCC (Schneider et al., 2011)

River	*Latitude*	*Longitude*
Rokan	0°- 2°N	100°-101°E
Siak	0° - 2°N	100°-102°E
Kampar	1°S – 1°N	100°-102°E
Indragiri	0 – 1°S	101°-104°E
Batang Hari	1°- 3°S	101°-104°E
Musi	2°- 5°S	102°-105°E

The full GPCC data covering the period between 1986 and 2013 was used to calculate the mean precipitation rate for the individual catchments. Precipitation rates and river discharges measured on the island of Borneo showed an annual mean evapotranspiration (ET) of 37.9% of disturbed and 67.7% of pristine peat lands (Moore et al., 2013). These values fall almost in the range of 41 - 72% determined for Indonesia (Baum et al., 2007; Kleinhans, 2003; Kumagai et al., 2005) suggesting a mean ET of 56.5 ±15.5%. Since already 90% of all peatlands on Sumatra and Borneo were disturbed in 2008 (Miettinen and Liew, 2010) we used an evapotranspiration of 37.9% and considered an error range of 15.5% for calculating the freshwater flux.

4.3.6 River catchments and peat coverage

An elevation model based on 30 arc-second data obtained from the shuttle radar topographic mission (SRTM, USGS, 2004) was established by using the geographical information system ArcGis with the extension ArcHydro in order to identify the individual river catchments and calculate the respective catchment areas. The peat area was obtained from the "Digital soil map of the world" (version 3.6, scale 1:5000000, resolution 3'x3'; FAO, 2003) and combined with the derived catchments to quantify the coverage in percentage (Table 4.1).

4.3.7 Mixing model principle

In order to better understand the processes controlling the DOC concentrations in rivers, a mixing model was produced (Figure 4.2). Since the majority of the available data was collected from the Siak, the mixing model was first of all developed based on data from the Siak. Later on the derived results were extrapolated and compared to data obtained from the other studied rivers.

In the model, the simulated DOC concentrations in the Siak were calculated as the product of mixing of three different water types: i) groundwater from peatlands, ii) surface runoff from peatlands and iii) freshwater discharges from parts of the catchment that are not covered by peatlands (non-peatlands), which are largely drained by the S. Tapung Kiri (Figure 4.1b, Figure 4.2). Freshwater discharges were calculated separately for the peat area and non-peat area within the catchment. The freshwater discharge from the peat area was divided into groundwater discharge and surface runoff based on the water storage capacity of the acrotelm, which is the upper, partly water-saturated soil horizon in which groundwater levels respond to varying precipitation rates (Holden, 2005). Acrotelm overflow and factors influencing

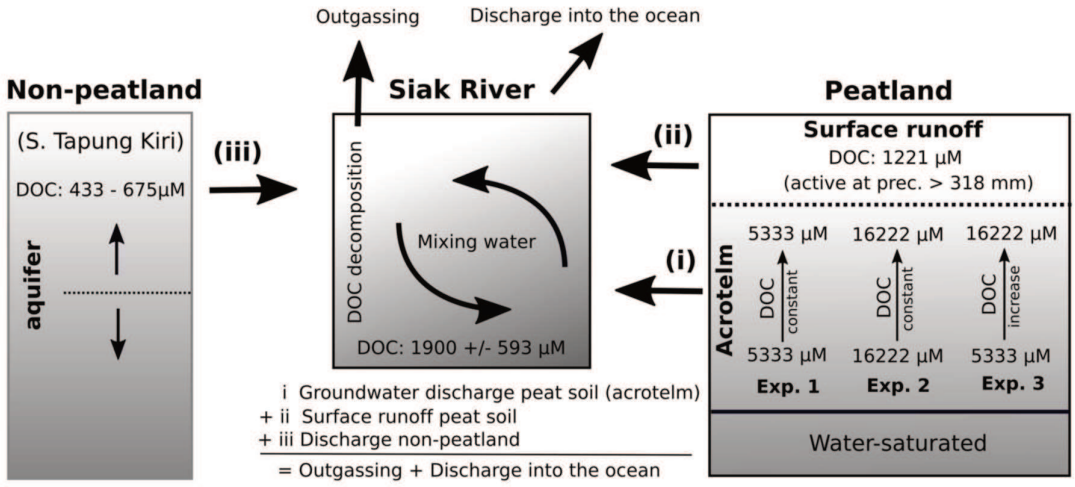

Figure 4.2 Schematic of the model structure with the three water types (i, ii, and iii) that mix within the Siak. The source waters originate from the non-peatlands, which are to a large extent drained by the S. Tapung Kiri (see **Figure 4.1**), and from the peatlands. In peatlands it was further distinguished between surface runoff and groundwater discharge from the acrotelm. Groundwater DOC concentrations were varied during the three experiments. Based on our observations the DOC concentration of the surface runoff was set to 1,221 µM and those in S. Tapung Kiri tended to increase from 433 to 675 µM with increasing precipitation rates (**Figure 4.3**,**Table 4.3**). DOC decomposition and outgassing in addition to DOC discharges into the ocean balance DOC inputs along with the source waters. More detailed information is given in the Supplementary Material.

DOC concentrations in the groundwater, as well as the DOC concentrations for the water types will be discussed in more detail in the following sections.

Besides the mixing of the different water types, the decomposition of DOC is the second factor controlling DOC concentrations in the Siak and was studied during a DOC decomposition experiment (Rixen et al., 2008). The results of this experiment, which included the photochemical and bacterial degradation of DOC, showed that roughly 27% of the DOC was degradable within a period of two weeks, whereas the remaining larger fraction was refractory on that respective time scale. The obtained equation, describing the DOC decomposition as a function of DOC concentration, was implemented into a box diffusion model that satisfactorily reproduced the oxygen concentrations in the Siak river, which are mainly controlled by the respiration of the labile DOC. In addition to the DOC concentration, the DOC decomposition equation within our mixing model also depends on time. The residence time of water within the Siak was derived from freshwater discharges and a fixed river profile. Accordingly, the residence time decreased with an increasing freshwater discharge, which in turn lowers the DOC decomposition in the rivers because there was less time to decompose DOC. Simulated DOC exports into the ocean finally result from the difference between the DOC inputs from the water types and the DOC decomposition in the

river. The simulated DOC concentrations were then compared to the DOC end-member concentrations obtained from the correlation between the measured DOC concentrations in the Siak estuary and the salinity.

4.4 Results

The highest so far reported DOC concentrations in the Siak catchment were measured during our expedition in March 2008 within groundwater obtained from peat soils (Figure 4.1). The DOC groundwater concentrations varied widely from 5,333 µM to 16,222 µM (Table 4.3). The lowest DOC concentrations in peat areas were measured with 1221.6 µM in surface runoff water (Table 4.3).

In the Siak the DOC concentration increased from approximately 500 to 1300 and from 1300 to 1900 μM around the S. Tapung Kanan/Kiri and Mandau junctions because S. Tapung Kanan and the Mandau are rivers draining relatively large peat areas and thus are enriched in DOC (Baum et al., 2007; Rixen et al., 2008). During our expeditions the DOC concentrations in the S. Tapung Kiri, which drains the non-peat areas within the Siak catchment, varied between 344 µM and 675 µM. DOC concentrations < 675 µM where only measured during expeditions at which the precipitation were < 300 mm, which might indicate that DOC concentrations decrease with decreasing precipitations rates as observed in many other rivers draining mineral soils (Figure 4.3). In the estuary, decreasing DOC concentrations correlating to increasing salinities indicate mixing between DOC-rich Siak water and DOC-poor ocean water (Figure 4.4b). During our expeditions in the Siak catchment, the DOC end-member concentrations varied between 636±88 and 2632±164 µM and increased with increasing precipitation rates up to 318 mm (Figure 4.5). After precipitation rates exceeded 318 mm the DOC concentrations dropped. The lowest DOC end-member concentrations were measured during our expedition in April 2013. Although this value is within the range of DOC end-member concentrations determined in the other studied rivers (Table 4.1) it represents a real exception for the Siak. The low DOC concentrations in the Siak estuary which finally lead to the low DOC end-member concentrations were assumed to be caused by enhanced DOC respiration within an senescent plankton bloom that occurred in the estuary during our expedition (Wit et al., 2015).

Table 4.3 Ground and surface water concentrations as measured during the expedition in March 2008.

Latitude (°N)	*Longitude (°E)*	*Soil Depth*	*DOC (µM)*
0.857166	101.41310	5 cm	5333.0
0.851500	101.41313	5 cm	6391.3
0.699790	101.18108	5 cm	15962.7
0.699790	101.18108	5 cm	1850.9
0.633310	101.96431	5 cm	16221.9
0.634640	101.96493	5 cm	8016.3
0.740690	101.18069	surface water	1221.6

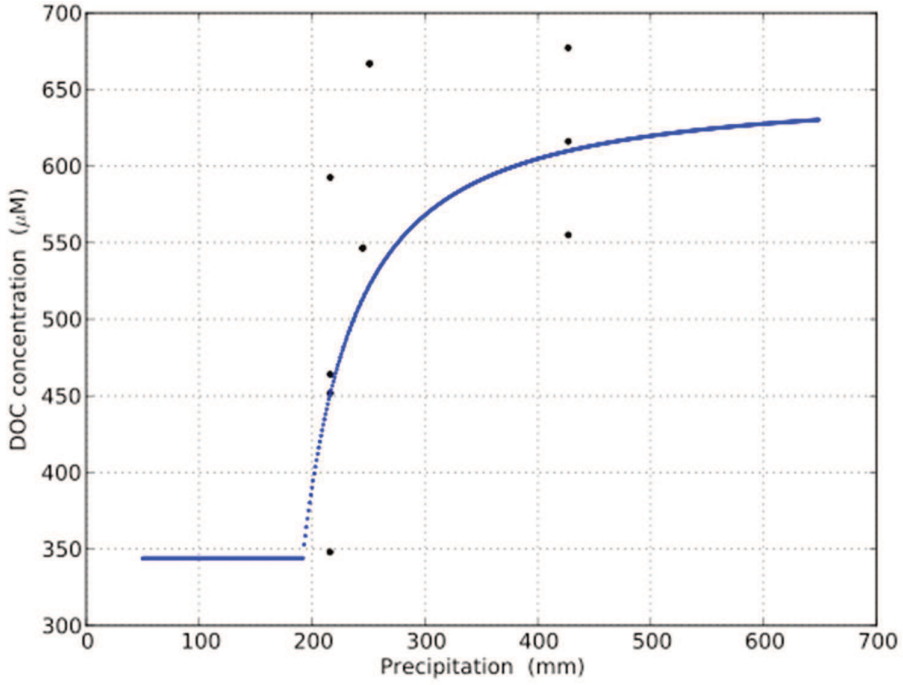

Figure 4.3 DOC concentrations versus precipitation rates. The circles indicate the DOC concentrations measured in the S. Tapung Kiri during our expeditions in March and September 2004, July 2005 and March 2006 and the blue curve are DOC concentrations derived from precipitation rates by using the equation: DOC_{Kiri} = (650 * (precipitation – 160)*1.22) / (60 + (precipitation – 160)*1.22).

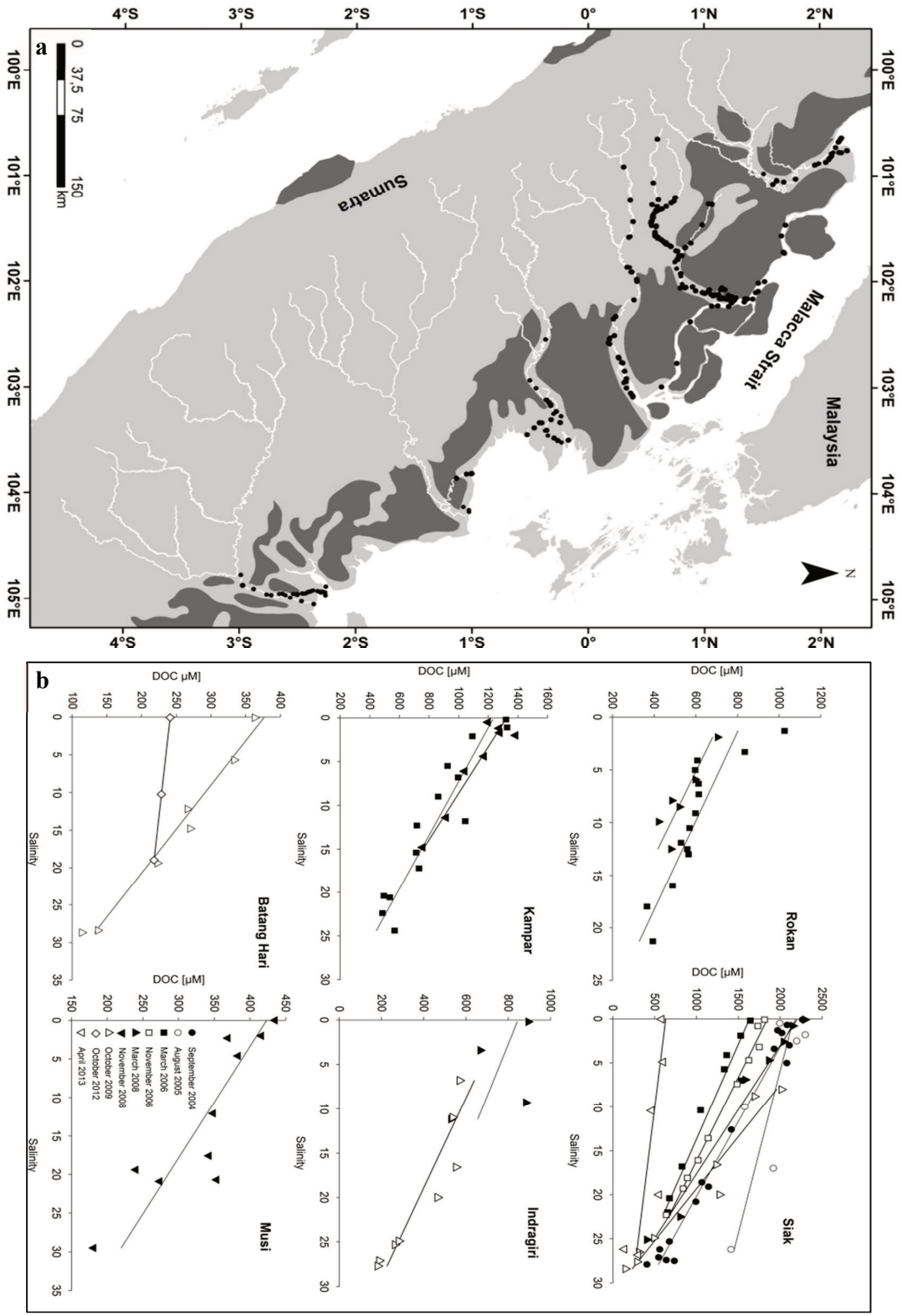

Figure 4.4 DOC sampling and salinity correlation. a) Working area and sampling sites at which DOC samples were taken and b) salinity versus DOC for the six Sumatran rivers.

4.5 Discussion

4.5.1 Acrotelm thickness

Due to the low DOC concentrations in the surface runoff water, flooding with a resulting acrotelm overflow is one explanation for decreasing DOC concentrations in Siak at high precipitation rates (Figure 4.5). A precipitation rate of 318 mm, beyond which the DOC concentrations decrease in the Siak, indicates accordingly the maximum water storage capacity of the acrotelm in the Siak catchment. In order to convert this maximum water storage capacity into acrotelm depth, evapotranspiration and pore volume need to be considered. The evapotranspiration of 37.9% would imply an acrotelm thickness of 19.7 cm if pore volume in peat soils would be 100% (318 * (1-0.379). Taking furthermore into account an organic matter density of 1 g cm^{-3} and a peat bulk density of 0.127 g cm^{-3} suggests a more realistic pore volume of 87.3 % (Warren et al., 2012) and results in an acrotelm thickness of 22.4 cm.

4.5.2 Leaching

In the Siak catchment the lower groundwater DOC concentrations of about 5,333 µM (Table 4.3) fall in the range of DOC concentrations measured in other peat soils (5,183 – 6,658 µM (Gandois et al., 2013). DOC groundwater concentrations of up to 16,222 µM are extremely high but can be caused by leaching of leaf litter produced by secondary forest plants within a couple of days (Yule and Gomez, 2009).

Contrary to secondary plants, leaves of endemic peat plants are more resistant to degradation (Lim et al., 2014; Treutter, 2006) and therefore less DOC is leached from endemic leaf litter. In DOC pore water profiles, such a reduced leaching is reflected in the absence of a pronounced DOC gradient (Gandois et al., 2013). DOC pore water profiles in soils with secondary vegetation are expected to show a strong gradient with higher DOC concentrations in the acrotelm top due to leaching of labile leaf litter and lower DOC concentrations at the acrotelm base where peat leaching dominates. This is however an expected observation that in the future needs to be proved by data, but in order to test whether such a soil DOC gradient helps to better explain the DOC end-member concentrations in the Siak, sensitivity experiments were carried out with our mixing model.

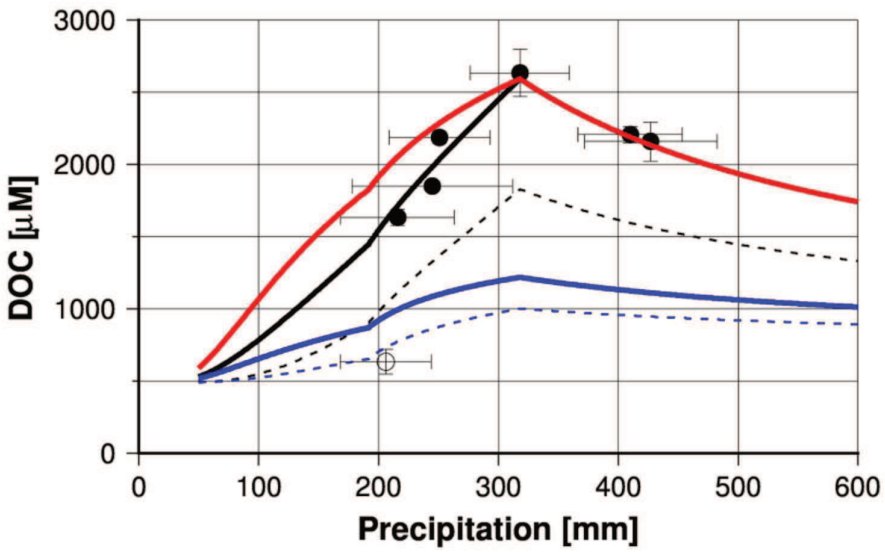

Figure 4.5 Mixing model DOC end-member results. DOC end-member concentrations obtained from data measured between 2004 and 2009 (black circles) and in 2013 (open circles) in the Siak (**Table 4.1**). Blue, red, and black lines show DOC end-member concentrations calculated by the model experiments number one (5,333 µM), two (16,222 µM) and three, respectively. The broken lines show also results of the experiment number one and three but instead of an evapotranspiration rate of 37.9% for disturbed peat lands an evapotranspiration of 67.7% was used which is assumed to be characteristic for pristine peat swamps.

4.5.3 Numerical leaching experiments for the Siak

Possible effects of leaf litter and peat leaching on the DOC concentrations in the Siak were studied by performing three model experiments (Figure 4.2) and comparing the results with the riverine DOC end-members (Figure 4.5). In the first two experiments, groundwater DOC concentrations were considered to be constant as generally assumed for peatlands. With a DOC concentration of 5,333 µM, the first experiment reflected leaf litter leaching from pristine peat soils, whereas the second experiment mimicked leaf litter leaching from secondary forest plants with a DOC concentration of 16,222 µM. During the third experiment, DOC concentrations increased from 5,333 µM at the base to 16,222 µM at the top of the acrotelm. The resulting linear DOC concentration gradient within the acrotelm corresponds to the assumption that endemic leaf litter leaching dominates at the base and secondary leaf litter leaching controls the DOC supply at the soil surface. DOC leaching became accordingly a function of the water level within the acrotelm and therewith also of the precipitation rates. The model experiments 1 and 2 showed increasing DOC concentrations with increasing precipitation rates prior to the acrotelm overflow at 318 mm precipitation, after which surface runoff diluted DOC concentrations (Figure 4.5). In the model the increasing DOC concentrations prior to the overflow were caused by reduced DOC decomposition as a

consequence of a lower residence time of water at higher precipitation rates. The first experiment (groundwater DOC concentration of 5,333 µM) results in simulated DOC concentrations lower than the measured end-members, whereas the second experiment (DOC groundwater concentration of 16,222 µM) leads to simulated DOC concentrations similar to those measured in the Siak during our expeditions. This suggests that leaf litter leaching from secondary vegetation could strongly affect the DOC concentration in the Siak, which is also obvious because peat soils in the Siak catchment are heavily disturbed with hardly any endemic vegetation left (Miettinen and Liew, 2010). The consistency between simulated and end-member DOC concentrations was further improved during the third experiment, indicating that leaching of leaf litter from secondary forest plants dominates at the top of the acrotelm and leaf litter leaching from endemic peat vegetation gains importance towards the base of the acrotelm.

Considering an evapotranspiration rate of 67.7%, as assumed to be characteristic for pristine peat swamps, instead of 37.9%, would not affect the trend but the values, which means that then all simulated DOC concentrations would fall below the measured DOC end-members. This implies that the evapotranspiration rates derived from the experiments carried out on Borneo of 37.9% apply also to Sumatra.

The concept of two DOC sources (leaf litter and peat) also agrees quite well with the radiocarbon ages of peat and DOC in rivers and the results derived from our DOC decomposition experiment, which showed that DOC in the rivers consists of a labile and a more refractory fraction (Rixen et al., 2008). The radiocarbon age of a peat sample obtained at a soil depth of 5 cm (Figure 4.1) revealed an age of 890±25 years BP. At high latitudes DOC can be younger than the surrounding peat because of vertical water movements (Clymo and Bryant, 2008), but since at our study site younger peat was already eroded a DOC age of 890±25 years could represent a minimum estimate. DOC ages in the Mandau, a main tributary of the Siak, were with 575±30 years BP similar to those measured in the disturbed channel on Borneo (Moore et al., 2013). Assuming that the secondary leaf-litter DOC is of modern age and DOC leached from peat is as old as the peat suggests that 65±5% of the DOC in the river could be derived from peat and 35±5% might originate from labile leaf litter. In combination with the results from the decomposition experiments and in line with the leaching characteristics of leaf litter this furthermore implies that a major share (65 – 73%) of the peat-derived DOC in the Siak is old and refractory on time scales of days to weeks. The smaller remaining fraction is young, labile, and originated from leaching of leaf litter produced by secondary forest plants. Since the decomposition of labile DOC was the main

factor controlling the consumption of dissolved oxygen, the hypoxic conditions in the Siak can be seen as a consequence of the re-growing secondary forest and its production of labile leaf litter.

If groundwater DOC concentrations in the Siak are controlled by two DOC sources in the acrotelm, the acrotelm thickness becomes an important factor for the leaching of carbon from soils. The deeper the acrotelm, the greater the distance between the groundwater and secondary leaf litter at the soil surface and the lower the mean DOC groundwater concentration. This reduction should be limited by the DOC groundwater concentrations of 5,333 µM caused by peat leaching at the bottom of the acrotelm. However, as indicated in experiment 1, such a low DOC groundwater concentration can only explain the DOC end-member concentration measured during our last expedition in April 2013 if one assumes an evapotranspiration of 57% as observed in pristine peat swamps (Figure 4.5). Considering however the overall status of Sumatran peat lands this appears unlikely which in turn supports the hitherto held assertion that an enhanced DOC respiration associated with the occurrence of a plankton bloom lowered the DOC concentrations in the Siak estuary in April 2013 (Wit et al., 2015).

4.5.4 Extrapolation of Siak results

So far we used the mixing model to calculate DOC end-member concentrations depending on precipitation rates and varying DOC concentrations in the acrotelm wherein the best fit between simulated and measured DOC end-member concentrations in the Siak could be obtained by assuming two DOC sources in the acrotelm: peat and secondary leaf litter. The next step was to study the impact of the peat coverage on the DOC end-member concentration. Therefore all model settings remained unchanged except the precipitation rate and the peat coverage. The precipitation rate was set at 227 mm, which is the monthly mean precipitation of all studied river catchments covering the period between 1986 and 2013 (Table 4.1), and instead of using the Siak peat coverage of 21.9% (Table 4.1) the peat coverage was set in a range from 0 to 100% (Figure 4.6). The resulting simulated DOC concentrations were multiplied by the freshwater flux to obtain the DOC yields (see Eq. 1, 2). Since the majority of DOC originates from peatlands, DOC yields are expected to increase with increasing peat coverage, which indeed is evident from the DOC yields obtained from the studied rivers. However, the Rokan river deviates from this trend with a lower DOC yield because coastal erosion, favored by mangrove deforestation (Butcher, 1996), increased suspended matter concentrations and DOC adsorption to suspended clay. Apart from that the

simulated DOC yields agree quite well with the data-based end-members. This agreement can further be improved by using an acrotelm depth of 57.4 cm instead of 22.4 cm, which is well within the depth-range of acrotelms found in drained forests and plantations (Hooijer et al., 2012).

By increasing the acrotelm depth from 22.4 to 57.4 cm, the DOC yield was reduced from 133 g C m^{-2} yr^{-1} to 96 g C m^{-2} yr^{-1} at a peat soil coverage of 100% (Figure 4.6). This is consistent with the observed DOC yield in a channel draining disturbed peatlands in Borneo (Moore et al., 2013) and suggests that these model results are representative for disturbed SE Asian peatlands. The modeled DOC soil leaching rate associated with the riverine DOC export yield of 96 g C m^{-2} yr^{-1} at the acrotelm depth of 57.4 cm amounts to 183 g C m^{-2} yr^{-1}, implying a DOC decomposition in the river of 87 g C m^{-2} yr^{-1}. This estimate for DOC decomposition falls within the range of the data-based estimate on CO_2 emissions from SE Asian peat lands of 105±27.5 g C m^{-2} yr^{-1} (Wit et al., 2015) and further supports the reliability of the model results.

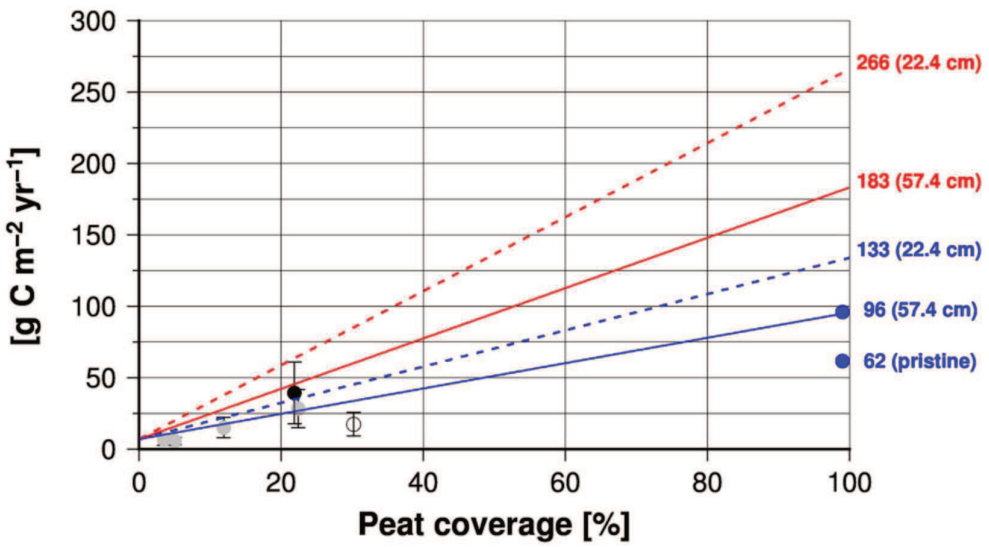

Figure 4.6 Mixing model mean DOC yield results. Mean DOC yields (discharge into the ocean) obtained from DOC end-member concentrations and the mean precipitations rates (1987 – 2013) in the respective river catchments (grey circles) versus peatland coverage of the catchments (data are given in **Table 4.1**). The black and open circle represents Siak and Rokan data. Blue dots show data from rivers draining pristine and disturbed peatlands in Borneo (Moore et al., 2013). The red and blue lines show the area normalized DOC leaching rates and riverine DOC yields, respectively, derived from the model versus peatland coverage of the catchments. Broken and solid lines indicate model results obtained by assuming an acrotelm depth of 22.4 and 57.4 cm, respectively. Numbers show leaching and export rates at 100% peat cover.

4.5.5 Anthropogenic perturbations

DOC concentrations of 5,661 µM measured in a channel draining pristine peat soils in Borneo (Moore et al., 2013) fall within the range of DOC pore water concentrations (Gandois et al., 2013), suggesting that DOC decomposition is of minor importance under natural conditions, as expected from the refractory characteristics of leaf litter of endemic peat plants. Under such a circumstance, the DOC yield obtained from the pristine river in Borneo of 62 g C m^{-2} yr^{-1} can be considered as the lowest estimate on DOC leaching. Compared to DOC leaching rates derived from the model of 183 g C m^{-2} yr^{-1}, this implies that leaching caused by changes in the vegetation cover has risen from 62 to 183 g C m^{-2} yr^{-1} representing an increase of almost 200% (Figure 4.7). In Borneo, changes in vegetation cover decreased evapotranspiration from 67.7 to 37.9%. This nearly doubles the freshwater flux fraction from 0.32 to 0.62 (Moore et al., 2013), which in principle could raise the peat leaching rate from 62 to ~118 g C m^{-2} yr^{-1}. Such an enhanced leaching rate is close to that of 108 g C m^{-2} yr^{-1} derived from our model by assuming a constant groundwater DOC concentration of 5,333 µM at a peat coverage of 100%. However, a peat leaching rate of 108 or 118 g C m^{-2} yr^{-1} contributes ~60% to the total leaching of 183 g C m^{-2} yr^{-1} (Figure 4.7). If deforestation of pristine peat swamp forests and the reduced evapotranspiration raised leaching of DOC from peat from 62 to 108 g C m^{-2} yr^{-1}, the increase from 108 to 183 g C m^{-2} yr^{-1} appears to be caused by leaching of leaf litter produced by secondary forest plants (Figure 4.7). This in turn implies that changes in the hydrological cycle and the regrowth of secondary forest plants explain 38% and 62% of the

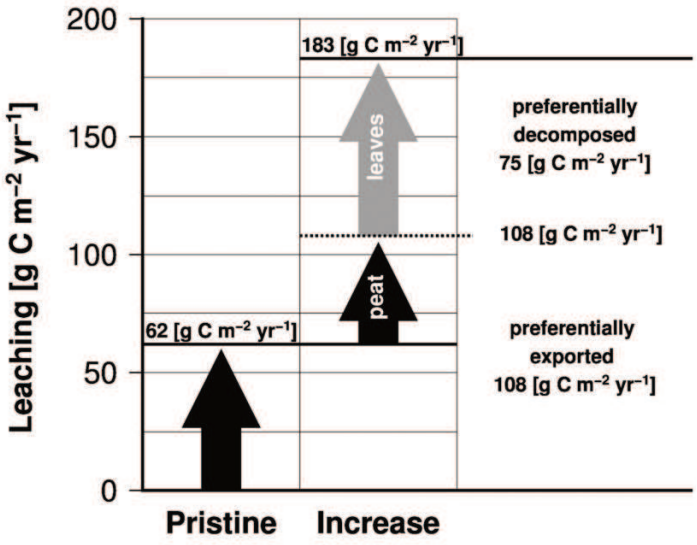

Figure 4.7 Leaching of organic carbon from pristine peat soils and the additional leaching caused by human impacts subdivided according to DOC sources (peat soil and leaf litter).

increase in DOC leaching from degraded peatlands, respectively.

4.5.6 Carbon budgets

In order to emphasize the role of DOC leaching it needs to be seen in the context of CO_2 losses from soils caused by aerobic peat respiration and the CO_2 uptake by the re-growing vegetation, which reduces carbon losses from the ecosystem (Figure 4.8). Estimates of CO_2 emissions from disturbed peat soils due to aerobic peat decomposition (Miettinen and Liew, 2010) and fires (van der Werf et al., 2008) of 53 and 128 Tg C yr^{-1}, respectively, and a disturbed peatland area of 0.24 10^{12} m^2 suggest a peat carbon loss of 744 g C m^{-2} yr^{-1}. The net ecosystem carbon loss from disturbed peatlands covered by secondary forest amounts to a carbon loss of 433 g C m^{-2} yr^{-1} (Hirano et al., 2007), indicating that re-growing biomass could reduce CO_2 emissions from disturbed peatlands into the atmosphere by 311 g C m^{-2} yr^{-1}. A leaching rate of 183 g C m^{-2} yr^{-1} increases carbon losses from the ecosystem by 42% from 433 to 616 g C m^{-2} yr^{-1} of which 48% (87 g C m^{-2} yr^{-1}) returns back into the atmosphere and 52% (96 g C m^{-2} yr^{-1}) is exported to the ocean. Since the leached DOC originates from

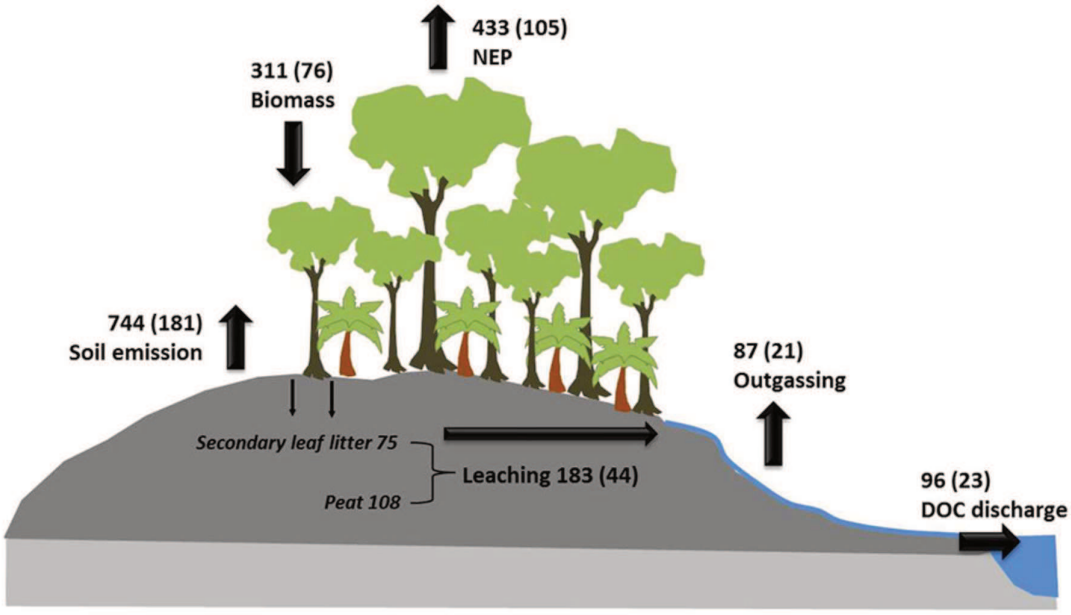

Figure 4.8 Carbon fluxes in disturbed peatlands. Net ecosystem carbon losses representing a negative net ecosystem production (NEP) (Hirano et al., 2007), CO_2 emissions from disturbed peat soils due to aerobic peat decomposition (Miettinen and Liew, 2010) and fires (van der Werf et al., 2008), carbon leaching, outgassing, and DOC discharge into the ocean. The carbon uptake by the growing biomass results from the difference between soil emission and NEP. River outgassing is the difference between leaching and DOC discharge into the ocean. The numbers and the numbers in brackets are fluxes in g C m^{-2} yr^{-1} and Tg C yr^{-1}, respectively.

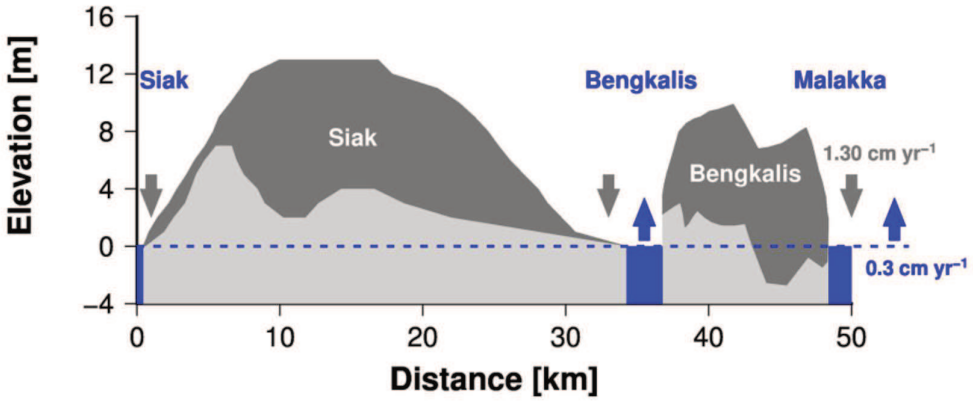

Figure 4.9 Cross-section through the Siak and Bengkalis peat domes. (Redrawn from Supardi and Subekty, 1993). The respective profile line is given in **Figure 4.1**b. Dark and light coloured areas represent the peat and underlying subsoils. Dark and blue arrows show the reduction of peat thickness caused by peat carbon losses and global mean sea level rise (Watson et al., 2015).

two different sources its role for the ecosystem varies: DOC leaching of labile leaf litter of 75 g C m^{-2} yr^{-1} reduces the carbon uptake by the re-growing biomass by 24% and its preferential decomposition in the river can lead to hypoxia as seen e.g. in the Siak river (Rixen et al., 2008; Rixen et al., 2010). The leaching of DOC from peat of 108 g C m^{-2} yr^{-1} represents in turn an irrecoverable loss of soil.

Assuming a peat carbon density of 65.35 kg m^{-3} (Warren et al., 2012) peat carbon losses caused by oxidation (744 g C m^{-2} yr^{-1}) and leaching (108 g C m^{-2} yr^{-1}) lower the peat thickness by approximately 1.30 cm yr^{-1} ((0.744 + 0.108) /65.35). Such a fast shrinking of coastal peat domes, that partly even form the coast as seen on the Island of Bengkalis (Figure 4.9), is a serious threat to the stability of the coastal peat plains that cover 10% of the Indonesian land mass.

4.6 Conclusion

In order to study processes controlling carbon leaching from tropical peat soils a mixing model was developed and validated by DOC concentrations measured in the groundwater, surface run off water, and river in the Siak catchment. This model was subsequently used to quantify carbon leaching from tropical peat soils wherein the obtained results were compared with data obtained from other Sumatran rivers. Since these rivers reveal peat soil coverages of <30.2%, also data obtained from the literature were used. Our results show that a reduced evapotranspiration and a resulting increased freshwater discharge in addition to the supply of labile leaf litter produced by re-growing secondary forests increase leaching of carbon by

~200%. Since the leached carbon originates from two different sources, namely peat and secondary vegetation, the resulting ecological consequences differ: Leached peat carbon is an irrecoverable loss of land that in addition to peat oxidation weakens the stability of peat-fringed coasts. This calls for mitigating strategies but reforestation by secondary forest plants bears an ecological threat. Leaching of their labile leaf litter supplies DOC of which the decomposition can lead to oxygen deficiencies in peat draining rivers.

4.7 End notes

4.7.1 Conflict of Interest Statement

Research was conducted in the absence of any commercial or financial relationships that could be construed as a potential conflict of interest.

4.7.2 Author Contribution Statement

TR, AB and JS conceived and led the research conducted in Sumatra. Data were collected by TR, AB, FW and JS. AB and FW performed chemical analyses. TR and FW conducted online measurements. TR and AB designed the study; FW and JS were involved in study design. TR led the writing of the paper. All authors discussed results and commented on the manuscript.

4.7.3 Acknowledgments

We would like to thank the Federal German Ministry of Education, Science, Research and Technology (BMBF Bonn, grant number 03F0392C) for its financial support.

4.8 Supplementary Material – Mixing model (written in Python)

4.8.1 Basic parameters:

Catchment area = 10423 km^2

Peat area = 10423 km^2 * 0.219 = 2,283 km^2 (peat coverage 21.9%)

Non-peat area = Catchment area - Peat area = 8140 km^2

Porosity = 0.873 %

4.8.2 Hydrological parameters:

Precipitation rates derived from Schneider et al. (2011) range between 50 to 450 mm (= l / m^2) for the period 1986 to 2013. Therefore the model was driven considering precipitation rates within the same range (Fig. 3a).

For calculating leaching and DOC yields depending on the peat coverage, as shown in Figure 3b, the mean precipitation rate of 227 mm was used.

Evapotranspiration = 37.9 % after (Moore et al., 2013)
Freshwater flux = precipitation – ((100-ET)/100.0) (mm = l/m^2)
Freshwater $flux_{flooding}$ = freshwater flux at a precipitation of 320 mm
Acrotelm depth = freshwater $flux_{flooding}$ / porosity / (-10.0) (cm)
Groundwater level:
GWL = acrotelm depth + (freshwater flux / porosity/10.0) (cm)
Groundwater discharge (GWD)
a) If ground water level < acrotelm depth: GWD = freshwater flux
b) If ground water level > acrotelm depth: GWD = freshwater $flux_{flooding}$
Surface runoff discharge (SRD) = freshwater flux – groundwater discharge
River water discharge (RWD) = freshwater flux * catchment area
River water discharge from non peatlands:
NP-RWD = freshwater flux * non-peat area
River water discharge from peat lands:
P-RWD = freshwater flux * peat area
Residence time of water in the Siak between west of the Mandau junction (river-km 285 km) and the mixing zone (river-km 340) in the estuary (see (Rixen et al., 2008))
Residence time = mean width (220 m) * mean depth (8 m) * distance (m) / groundwater discharge (m^3/hour)

4.8.3 DOC concentrations in the source waters:

DOC concentration in the groundwater in µM
a) Experiment 1 and 2:
DOC_{GWL}= 5,333 µM (experiment 1)
DOC_{GWL}=16,221 µM (experiment 2)
b) Experiment 3:
DOC_{GWL}= m * GWL + b
m and b are derived by assuming a DOC concentration at the acrotelm base of 5333 µM and 16221 µM at the acrotelm top
DOC concentration in the surface runoff water (DOC_{surf}) = 1221 µM (see Table S3)

DOC concentration in non-peat river water as obtained from our data measure in S. Tapung Kiri (DOC_{Kiri}) (see Figure S1)

a) Precipitation rate < 192 mm: DOC_{Kiri} = 344 µM

b) Precipitation rate > 192 mm:

DOC_{Kiri} = (650 * (precipitation – 160)*1.22) / (60 + (precipitation – 160)*1.22)

For calculating leaching and DOC yields depending on the peat coverage the DOC end-member concentration of the S. Tapung Kiri (344 µM) was used as DOC_{Kiri}.

4.8.4 DOC concentrations caused by mixing:

DOC concentrations in µM caused by mixing of groundwater and surface runoff:

DOC_{peat} = ((SRD * DOC_{surf}) + (GWD * DOC_{GWL})) / (freshwater flux)

DOC concentrations in µM caused by mixing of river waters from the peat and non-peat lands:

DOC_{input} = ((NP-RWD * DOC_{Kiri}) + (P-RWD * DOC_{peat})) / (RWD)

4.8.5 DOC decomposition in the Siak:

DOC decomposition in µM in the Siak (Rixen et al., 2008) (see Fig. S4):

t0 = (log((DOC_{input} – 1011.0)/390.0))/(-0.016)

t1 = t0 + residence time

DOC_{Siak} = (390 * exp(-0.016 * t1) + 1011).

V

The invisible carbon footprint: from land use change to coral reef dissolution in Sumatra, Indonesia

Francisca Wit[1*], Tim Rixen[1,3], Antje Baum[1], Widodo Setiyo Pranowo[2] and Andreas A. Hutahaean[4]

1) *Francisca Wit (*Corresponding author), Leibniz Center for Tropical Marine Research (ZMT), Fahrenheitstrasse 6, 28359 Bremen, Germany (francisca.wit@leibniz-zmt.de)*
2) *Research & Development Center for Marine & Coastal Resources (P3SDLP), Gedung II BALITBANGKP, Jalan Pasir Putih II, Ancol Timur, Jakarta, 14430, Indonesia*
3) *Institute of Geology, University of Hamburg, Bundesstrasse 55, 20146 Hamburg, Germany*
4) *Coordinating Ministry of Maritime Affairs, Jalan. MH. Thamrin No. 8, Jakarta 10340, Indonesia*

Key Points:

- Human-induced soil carbon leaching increases respiration of the labile organic matter and thereby the CO_2 emission in the rivers as well as in the estuaries and coastal ocean.
- Besides CO_2 emissions, respiration of organic matter is taking its toll by enhancing carbonate dissolution.
- This *invisible carbon footprint* threatens benthic ecosystem and extents the effects of LUC beyond the terrestrial realm.

Submitted at *Nature Climate Change*

Abstract

In Indonesia, land use change (LUC) in the form of peatland degradation induces carbon loss through direct CO_2 emissions, but also via soil leaching of which circa 50% is decomposed and emitted as CO_2 from the rivers. However, the fate of the remaining exported leached carbon is uncertain. Here, we show that the majority of this carbon is respired in the estuaries and emitted to the atmosphere. However, a portion is adsorbed into the marine carbon pool where it favors $CaCO_3$ dissolution. Therefore, impacts of LUC are not only limited to CO_2 emissions, but also affect marine ecosystems such as coral reefs. We conclude that the effects of LUC stretch beyond the terrestrial realm and, considering the ecological and economical importance of such ecosystems, it is important that this so far invisible carbon footprint, as well as the aquatic and marine CO_2 emissions, are included in climate mitigation strategies.

5.1 Introduction

Peatland degradation in Southeast Asia is recognized as an important carbon source to the atmosphere (Page et al. 2010) albeit so far not yet considered in all global estimates of CO_2 emissions. It would increase the LUC emissions from 1100 Tg C yr^{-1} (ref. (Philippe Ciais et al. 2013)) to 1389 ±938 Tg C yr^{-1} (26%) only by considering CO_2 emissions caused by peat oxidation and forest fires (289 ±138 Tg C yr^{-1}) (ref. (Houghton et al. 2012)). In Indonesia, regrowth of secondary vegetation could reduce this CO_2 emission to 105 Tg C yr^{-1} (ref. (Hirano et al. 2007)). However, this estimate would again enhance by 42% to 149 Tg C yr^{-1}, as a recent study (Rixen et al. 2016) revealed that degradation of peatlands has increased carbon leaching from soils by 200% with a leaching rate of 183 g C m^{-2} yr^{-1}, as opposed to 62 g C m^{-2} yr^{-1} from pristine peatlands (Moore et al. 2013). This increase results partly from changes in the hydrological cycle due to drainage (38%), but is primarily due to regrowth of secondary vegetation (62%) with leaves consisting of relatively labile organic carbon. Despite the carbon-enriched peat soils and enhanced leaching rate, the location of the peatlands near the coast limits the decomposition of leached carbon in the rivers by reducing its residence time in the river, which leads to a relatively modest river outgassing rate of 21 – 25 Tg C yr^{-1} (87 – 109 g C m^{-2} yr^{-1}) in Indonesian disturbed peatlands (Rixen et al. 2016; Wit et al. 2015). With roughly half of the carbon that enters the freshwater system being decomposed and emitted into the atmosphere, it remains unclear what the fate of the exported riverine carbon is once it has reached the estuaries and coastal ocean. In general, tropical estuaries and coastal

oceans are heterotrophic systems emitting CO_2 (Sarma et al. 2012; Noriega & Araujo 2014; Borges et al. 2005; Chen et al. 2013; Cai 2011; Regnier et al. 2013). In contrast, a recent study (Goulven G Laruelle et al. 2014) shows that coastal oceans in west Southeast Asia are considered to be a carbon sink, which would imply that the carbon that is leached from peat soils and exported via the rivers to the coastal ocean is absorbed in the water column.

In this study, we aim to resolve these knowledge gaps in Sumatra, Indonesia, by quantifying the riverine carbon export and investigate the estuarine and marine processes to better understand the fate of terrestrial carbon in the coastal ocean.

5.2 Methods

5.2.1 Study area

Tropical peatlands in Sumatra cover approximately 15.6% (Miettinen et al. 2012) or 72,431 km^2 of the land area with a thickness between 2 and 10 m (Hooijer et al. 2006) and are mostly located on the northern coastal plains. The large majority of these peatlands are disturbed as a consequence of deforestation and drainage to make way for agricultural cropland and in particular palm oil plantations (Miettinen et al. 2012). Indeed, only a small portion of circa 10% of tropical peatlands in Southeast Asia is pristine (Miettinen & Liew 2010). The study area is focused on the estuaries and northern coastal ocean of Sumatra, Indonesia, in order to cover the potential influence of the peatland degradation outside their catchments. The investigated estuaries belong in particular to the Musi, Indragiri and Siak rivers, but include also the outer estuaries of other rivers, such as the Batanghari, Kampar and Rokan, encountered during the trajectory along the coastline (Figure 5.1). The river catchments contain various amounts of peatland coverage, ranging from 3.5% in the Musi up to 30.2% in the Rokan catchment (Table 5.2).

Sumatra is subject to the Malaysian-Australian monsoon as a consequence of the meridional variation of the intertropical convergence zone. During the wet season, which lasts from October to April, the monsoon brings heavy rains from the north, whereas from May to September dry air currents from Australia induce a dry season (Gentilli et al. 2014). Precipitation rates vary between 123 mm in July to 312 mm in November with an annual sum of 2,696 mm in Pekanbaru, Central Sumatra (Schwarz 2014).

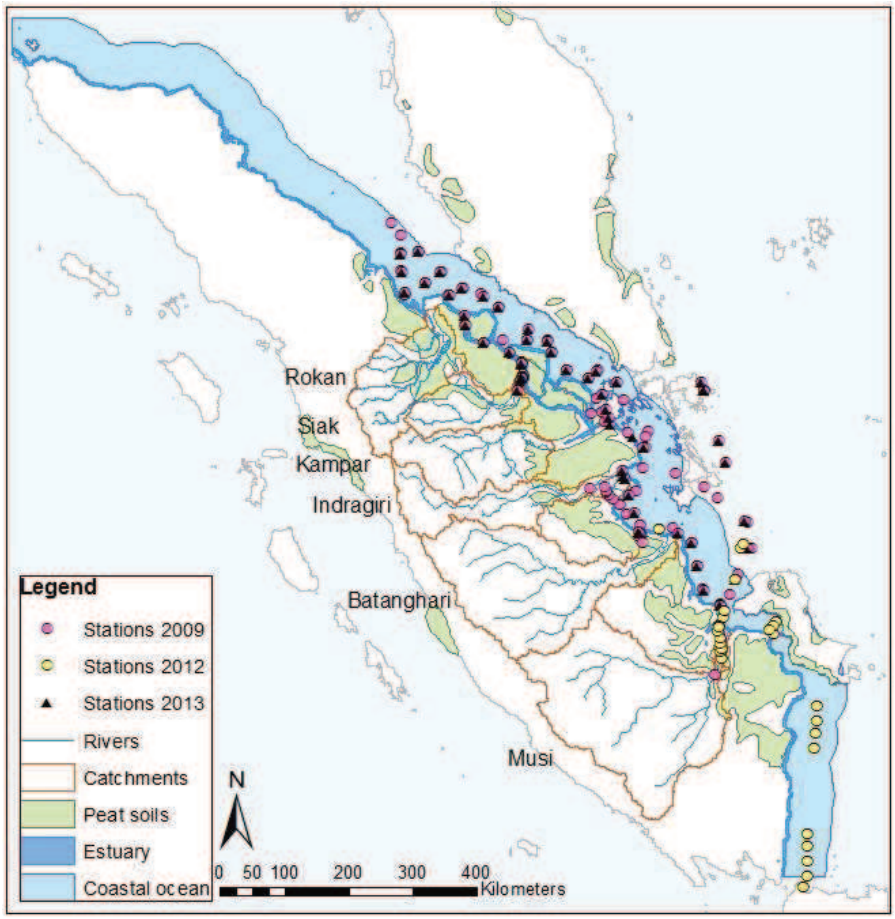

Figure 5.1 Study area and sample stations in 2009, 2012 and 2013 along the coast of Sumatra, Indonesia.

5.2.2 Expeditions

A total of three expeditions were carried out in October 2009, October 2012 and April 2013. In 2009 and 2013, the cruises started in the Musi river and continued along the coastline while visiting the Batanghari, Indragiri, Kampar, Siak and Rokan rivers and estuaries and returned through the coastal ocean. A total of 72 and 57 sampling stations were made in 2009 and 2013, respectively. In 2012 the cruise took off in the Banten Bay, West Java, along the coast to visit the Musi and Batanghari rivers, with a total of 32 sampling stations.

5.2.3 Sampling methods

Salinity, pCO_2 and temperature were measured continuously by means of underway instruments, which were connected via a through-flow system and supplied with surface water from an approximate depth of 1 m. Salinity was measured using a Seabird SBE 45 Micro TSG sensor, whereas temperature was measured via the integrated sensor of the

Meinsberg EGA 140 SMEK pH sensor. pCO_2 measurements were carried out with a Li-Cor 7,000 pCO_2 analyzer in 2009 and 2012, and a Contros HydroC CO_2 Flow Through Sensor in 2012 and 2013. Both pCO_2 devices were calibrated prior to the expeditions, of which the Contros HydroC device at 100, 448 and 800 ppm. The Li-Cor 7,000 device was calibrated using certificated NOAA reference gases (#CB08923 with 359.83 ppm, #CA06265 with 1,021.94 ppm) and another certificated calibration gas with 8,000 ppm. Wind parameters were measured using pre-installed equipment available on the vessel in 2009 and by means of a Lambrecht Ultrasonik anemometer in 2012, both at a height of 10 m above sea level.
In addition to continuous measurements, water samples were taken at each station using a Niskin bottle at circa 1.5 m depth. After a total storage (during and after expedition) of maximum three weeks, the samples were analyzed in the laboratory in Bremen, Germany. Samples for $\delta^{13}C_{DIC}$ were stored in amber-colored 20 ml bottles, deprived of air, intoxicated with mercuric chloride ($HgCl_2$) and analysed using the Finnigan GasBench II. In this instrument, organic compounds eluting from a GC column are converted into simple gases when traversing a capillary micro-reactor. Accordingly, all compound specific isotope ratios are analyzed in the IRMS. DOC samples were filtered (0.45 µm) into 60 ml high-density polyethylene (HDPC) bottles and acidified with phosphoric acid (20%) up to pH 2.0. By means of a Shimadzu TOC-VCPH Total Organic Carbon Analyzer, the samples were combusted at 680 °C within a quartz column and the released CO_2 was measured using the oxidative combustion-infrared analysis. The relative standard error for the method was ±1%. Alkalinity samples were collected in 250 ml glass bottles in 2009 and 2012 and in 125 ml LDPE flasks in 2013, deprived of air, intoxicated with $HgCl_2$ and analyzed using a VINDTA 3S instrument. Known amounts of sampled seawater were titrated with constant increments of 0.15 ml of hydrochloric acid (HCl) until a total amount of 4.2 ml HCl was reached. The HCl in the device was calibrated with a sodium chloride solution to approximate the ionic strength of seawater. The process of the open cell titration allowed the assumption that the total amount of DIC was approximately zero in the pH region of 3,0 – 3,5. The process was monitored using a pH glass electrode cell and the total alkalinity (TA) was calculated from the titrant volume and electromotoric force using a non-linear least-squares approach that corrected for the reactions with sulphate and fluoride ions.

5.2.4 CO_2 flux and piston velocity calculations for estuaries and coastal ocean

CO_2 fluxes (F) were calculated from the pCO_2 measurements of the continuous data using:

$$F = K_{CO2} \times K_0 \times \Delta pCO_2 \quad (1)$$

where K_{CO2} is the CO_2 piston velocity, K_0 the solubility of CO_2 in seawater (Weiss 1974) and ΔpCO_2 is the sea-air pCO_2 difference with an average atmospheric CO_2 concentration of circa 390 ppm, as measured during the cruises.

Although piston velocities are affected by many processes such as surface wave types, formation of air bubbles, humidity and temperature gradients and organic film coating, in the coastal systems and ocean piston velocities are primarily influenced by wind speed and the Schmidt number (Sarmiento & Gruber 2005). Therefore, piston velocity calculations related to wind speed have been chosen for this study. As calculations from Wanninkhof (Wanninkhof 1992) and Nightingale et al. (Nightingale et al. 2000) are widely used in the literature (Ekayanti & Rahman as-syakur 2011; Takahashi et al. 2009; Müller et al. 2015), both formulas have been used to calculate K_{CO2} for comparative matters. CO_2 calculations based on Wanninkhof's principles were 9.2% higher than Nightingale's and are used to represent a maximum estimate, which results in a lower invisible carbon footprint. The results based on Nightingale's principle are summarized in Table 5.1.

$$K_{W92} = 0.31 * U^2 * (Sc/600)^{-0.5} \quad (2)$$

$$K_N = (0.222 * U^2 + 0.333 * U) * (Sc/600)^{-0.5} \quad (3)$$

where K_{W92} and K_N are the formulas for Wanninkhof and Nightingale, respectively. U is wind speed in m s^{-1} at a height of 10 m above sea level and Sc is the Schmidt number for CO_2 (kinematic viscosity of water divided by the diffusion coefficient of CO_2 in water) in seawater determined for temperatures between 0 and 30 °C (Wanninkhof 1992) calculated by:

$$Sc = 2073.1 + -125.62 * T + 3.6276 * T^2 + -0.043219 * T^3 \quad (4)$$

where T is temperature in °C. Although wind speed was measured during the cruises in 2009 and 2012 with averages of 2.39±0.01 m s^{-1} and 3.97±0.02 m s^{-1}, respectively. However, the annual wind speed derived from QuikSCAT (Ricciardulli et al. 2011) by averaging monthly

Table 5.1 CO_2 outgassing fluxes for the rivers, estuaries and coastal ocean of Sumatra according to Nightingale's principle based on averaged concentrations measured during expeditions from 2009 to 2013. Errors are represented as the standard error.

Location		Estuaries	Coastal ocean	Subtotal marine
Area	km^2	10818	127674	138492
Wind speed	m/s	5.59±0.41	5.59±0.41	/
K_N	cm hr^{-1}	10.9±1.4	10.9±1.4	/
pCO_2 conc.	µatm	2038±56	554±1	/
CO_2 yield	g C m^{-2} yr^{-1}	609.2±79.9	44.9±5.9	/
CO_2 flux	Tg yr^{-1}	6.6±0.9	5.7±0.8	12.3±1.6

K is based on Nightingale. The spread of the K_N, CO_2 yields and fluxes are best/worst case scenarios, calculated based on the s.d. of the wind speed. The spread of the pCO_2 is the s.e.

Table 5.2 Precipitation, discharge and end-member concentrations of DOC, DIC, POC and PIC for the rivers. Uncertainties of the values per expedition are the standard deviation, whereas uncertainties of the averages are the standard error.

River	Expedition	Precipitation	Discharge	DOC	DIC	POC	PIC
		mm	m^3 s^{-1}	µmol l^{-1}	µmol l^{-1}	µmol l^{-1}	µmol l^{-1}
Musi	Mar 2008	352	4735	/	/	117	/
	Nov 2008	436	5865	423±21	/	242	/
	Oct 2009	197	2650	223±5	/	70	8
	Oct 2012	249	3350	264±5	748±42	/	/
	Apr 2013	238	3202	/	/	/	/
	Average	**294±44**	**3961±587**	**303±61**	**748±42**	**143±51**	**8±-**
Batanghari	Oct 2009	214	2270	377±10	/	109	10
	Oct 2012	249	2641	241±1	/	/	/
	Apr 2013	190	2015	314±0	/	/	/
	Average	**218±17**	**2309±182**	**311±39**	**/**	**109±-**	**10±-**
Indragiri	Mar 2008	366	1554	846±159	/	449	/
	Nov 2008	291	1236	/	/	304	/
	Oct 2009	272	1155	774±71	/	692	57
	Apr 2013	332	1410	651±5	409±12	/	/
	Average	**315±21**	**1339±89**	**757±57**	**409±12**	**482±113**	**57±-**
Kampar	Mar 2006	290	1795	1236±51	/	103	/
	Mar 2008	429	2655	/	/	133	/
	Nov 2008	281	1739	1325±39	/	232	/
	Average	**333±51**	**2063±297**	**1280±45**	**/**	**156±39**	**/**
Siak	Sep 2004	250	616	2187±40	/	492	/
	Aug 2005	426	1049	2159±136	/	836	/
	Mar 2006	216	532	1633±55	/	316	/
	Nov 2006	244	601	1849±22	/	/	/
	Mar 2008	409	1007	2205±56	/	443	/
	Nov 2008	273	672	/	/	135	/
	Oct 2009	317	781	2632±164	/	773	0.00
	Apr 2013	205	505	633±88	291±11	/	/
	Average	**293±46**	**720±74**	**1900±242**	**291±11**	**499±109**	**0.00±-**
Rokan	Apr 2006	300	1365	833±50	/	/	/
	Mar 2008	438	1993	728±54	/	1017	/
	Nov 2008	255	1160	/	/	1052	/
	Average	**331±67**	**1506±307**	**781±53**	**/**	**1034±18**	**/**

measurements between 2001 and 2008 within the coastal ocean area (Figure 5.1) resulted in an annual average wind speed of 5.59±0.41 m s^{-1}. Therefore, the QuickSCAT average was used to get a maximum estimate on emissions.

5.2.5 Carbon export and end-members

Carbon exports are comprised of riverine export rates of POC, PIC, DOC and DIC into the estuaries and coastal ocean. DIC (μmol l^{-1}) was calculated using the co2sys program with TA and pCO_2 measurements as input parameters. Other components related to the carbonate system, such the aragonite and calcite saturation state, were calculated simultaneously.

Exports were calculated by multiplying the average carbon end-member concentration with discharge, which was based on averaged monthly precipitation rates (Table 5.2) and assuming an evapotranspiration rate of 37.9% (Moore et al. 2013). DOC and DIC end-member concentrations per expedition were derived through correlating their concentrations with salinity, where the y-intercept at salinity 0 represents the end-member concentration. POC and PIC concentrations were derived from stations in a salinity range of 0 – 1, as it was not possible to obtain an end-member due to few data points. Exports normalized to catchment area represent the yield.

5.2.6 Surface area calculations

Catchment areas were defined by means of a relief model in ArcGIS 9.3 with the ArcHydro extension, which was derived from SRTM90m digital elevation model of the Consortium for Spatial Information of the Consultative Group for International Agricultural Research (CGIAR-CSI). Peat coverage in each catchment was determined by overlaying the determined catchment areas by the FAO soil map of the world (FAO/UNESCO 2004). The peat coverage for Sumatra was derived from Miettinen et al. (Miettinen et al. 2012).

Generally, the border between estuaries and coastal ocean is predetermined at a salinity equal to or more than 30 (Bauer et al. 2013). However, in this study the correlation between salinity and the aragonite saturation state off the coast of Sumatra shows a clear distinction of this border, indicated by Ω_{AR} values of ≤1 below salinity 25, and a rapid increase of Ω_{AR} ≥1 at salinities ≥25 (Figure 5.7). Therefore, the border between estuaries and coastal ocean is here defined at a salinity equal to or higher than 25. By correlating the salinity and distance to shore, this border is found at an approximate distance of 3 km (Figure 5.2). Based on this

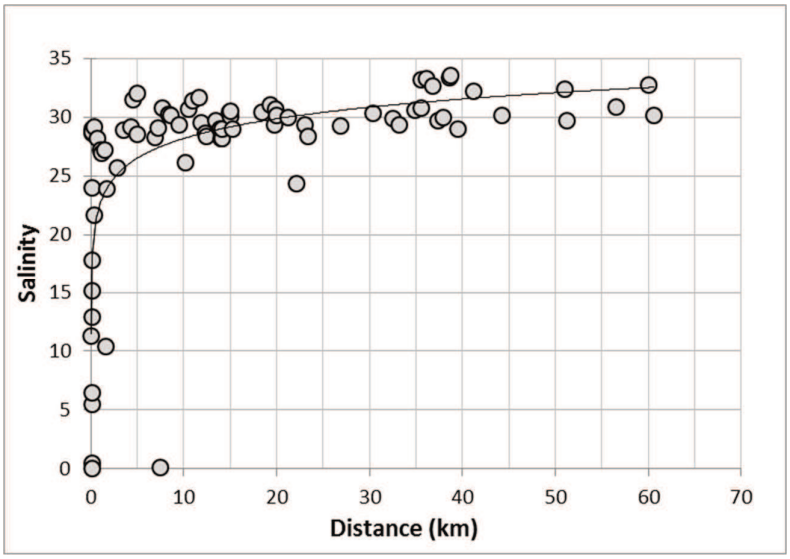

Figure 5.2 Correlation salinity and distance from shore. Salinity 25, which is considered the border between the estuaries and coastal ocean, is located at approximately 3 km distance. The border between the coastal ocean and open ocean is located at circa 67 km distance.

distance, the surface area of the estuaries was estimated using ArcGIS 10.4 and, assuming that estuaries influence the entire coastline, amounts to 10,818 km^2. The perimeter of the coastal ocean is based on the correlation between salinity and $\delta^{13}C$, where the terrestrial influence, characterized as $\delta^{13}C$ values below the marine $\delta^{13}C$ signature of circa +1‰ (Sonnerup & Quay 2012), reached up to a salinity of circa 32.8. This salinity coincided with a distance of circa 67 km, which resulted in a surface area of 127,674 km^2.

5.2.7 Mixing lines

In the estuaries, TA and DIC concentrations increase in a linear fashion as low concentration river waters mix with high concentration coastal ocean waters. This linear relationship along a salinity gradient is referred to as a mixing line and represents the expected TA and DIC concentrations at a specific salinity as a consequence of mixing. Mixing lines were calculated for the Musi, Indragiri and Siak estuaries as a linear correlation between salinity and TA or DIC by including their respective estuary stations and the coastal ocean dataset (Figure 5.3). Based on these TA and DIC mixing lines calculated for the Musi, Indragiri and Siak estuaries, pCO_2 mixing lines were calculated using co2sys with the TA and DIC concentrations of the mixing lines as input parameters, in addition to temperature, salinity and air pressure. The pCO_2 (non-linear) mixing lines represent the expected decrease in pCO_2 concentrations along the salinity gradient caused by mixing.

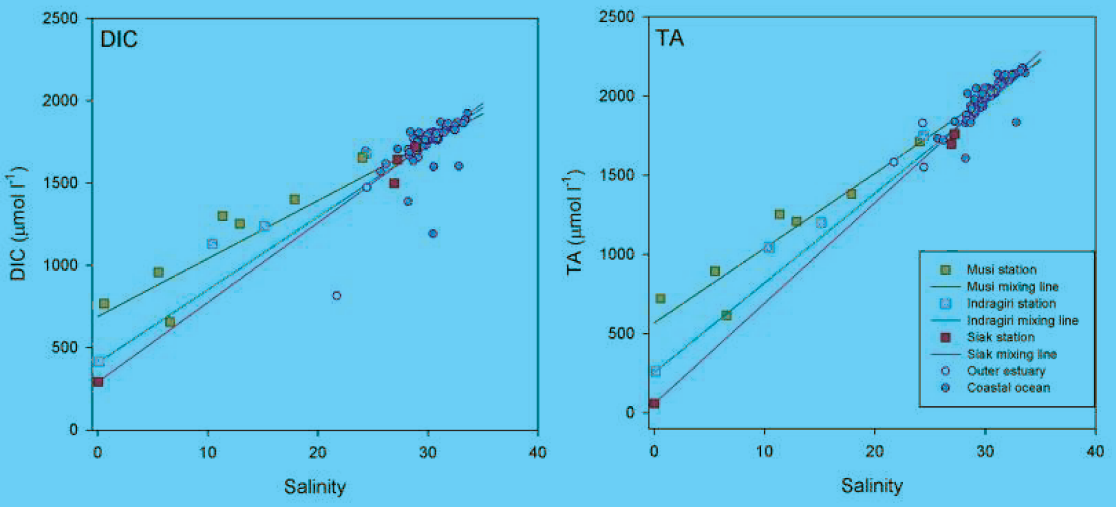

Figure 5.3 Mixing lines for DIC (a) and TA (b) for the Musi, Indragiri and Siak rivers, as well as the average mixing line for Sumatra, which is extended to salinity 35 to represent the coastal ocean. The standard error of the Sumatra mixing line is indicated as dotted lines.

5.2.8 Calibration experiment

As pCO_2 was measured with different devices in 2009 and 2013, a CO_2 calibration experiment was conducted to validate the Contros measurements, during which different concentrations of CO_2 gas were delivered using a gas mixing system. The gas concentrations delivered by the gas mixing system were first monitored and compared by the mixing system regulator, the Li-Cor 7000, the Li-820 and the cavity ring-down spectrometer (Picarro G2201-i) in a range from circa 500 to 6000 ppm (Figure 5.4a). The gas was then used to calibrate seawater in a range of 500 – 5000 ppm that was pumped into the Li-Cor 7000 equilibrator

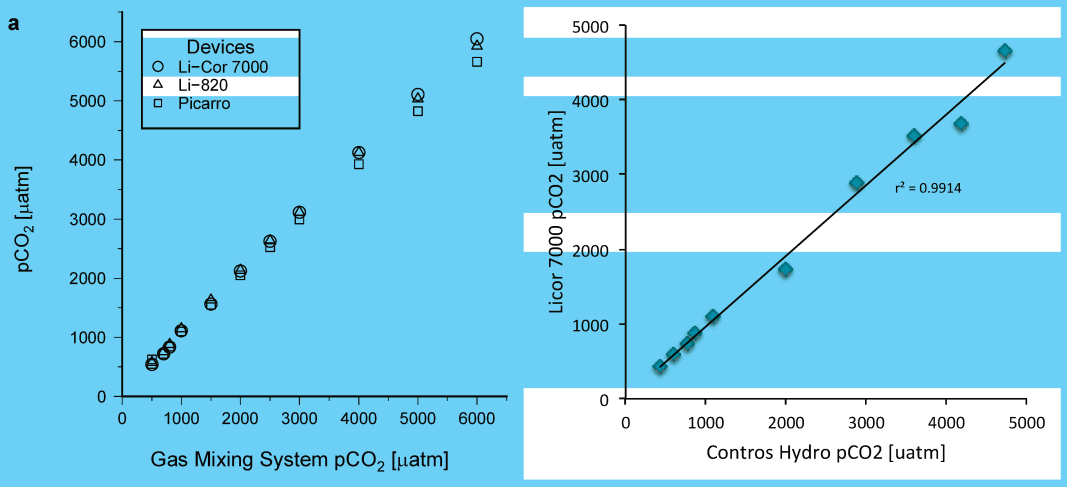

Figure 5.4 Calibration experiment results. a) Monitor results of calibration gas using the mixing system, Li-Cor 7000, Li-820 and Picarro devices. b) Calibration experiment results, $r^2 = 0.99$

and the Contros sensor. The measured pCO_2 concentrations were highly correlated (Figure 5.4b), especially in the lower concentration range common in the coast, which justified the Contros measurements.

5.2.9 Uncertainty estimates

The errors associated with the averaged parameters in the rivers, estuaries and coastal ocean are presented as the standard error (s.e.). The error range of the alkalinity is based on the standard error of the seawater standards measured during the sample analysis and applied to the respective samples. The error of DIC can be seen as best/worst case scenario, as the errors of TA and pCO_2 have been integrated throughout the co2sys calculations. The error range of the CO_2 yields and fluxes in the estuaries and coastal ocean are the result of the standard deviation of the piston velocities in turn as a consequence of the standard deviation of the wind speed (5.59±0.41 m s^{-1}), which was integrated in the CO_2 yield and flux calculations to give a best/worst case scenario.

5.3 Results and discussion

5.3.1 Riverine carbon processes and exports

In Sumatra six rivers were investigated, namely the Musi, Batanghari, Indragiri, Kampar, Siak and Rokan (Figure 5.1), of which the river catchments contain various amounts of peatland coverage, ranging from 3.5% in the Musi up to 30.2% in the Rokan catchment. Through leaching, carbon is mobilized from the peat soils into the rivers, which is further enhanced through disturbance (Moore et al. 2013) and the leaves of secondary vegetation that are more labile compared to those of primary peat swamp vegetation (Rixen et al. 2016). The export ratio between total organic carbon and total inorganic carbon (TOC:TIC) increases with increasing peat coverage as organic carbon is leached from the overlying peat soils, which simultaneously reduce the contribution of dissolved (inorganic) carbonate derived from weathering of underlying mineral soils to the rivers (Huang et al. 2012; FAO/UNESCO 2004). The relative importance of dissolved inorganic carbon (DIC) derived from respiration and silicate weathering can also be quantified by $\delta^{13}C_{DIC}$ isotopes. The riverine $\delta^{13}C_{DIC}$ is a mixture between low isotopic $\delta^{13}C_{CO2}$ values from decomposed plant material, which amounts to an average of -28.0±1.5‰ as derived from leached terrestrial dissolved organic carbon (DOC) measured in the Siak, Rokan and Kampar rivers in 2006, and HCO_3^- derived

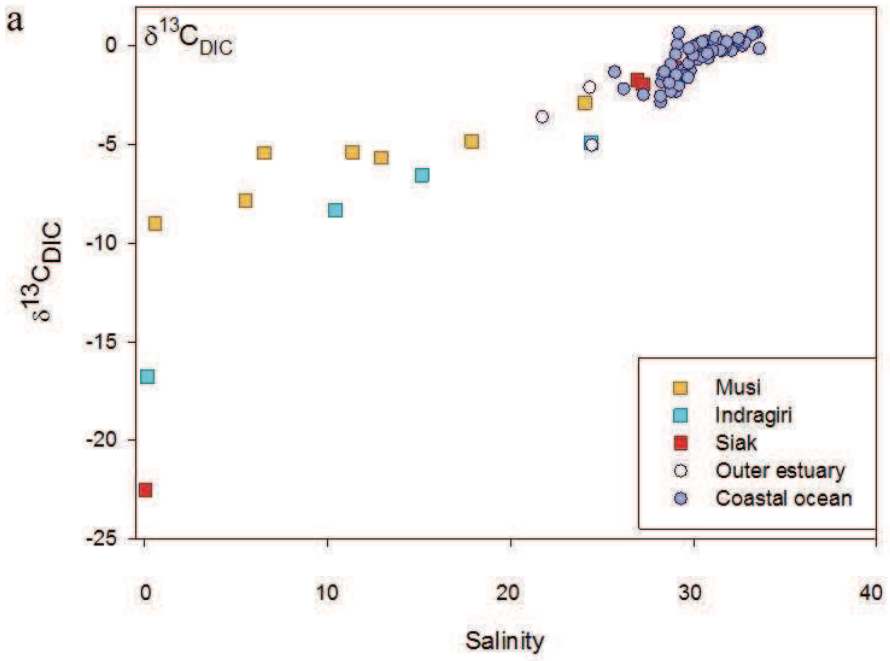

Figure 5.5 $\delta^{13}C_{DIC}$ values plotted against salinity.

from weathering of mineral soils (Polsenaere & Abril 2012), which have an isotopic signature of about 0‰ (Schindlbacher et al. 2015). The Siak river has a $\delta^{13}C_{DIC}$ of -22.5‰ as its DIC is composed primarily of CO_2 derived from decomposed terrestrial DOC and less of DIC from weathering (Figure 5.5). In the Musi and Indragiri, which have a small peat coverage, $\delta^{13}C_{DIC}$ values are higher with -16.8‰ and -9.0‰, respectively, which indicates that mineral soil weathering plays a more active role in these catchments.

The dissolved and particulate organic and inorganic carbon fluxes have been calculated based on measurements carried out between 2004 and 2013 (Table 5.2) and were interpolated to encompass Sumatra. On average 72% of the exported carbon from Sumatra is organic with 10.72 ±0.12 Tg C yr^{-1} of DOC and 4.87 ±0.08 Tg C yr^{-1} of particulate organic carbon (POC), adding up to 15.59 ±0.20 Tg C yr^{-1} of TOC (Table 5.3). The export of TIC amounts to 6.05 ±0.19 Tg C yr^{-1}, mostly consisting of DIC with 5.82 ±0.19 Tg C yr^{-1}, whereas particulate inorganic carbon (PIC) contributes on a marginal level with 0.23 ±0.00 Tg C yr^{-1}. As a whole, Indonesia, with a peat coverage of 11.9% (Wit et al. 2015), has a TOC export of 53.06 Tg yr^{-1} and a TIC export of 25.65 Tg C yr^{-1}. In comparison, the Amazon river has riverine carbon exports of 36 Tg C yr^{-1} of TOC and 35 Tg C yr^{-1} of TIC (Richey et al. 2002), which shows that Indonesia, regardless of its relatively small size of 1.9 million km^2 (Wit et al. 2015) compared to the Amazon catchment of 3.9 million km^2 (Richey et al. 2002), plays a crucial

role with respect to carbon exports. Its relatively large riverine export of organic carbon shifts the attention to the fate of this organic carbon in the estuaries.

Table 5.3 Carbon export rates from rivers in Sumatra based on averaged concentrations measured during expeditions from 2009 to 2013, including POC and PIC data from cruises in 2004, 2005, 2006 and 2008. Errors are represented as the standard error.

Location		Musi	Batanghari	Indragiri	Kampar*	Siak	Rokan*	Sumatra*
Catchment	km^2	56931	44890	17968	26195	10423	19258	464301
River area	km^2	245	269	174	210	81	154	3714
Peat cover	%	3.5	5	11.9	22.4	21.9	30.2	15.6
Discharge	$m^3\ s^{-1}$	3961±587	2309±182	1339±89	2063±297	720±74	1506±307	31820±3606
$\delta^{13}C_{DIC}$	‰	-9.0	-	-16.8	-	-22.5	-	-
DOC conc.	µM	303±61	311±39	757±99	1280±63	1900±640	781±53	890±159
DOC yield	$g\ C\ m^{-1}\ yr^{-1}$	8.00±3.91	6.05±0.62	21.37±4.99	32.65±0.88	49.71±27.26	23.13±3.09	23.09±6.79
DOC flux	$Tg\ C\ yr^{-1}$	0.46±0.22	0.27±0.03	0.38±0.09	0.86±0.02	0.52±0.28	0.45±0.06	10.72±0.12
DIC conc.	µM	748±42	671±21	409±12	294±21	291±11	333±21	483±137
DIC yield	$g\ C\ m^{-1}\ yr^{-1}$	19.71±0.16	13.08±0.03	11.53±0.02	7.49±0.09	7.62±0.03	9.86±0.13	12.53±0.40
DIC flux	$Tg\ C\ yr^{-1}$	1.12±0.01	0.59±0.00	0.21±0.00	0.20±0.00	0.08±0.00	0.19±0.00	5.82±0.19
POC conc.	µM	143±51	109±-	482±113	156±39	499±109	1034±18	404±55
POC yield	$g\ C\ m^{-1}\ yr^{-1}$	3.76±0.20	2.12±-	13.60±0.21	3.98±0.17	13.06±0.29	30.64±0.11	10.48±0.16
POC flux	$Tg\ C\ yr^{-1}$	0.21±0.01	0.10±0.00	0.24±0.00	0.10±0.00	0.14±0.00	0.59±0.00	4.87±0.08
PIC conc.	µM	8±0.17	10±0.20	57±1.14	-	0±0.00	-	19±0.38
PIC yield	$g\ C\ m^{-1}\ yr^{-1}$	0.22±0.00	0.20±0.00	1.60±0.00	-	0.00±0.00	-	0.49±0.00
PIC flux	$Tg\ C\ yr^{-1}$	0.01±0.00	0.01±0.00	0.03±0.00	-	0.00±0.00	-	0.23±0.00
Tot.C exp.	$Tg\ C\ yr^{-1}$	1.80±0.24	0.96±0.03	0.86±0.09	1.16±0.02	0.73±0.28	1.23±0.06	21.63±0.39
CO_2:C_{exp} ratio	-	27:73	29:71	43:57	52:48	38:62	49:51	43:57
OC:IC ratio	-	37:63	38:62	73:27	83:17	89:11	85:15	72:28

* DIC concentrations for the Kampar, Rokan and Sumatra were derived from the correlation between DIC concentrations and peat coverage of the Musi, Batanghari and Siak rivers.

5.3.2 Carbon fluxes and processes in the estuaries and coastal ocean

As river waters reach the estuaries and coastal ocean of Sumatra, pCO_2 levels rapidly decrease. In order to investigate to which extent mixing with low pCO_2 ocean waters is responsible for this measured decrease, pCO_2 mixing lines were calculated and represent the expected decrease in pCO_2 concentrations along the salinity gradient caused by mixing. They are visualized along with the measured pCO_2 concentrations for the Musi, Indragiri and Siak estuaries in Figure 5.6. The pCO_2 mixing lines are initially relatively high in accordance with the measurements, but quickly decrease exponentially. However, the higher pCO_2 measurements indicate that additional CO_2 is produced that increases the pCO_2 beyond the level expected during mixing. This confirms the general observation that especially the estuaries are heterotrophic systems, where respiration and decomposition of organic carbon are dominant processes. The $\delta^{13}C_{DIC}$ data shows the influence of terrestrial carbon in the estuaries and coastal ocean. However, its increase with increasing salinity is in a linear

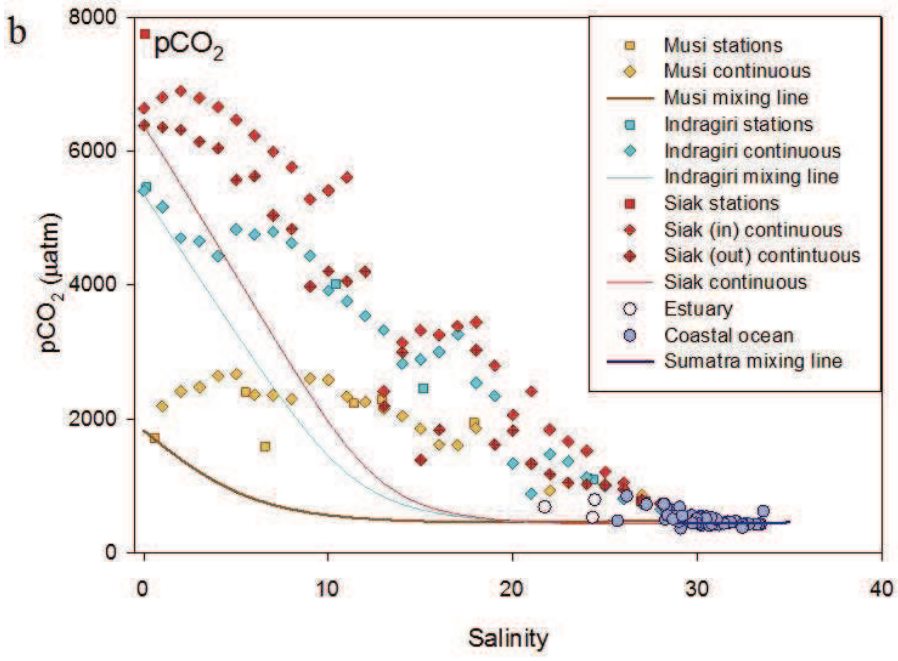

Figure 5.6 Measured pCO_2 concentrations (dots) and expected pCO_2 concentrations during mixing in the estuaries (mixing lines). To complement the figure with respect to pCO_2 measurements in the estuaries, the continuous pCO_2 measurements were used to calculate the average pCO_2 at each salinity point in the respective rivers (continuous). As the trip in the Siak river covered two days with a break upstream, the pCO_2 data is divided between 'In' and 'Out' to highlight the difference in pCO_2 concentrations. During the way into the Siak the pCO_2 concentrations are slightly lower than during the way out. This is presumably due to a plankton bloom that occurred as relatively low DOC concentrations allowed for enhanced light availability, which absorbed CO_2 for photosynthesis (Wit et al. 2015)(Wit et al. 2015)(Wit et al. 2015).

Table 5.4 CO_2 outgassing fluxes of the rivers, estuaries and coastal ocean of Sumatra according to Wanninkhof's principle based on averaged concentrations measured during expeditions from 2009 to 2013. Errors are represented as the standard error.

Location		Estuaries	Coastal ocean	Subtotal marine
Area	km^2	10818	127674	138492
Wind speed	m/s	5.59±0.41	5.59±0.41	/
K_W	cm hr^{-1}	12.0±1.8	12.0±1.8	/
pCO_2 conc.	µatm	2038±56	554±1	/
CO_2 yield	g C m^{-2} yr^{-1}	670.7±98.4	49.4±7.2	/
CO_2 flux	Tg yr^{-1}	7.3±1.1	6.3±0.9	13.6±2.0

K is based on Wanninkhof. The spread of the K_W, CO_2 yields and fluxes are best/worst case scenarios, calculated based on the s.d. of the wind speed. The spread of the pCO_2 is the s.e.

fashion, thereby seemingly due to mixing. Decomposition of terrestrial organic carbon would result in more negative values, expressed in a theoretical curve below the observed linear correlation. On the other hand, outgassing of CO_2 at a pCO_2 twice or more that of the atmosphere raises the $\delta^{13}C_{DIC}$ values (Doctor et al. 2008), providing a theoretical curve above the observed correlation. Both processes occur in the estuaries and balance the resulting $\delta^{13}C_{DIC}$ values to appear linear.

In order to quantify how much of the respired exported carbon is emitted as CO_2 to the atmosphere, the CO_2 yields of the estuaries and coastal ocean were calculated and amount to 670.7 ±98.4 g C m^{-2} yr^{-1} and 49.4 ±7.2 g C m^{-2} yr^{-1}, respectively (Table 5.4). Multiplied by their surface areas, this results in a CO_2 flux of 7.3 ±1.1 Tg C yr^{-1} in the estuaries and 6.3 ±0.9 Tg C yr^{-1} in the coastal ocean. This finding is contradictory to a recent study that predicts the coastal ocean of Southeast Asia to be a carbon sink (G.G. Laruelle et al. 2014). Whereas this may be the case for the northern part of Southeast Asia from where this data point is extrapolated due to data scarcity, our data shows that the coastal ocean of Sumatra is instead a carbon source. Indeed, it appears that the short residence time of the rivers creates relatively modest CO_2 emissions in the rivers with 16.5 Tg C yr^{-1} in Sumatra (Wit et al. 2015), but in fact shifts this process of CO_2 emission to the estuaries and coastal ocean where the exported organic carbon is respired, thereby causing a combined CO_2 emission of 13.6 ±2.0 Tg C yr^{-1}. In regard to the total carbon export of 21.6 Tg C yr^{-1}, this suggests that the excess of 8.0 Tg C yr^{-1} is either exported into the sediments or it is adsorbed by marine waters. Although actual sedimentation rates in Southeast Asia are uncertain, globally it is estimated that approximately 10% of the exported terrestrial organic carbon is sequestered in continental margin sediments (Schlünz & Schneider 2000). Assuming a similar burial rate for Sumatra and its TOC export of 15.6 Tg C yr^{-1}, this results in a sedimentation rate of 1.6 Tg C yr^{-1}, which would reduce the excess of exported carbon from 8.0 to 6.4 Tg C yr^{-1}. The remaining excess of carbon may be partially exported to the open ocean (Andersson et al. 2005), but is

most presumably further remineralized to form CO_2 (Blair & Aller 2012). In addition to the exported DIC_{CO2}, this may be used for photosynthesis or alternatively is absorbed by marine waters through carbonate dissolution, which shifts the carbonate system towards lower CO_2 concentrations.

5.3.3 Carbonate dissolution

Marine organisms primarily use two major forms of $CaCO_3$, namely aragonite (corals and many mollusks) and calcite (coccolithophores, foraminifera and some mollusks)(Scott C Doney 2010). The saturation states of aragonite (Ω_{AR}) and calcite (Ω_{CA}) found in the Sumatran estuaries range between 0 – 1.1, which encourages carbonate dissolution (Scott C Doney 2010) and impede the growth of carbonate-producing organisms. In the coastal ocean, the values increase up to 3.5 for Ω_{AR} and 5.5 for Ω_{CA} (Figure 5.7). This gradient from the estuaries to the coastal ocean is notably reflected by the mollusk species richness and abundance, which is correlated to the sediment carbonate content (Michel et al. 2015), and hence Ω_{AR} / Ω_{CA}. Indeed, the minor sediment carbonate content in the river mouths (0-4%) and Malacca Strait (<1%) allow few mollusk species to thrive with very low abundance, whereas the increased carbonate content in East Sumatra (2-79%) and the Tuju Islands (27-92%) show increased species richness and mollusk abundance (Michel et al. 2015). Nonetheless, taking into account that calcification rates and cementation sharply decrease at $\Omega_{AR} < 4$ (Langdon & Atkinson 2005) and $\Omega_{AR} < 3$ (Manzello et al. 2008), respectively, the findings indicate that calcification rates in the coastal ocean are not optimal.

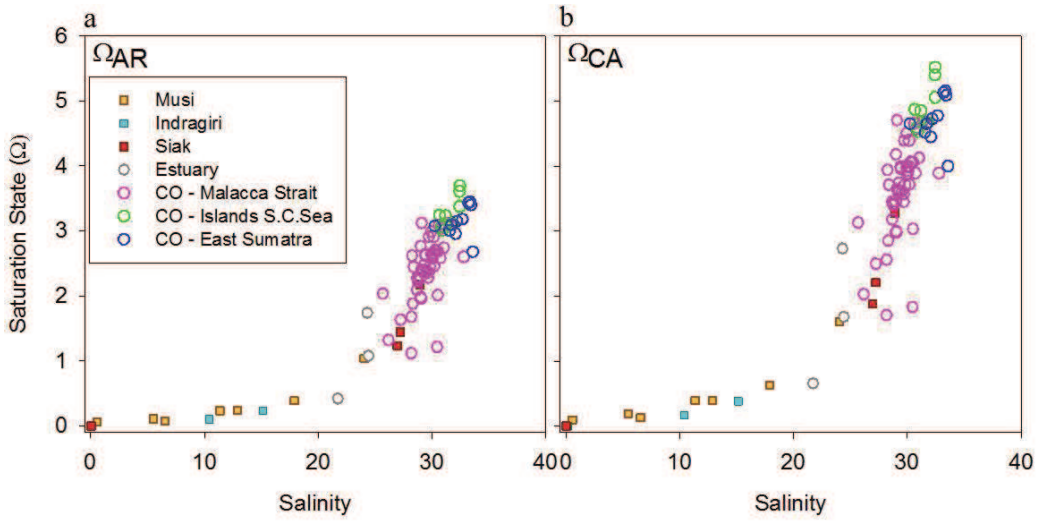

Figure 5.7 Saturation states of a) aragonite (Ω_{AR}) and b) calcite (Ω_{CA}) versus salinity for the estuaries and three regions of the coastal ocean (C.O.) of Sumatra: the Malacca Strait, islands in the South China Sea and East Sumatra.

In order to visualize the balance between $CaCO_3$ dissolution and formation, the measured total alkalinity (TA) and DIC concentrations were compared to their respective mixing lines (Figure 5.3). The DIC and TA deviations were then plotted against each other to visualize their ratio, which sheds light on the occurring processes (Figure 5.8). In accordance with their low Ω_{AR}, most of the estuarine data points show the largest dissolution and are offset to the right due to additional DIC in the form of respired CO_2. This confirms our previous observation that, besides $CaCO_3$ dissolution as evident from this plot and the Ω_{AR} / Ω_{CA}, respiration is an active process in the estuaries. Whereas optimal Ω_{AR} and Ω_{CA} conditions in the coastal ocean would result in its data points along the $CaCO_3$ formation, the cluster is shifted toward dissolution instead, with an offset towards respiration. This indicates that ocean acidification as a consequence of oversaturation of respired CO_2 is taking its toll in the

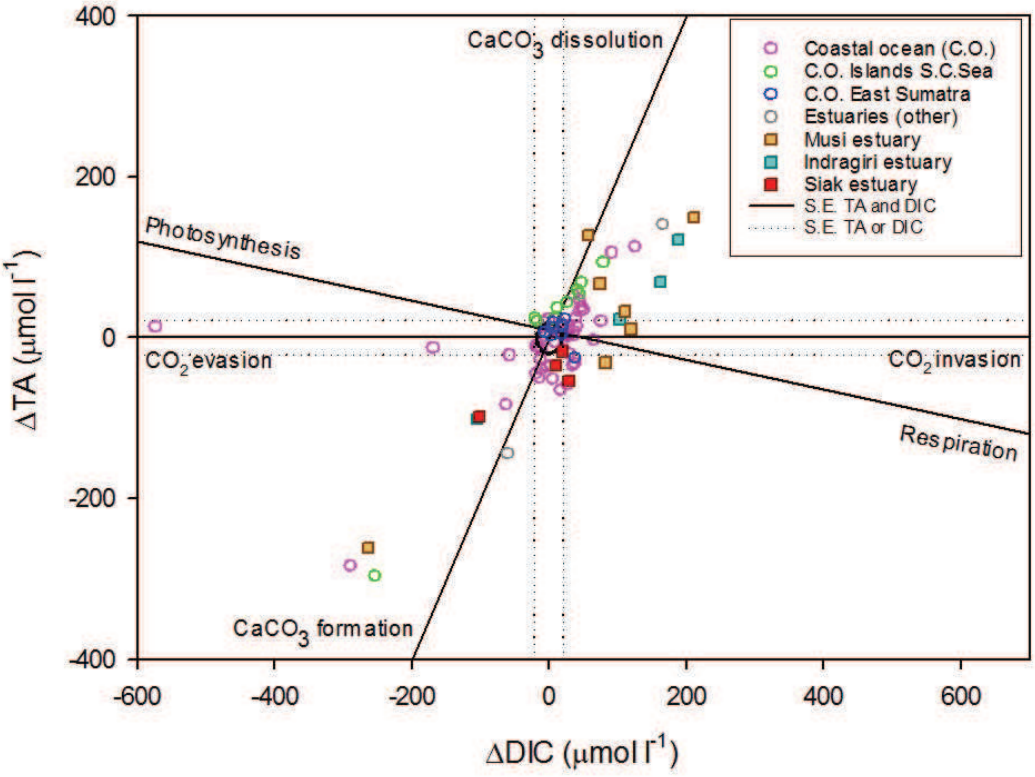

Figure 5.8 Deviations of DIC and TA for the Musi, Indragiri and Siak estuaries, as well as other estuaries and the coastal ocean (C.O.). The black solid lines show the processes that occur corresponding to the ratio of increase or decrease of DIC and TA, namely photosynthesis/respiration, CO_2 invasion/evasion and $CaCO_3$ formation/dissolution. Data points within the black s.e. circle have no significant deviations for both TA or DIC and indicate the process of mixing, whereas the direction and degree of deviation away from the s.e. circle point to other processes as indicated by the black solid lines in the plot. Data points in between lines show a mixture of the neighboring processes. Modified after Zeebe & Wolf-Gladrow (2001).

coastal ocean as well, through reduced calcification rates, but also reef dissolution. Indeed, coral reefs relatively close to the study site were recently identified as 'dark spots', characterized among other things to be affected by environmental shocks such as coral bleaching (Cinner et al. 2016), the latter of which may be an effect of lowered saturation states (Anthony et al. 2008). The disappearance of carbonate-producing reef organisms would have vast ecological and economic impacts as the trophic system becomes disturbed, thereby affecting biodiversity, sediment production and sequestration, in addition to destabilization of the coast (Bunkley-Williams & Williams 1990).

5.3.4 The invisible carbon footprint

In Sumatra 62.7% of the exported total carbon (13.6 of 21.6 Tg yr^{-1}) is emitted from the estuaries and coastal ocean and 10% of its organic carbon export is assumed to be sequestered in the sediments. Adopting similar emission and burial percentages for entire Indonesia with its total carbon export of 78.7 Tg yr^{-1} and organic carbon export of 53.1 Tg yr^{-1}, the CO_2 emissions from the estuaries and coastal ocean result in a total of 49.4 Tg yr^{-1} with another 5.3 Tg yr^{-1} buried in the sediments (Figure 5.9). The remaining exported carbon of 24.1 Tg C yr^{-1} (30.6%) remains in the marine waters where it further respires and favors $CaCO_3$

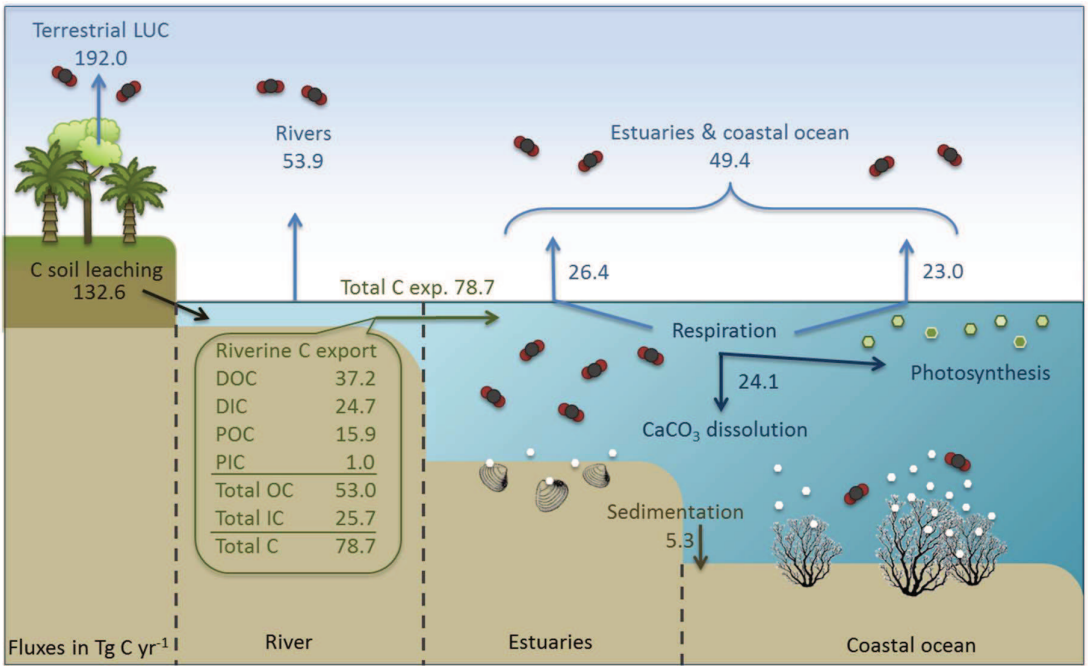

Figure 5.9 Overview of the carbon fluxes (Tg C yr^{-1}) in the rivers, estuaries and coastal ocean in Indonesia. With the exception of the terrestrial LUC emissions, all fluxes include a portion of the natural background emission from pristine peatlands of 13.0 Tg yr^{-1} in total.

dissolution by lowering the saturation states. As saturation states are lowered by inputs of Ca^{2+}-poor and acidic freshwater, this situation is induced by the peatlands, which overlie mineral soils thereby reducing weathering, and moreover produce an acidic CO_2-rich environment through decomposition of leached organic carbon in the rivers that extends into the estuaries and beyond. Having greatly increased DOC leaching from peat soils through degradation and land use change by 200% as compared to the natural situation (Rixen et al. 2016), anthropogenic disturbance may therefore be seen as a primary contributor to the low saturation states in the estuaries and, to a lesser extent, the coastal ocean. The respired carbon that remains in the ocean and favors carbonate dissolution can therefore be viewed as the invisible carbon footprint induced by LUC, which should be considered in terms of ocean acidification. UNESCO already recognizes ocean acidification as a serious threat and urges the United Nations Framework Convention on Climate Change (UNFCCC) to consider its negative effects on the ocean chemistry and marine ecosystem (UNESCO 2017). In addition, the UN Sustainable Development Goal 14 'Life below water' (UN 2017) aims to sustainably use marine resources and address the impact of ocean acidification. However, whereas this study shows that the effects of LUC stretch beyond the terrestrial realm, the invisible carbon footprint is currently overlooked in mitigation policies alongside the CO_2 emissions from the rivers, estuaries and coastal ocean, as the focus is on reducing direct terrestrial carbon emissions (Myers 2007; Smith P. et al. 2014; UNFCCC 2017).

In Southeast Asia, approximately 6% of the peatlands remain pristine, whereas 11% is covered by secondary vegetation and 81% is degraded and converted peatland cover (Miettinen et al. 2016). Assuming an even distribution, a peatland cover of 2.3 $*10^6$ km^2 and a yield of 433 g C m^{-2} yr^{-1} (Hirano et al. 2007), the direct terrestrial CO_2 emission from secondary vegetation in Indonesia amounts to 10.9 Tg C yr^{-1}. Its direct terrestrial CO_2 emissions due to LUC via peat oxidation and fires from the degraded and converted peatland cover result in 109.9 Tg yr^{-1} (Hooijer et al. 2010) and 82.1 Tg yr^{-1} (van der Werf et al. 2008), respectively, which amounts to a total direct terrestrial CO_2 emission of 192.0 Tg yr^{-1}. Carbon loss due to indirect emissions from the rivers (53.9 Tg yr^{-1}, (Wit et al. 2015)), estuaries and coastal ocean (49.4 Tg yr^{-1}), as well as the invisible carbon footprint (24.1 Tg yr^{-1}), amounts to 127.3 Tg C yr^{-1}. The natural indirect peatland emission can be deduced from the TOC leaching rate of pristine peatlands of 63 g m^{-2} yr^{-1} (Moore et al. 2013), excluding a 10% sedimentation rate, and amounts to 13.0 Tg C yr^{-1}. Subtracting this natural indirect emission results in a total indirect LUC emission of 114.3 Tg C yr^{-1}. Including the direct emissions of 192.0 Tg C yr^{-1}, the total carbon loss due to LUC amounts to 306.3 Tg yr^{-1}, which represents

an increase of 60% with respect to the direct terrestrial emissions. Considering this large impact along with the environmental and economic effects on global climate and the marine ecosystem, it is of vital importance that LUC mitigation policies are not only limited to direct terrestrial greenhouse gas emissions, but also incorporate the aquatic and marine CO_2 emissions as well as the invisible carbon footprint.

5.4 End notes

5.4.1 Acknowledgements

We would like to thank all scientists and students from the University of Pekanbaru for the fieldwork assistance and the captain and crew of the Matahari-ku ship for their support. We are also grateful to the Federal German Ministry of Education, Science, Research and Technology (BMBF, Bonn grant number 03F0642–ZMT). Maps were drawn using ArcGIS 10.3 and calculations were executed with ArcGIS 10.2 and Python software, version 2.7

5.4.2 Author contributions

F.W. and T.R. designed the study. T.R. performed the Sumatra field data collection and A.B. the laboratory analysis in 2009. F.W. performed field data collection and laboratory analysis in 2012 and 2013. F.W. performed the data analysis and calculations and led the writing of the paper, including graph and table design. All authors discussed results and commented on the manuscript.

5.4.3 Author information

Data deposition statement

Reprint and permissions information is available at www.nature.com/reprints.

Competing financial interests

The authors declare no competing financial interests.

Corresponding author line

Correspondence and requests for materials should be addressed to F.W.
(francisca.wit@leibniz-zmt.de)

VI
General discussion

6.1 Grand picture

Globally, land use change is recognized as an important carbon source as it is responsible for circa 12.5% of anthropogenic greenhouse gas emissions in 2001–2010 (Friedlingstein et al. 2010). Increased awareness of CO_2 emissions due to deforestation and degradation has initiated the REDD, later REDD+, policy, which stands for 'Reducing Emissions from Deforestation and forest Degradation in developing countries, and the role of conservation, sustainable management of forests, and enhancement of forest carbon stocks in developing countries' (UNFCCC 2007, Couwenberg et al. 2010). Especially in Southeast Asia and Indonesia, where large-scale deforestation and peatland degradation occur, efforts have increased to quantify direct CO_2 emissions from peat soils as a consequence of oxidation, subsidence and deforestation (van der Werf et al. 2009; Hooijer et al. 2012; Hooijer et al. 2010; Hirano et al. 2007). More recently in Borneo it was discovered that peatland degradation actually increases the fluvial total organic carbon flux in river channels significantly compared to pristine peatlands (Moore et al. 2013), thereby shifting the focus of the impact of peatland degradation to a broader spectrum. Indeed, the findings of this PhD study bring attention to the fact that the impacts of tropical peatland degradation in Southeast Asia are not limited to direct CO_2 emissions due to drainage and deforestation, but also greatly affect the carbon cycle of adjacent freshwater and marine environments through a variety of processes. Besides the direct CO_2 emissions, peatland degradation induces enhanced mobilization of organic carbon from soils. By means of a mixing model it was shown that dissolved organic carbon leaching from disturbed peat soils has increased by 200% from 62 to 183 g m^{-2} yr^{-1} as a consequence of hydrological changes and secondary vegetation. Increased freshwater fluxes due to reduced evapotranspiration account for 38% of the increase in carbon leaching. Contrary to endemic plants, leaves of secondary vegetation are less resistant to degradation and therefore more DOC is leached from secondary leaf litter,

which is responsible for the remaining 62% increase. Once the organic carbon has reached the rivers, it is either respired and emitted to the atmosphere (river outgassing) or exported to the coastal ocean (riverine carbon export). In six rivers in Southeast Asia, namely the Musi, Batanghari, Indragiri and Siak rivers in Sumatra, Indonesia, and the Lupar and Saribas rivers in Sarawak, Malaysia, correlations of pCO_2, DOC and oxygen concentrations show that the DOC concentration is the main factor controlling the CO_2 and oxygen concentrations in the rivers through the process of decomposition. Subsequently, it is disturbed peat coverage that controls the DOC concentrations through carbon leaching from peat soils, with increasing DOC concentrations as the share of disturbed peatland coverage in the catchment increases. Although positively correlated, CO_2 concentrations start to level off at a peat coverage higher than 25%, despite continuously increasing DOC concentrations. This may be attributed to a limitation of bacterial production as a consequence of low pH due to an acidic environment, oxygen depletion or the refractory nature of peat-derived DOC. Based on the regression between peat coverage and CO_2 yield, the CO_2 fluxes from rivers in Malaysia, Indonesia and Southeast Asia have been estimated to be 6.2±1.6, 53.9 ±12.4 and 66.9±15.7 Tg C yr^{-1}, respectively. However, compared to flux predictions from global estimates, these fluxes are rather moderate. The primary reasons for this include the short residence time of the river waters and the location of peat close to the coast, which further shortens the time available for decomposition. By comparing the CO_2 emissions with the riverine DOC fluxes, it appears that 53.3% of the carbon that enters the freshwater system in Southeast Asia is emitted as CO_2 to the atmosphere, whereas the remaining 46.7% is exported to the coastal ocean. Using mixing lines based on total alkalinity (TA), DIC and pCO_2 measurements in the estuaries and coastal ocean of Sumatra, it was shown that the majority of this exported carbon is respired in the estuaries. In total, circa 63% of the respired exported total carbon is emitted to the atmosphere in the estuaries and coastal ocean, whereas circa 6% of its organic content is assumed to be sequestered in the sediments and circa 31% is absorbed in the water column. Here, the respired CO_2 contributes to ocean acidification and lowers the aragonite and calcite saturation states (Ω_{AR} / Ω_{CA}). This induces carbonate dissolution of the carbonate content in sediments, but also calcifying organisms and possibly even coral reefs. Indeed, the carbonate content of the sediments has a positive correlation to the number of mollusk species and their abundance, and shows an increasing gradient from the river mouths towards the ocean in accordance with increasing Ω_{AR} / Ω_{CA}. Furthermore, coral reefs relatively close to the study site were recently identified as ‘dark spots’, characterized among other things to be affected by environmental shocks such as coral bleaching which may be an effect of lowered

saturation states. The disappearance of these carbonate-producing reef organisms in general would have vast ecological and economic impacts as the trophic system becomes disturbed affecting biodiversity, sediment production and sequestration, in addition to destabilization of the coast, all of which ultimately affect tourism and fisheries (Bunkley-Williams & Williams 1990). As saturation states are lowered by inputs of Ca^{2+}-poor and acidic freshwater, this situation is induced by the peatlands, which overlie mineral soils thereby reducing weathering, and moreover produce an acidic CO_2-rich environment through decomposition of leached organic carbon in the rivers. Having greatly increased the DOC leaching from soils through degradation and land use change, human disturbance may therefore be seen as the main contributor to the low saturation states in the estuaries and coastal ocean. The portion of respired exported carbon that remains in the ocean can therefore be viewed as the invisible carbon footprint induced by LUC. Therefore, it should be considered in greenhouse gas mitigation policies, especially in terms of ocean acidification, alongside the consequential river outgassing and marine CO_2 emissions. UNESCO recognizes the effects of ocean acidification on the ocean chemistry and marine ecosystem and has urged the United Nations Framework Convention on Climate Change (UNFCCC) to consider these impacts. Additionally, the UN Sustainable Development Goal 14 'Life below water', aims to sustainably use marine resources and address the impact of ocean acidification. However, currently UNFCCC greenhouse gas mitigation policies such as REDD+ are focused on reducing direct, terrestrial CO_2 emissions (UNFCCC 2008).

6.2 Perspectives and outlook for Indonesia

With respect to land use change in Indonesia, the direct terrestrial emissions from the 81% of degraded and converted peatland cover (Miettinen et al. 2016) via peat oxidation and forest fires add up to 109.9 Tg yr^{-1} (Hooijer et al. 2010) and 82.1 Tg yr^{-1} (van der Werf et al. 2008), respectively. Secondary vegetation involves a land use change which remains a carbon loss through a negative net ecosystem production (NEP) of 433 g m^{-2} yr^{-1} (Hirano et al. 2007) and, considering that it covers approximately 11% of the peatland coverage (Miettinen et al. 2016) of 2.3 *10^6 km^2, contributes 10.9 Tg C yr^{-1} to LUC emissions. Therefore, the total direct terrestrial CO_2 emissions due to LUC in Indonesia amount to 192.0 Tg C yr^{-1}. However, based on the findings of this PhD study, the effects of land use change and peat degradation exceed the terrestrial boundaries and also influence freshwater and marine systems. Indeed, carbon loss due to indirect emissions from the rivers (53.9 Tg yr^{-1}, (Wit et al. 2015)), estuaries and coastal ocean (49.4 Tg yr^{-1}), as well as the invisible carbon footprint (24.1 Tg yr^{-1}) and

excluding the natural emissions from pristine peatlands (13.0 Tg C yr^{-1}) amounts to 114.3 Tg C yr^{-1}. Therefore, the total carbon loss due to LUC amounts to 306.3 Tg yr^{-1}, which represents an increase of 60% with respect to the direct terrestrial emissions. In comparison, Indonesia ranked 12th place in the world list of emissions from fossil-fuel burning, cement production and gas flaring in 2013 with 130.7 Tg yr^{-1} (Boden et al. 2016). Along with the environmental and economic effects on global climate and the marine ecosystem, it is therefore of vital importance that LUC mitigation policies are not only limited to direct terrestrial greenhouse gas emissions, but also incorporate the aquatic and marine CO_2 emissions as well as the invisible carbon footprint.

Besides CO_2 emissions, ocean acidification and carbonate dissolution, land use change and peat degradation also result in soil subsidence as a consequence of oxidation and water loss. With an estimated subsidence of 1.3 cm yr^{-1}, soil subsidence forms a threat to the stability of the coastal peat plains, which cover 10% of the Indonesian land mass, which should not be underestimated.

With respect to the development of climate change mitigation strategies as one of the overarching goals of SPICE and CISKA, the advice is to develop measures for an additional 60% of CO_2 uptake in addition to terrestrial LUC carbon losses, in order to compensate for carbon losses due to indirect LUC emissions from the rivers, estuaries and coastal ocean, as well as the invisible carbon footprint. This may be best achieved by starting at the source of the problem, which would mean to reduce soil carbon leaching and thereby fluvial carbon export in order to mitigate the impact of CO_2 emissions, ocean acidification and carbonate dissolution. Although efforts are made with respect to reforestation, the findings of this PhD study indicate that the secondary vegetation enhances carbon leaching from soils due to hydrological changes and relatively labile DOC from the leaves. To negate these effects, it would be more beneficial to use endemic vegetation for reforestation purposes.

Furthermore, restoring the high water table in the peatlands will lead to reduced flooding through enhanced water retention and reduce forest fires (Miettinen & Liew 2010; Turetsky et al. 2015), and will enhance carbon sequestration and reverse soil subsidence in the process (Hooijer et al. 2006).

6.3 Global relevance

In terms of global relevance, the findings of this study show that Southeast Asia is not such a hotspot for tropical river outgassing as previously thought. Indeed, with 66.9 Tg C yr^{-1} for Southeast Asia and 53.9 Tg C yr^{-1} for Indonesia, river outgassing fluxes are rather moderate.

This can primarily be accounted to the location of the peatlands near the coast, which limits the decomposition of leached carbon in the rivers by reducing its residence time in the river. However, Southeast Asia remains to have one of the largest exports with respect to organic carbon (Harrison et al. 2005), which in Indonesia amounts to 53.1 Tg C yr^{-1} as calculated in this study. In large rivers having a longer residence time, the majority of the organic carbon can be decomposed and emitted to the atmosphere, resulting in a large CO_2:TOC ratio of for instance 13:1 in the case of the Amazon river (Richey et al. 2002). However, the CO_2:TOC ratio in Indonesia is approximately 1:1, which means that a relatively large share of organic carbon is exported to the estuaries and coastal ocean. Indeed, it appears that the short residence time of rivers creates relatively modest CO_2 emissions in the rivers, but in fact shifts this process of CO_2 emission to the estuaries and coastal ocean where the majority of the exported organic carbon is respired.

Furthermore, this study shows that the effects of land use change reach beyond the terrestrial realm and also affect the estuaries and coastal ocean. In addition, the effects are not only concerned with CO_2 emissions, but due to the fact that not all respired CO_2 is emitted to the atmosphere, another consequence entails direct ocean acidification. This results in lower aragonite and calcite saturation states as the CO_3^{2-} concentration is reduced as the marine carbonate system aims to buffer the increase in CO_2 concentration. At Ω_{AR} / Ω_{CA} < 1, this favors net carbonate dissolution of carbonate sediments, but also calcifying organisms such as mollusks and coral reefs, thereby lowering their calcification rates. As large organic carbon exports are not limited to Indonesia and Southeast Asia, these processes may in fact be applicable to more tropical estuaries and coastal oceans.

Finally, in contrast to secondary plants, leaves of endemic tropical peat plants are more resistant to degradation and therefore less DOC is leached from endemic leaf litter. Therefore, afforestation of secondary vegetation with relatively labile leaf content may reduce the potential terrestrial CO_2 emissions by its ecosystem production, but at the same time increases carbon leaching from the soils. For restoration purposes in tropical peat areas, it is therefore important to aim to restore the original circumstances with respect to groundwater table, as well as endemic plant species.

VII

Main conclusions

7.1 Background

In Southeast Asia and Indonesia, land use change (LUC) occurs in the form of large-scale deforestation and peatland degradation for agricultural purposes, which causes terrestrial CO_2 emissions from peat soils as a consequence of oxidation, subsidence and forest fires. However, the consequences of this peatland degradation for the aquatic and marine environment and carbon cycle are less well known. In the framework of the SPICE III – CISKA subproject 1, the impacts of land use change in Indonesia were determined by the quantification of the inorganic and organic carbon fluxes and CO_2 emissions from the rivers, estuaries and coastal ocean into the atmosphere as well as the marine carbonate system in order to subsequently develop sustainable mitigation strategies to reduce CO_2 emissions. Below the main conclusions of this study are listed per topic.

7.2 Manuscript 1: River outgassing

- DOC concentrations in the rivers are positively correlated with pCO_2 concentrations and inversely correlated with oxygen concentrations, which shows that DOC decomposition is the main factor controlling the pCO_2 concentrations in the rivers.
- DOC and pCO_2 yields are positively correlated with disturbed peatland coverage, which shows that DOC leaching from peat soils is the source for the CO_2 production via decomposition.
- As opposed to the DOC yield, the CO_2 yield levels off after a disturbed peat coverage larger than 25%. This may be attributed to reduced microbial productivity as a consequence of oxygen depletion, low pH or refractory content of the DOC substrate.
- In Southeast Asia, approximately 53.5% of the carbon that enters the rivers is decomposed and emitted as CO_2 to the atmosphere.

- River outgassing in Malaysia, Indonesia and Southeast Asia amounts to 6.2 Tg C yr^{-1}, 53.9 Tg C yr^{-1} and 66.9 Tg C yr^{-1}, respectively.
- River outgassing in Southeast Asia is moderate when compared to global model findings and is not a river outgassing hotspot as previously thought.
- The reasons for the moderate river outgassing is the relatively short residence time of the river waters, which inhibits the available time for DOC decomposition in the rivers. In addition, the peatlands, which are the main source of DOC, are located on the coastal plains, which further shortens the available decomposition time.

7.3 Manuscript 2: Carbon leaching

- The results of the mixing model experiments showed that leaching of leaf litter from secondary forest plants dominates at the top of the acrotelm (DOC groundwater concentration of 16,222 μM) and leaf litter leaching from endemic peat vegetation gains importance toward the base of the acrotelm (DOC groundwater concentration of 5,333 μM) with an approximate acrotelm depth of 57.4 cm.
- Soil carbon leaching has increased from 62 g m^{-2} yr^{-1} in pristine peatlands to 183 g m^{-2} yr^{-1} in disturbed peatlands, which is an increase of almost 200%.
- Changes in the hydrological cycle and the regrowth of secondary forest plants explain 38% and 62% of the increase in DOC leaching from degraded peatlands, respectively. The reduced evapotranspiration increases freshwater discharge, whereas the secondary forest plants produce labile DOC, which is relatively easily degraded and leached from the soil.
- Peat carbon losses by oxidation and leaching lower the peat thickness by 1.30 cm yr^{-1}, which is a serious threat to the stability of the coastal peat plains that cover 10% of the Indonesian land mass.
- Leached ancient peat carbon is an irrecoverable loss of land that weakens the stability of peat-fringed coasts.
- Leached labile leaf litter of secondary vegetation supplies DOC of which the decomposition can lead to oxygen deficiencies in peat draining rivers.

7.4 Manuscript 3: Carbon export and coastal ocean processes

- The riverine carbon export of Sumatra amounts to 21.63 Tg C yr^{-1}, of which 10.72 Tg C yr^{-1} DOC, 5.82 Tg C yr^{-1} DIC, 4.87 Tg C yr^{-1} POC and 0.23 Tg C yr^{-1} PIC.

- The majority of the exported organic carbon is decomposed in the estuaries and emitted to the atmosphere with a CO_2 yield of 670.7 ±98.4 g C m^{-2} yr^{-1}.
- The coastal ocean of Sumatra is a carbon source with a CO_2 yield of circa 49.4 ±7.2 g m^{-2} yr^{-1}, which is in contrast with an earlier study that claimed it to be a carbon sink.
- The respired CO_2 that does not emit into the atmosphere remains in the marine water column, where it contributes to ocean acidification, lowers the saturation states and induces carbonate dissolution. With human disturbance as the main cause through enhanced carbon exports due to land use change, this carbon is therefore referred to as the invisible carbon footprint (ICFP).
- In Indonesia, direct LUC emissions from disturbed peatlands include secondary vegetation (10.9 Tg C yr^{-1}), forest fires (82.1 Tg C yr^{-1}) and peat oxidation (109.9 Tg C yr^{-1}) and amounts to 192.0 Tg C yr^{-1}. Indirect emissions from river outgassing (53.9 Tg C yr^{-1}), CO_2 emissions from estuaries and coastal ocean (49.4 Tg C yr^{-1}) and the invisible carbon footprint (24.1 Tg C yr^{-1}) amount to 114.3 Tg C yr^{-1}. This results in a total LUC emission of 306.3 Tg C yr^{-1}.
- Considering this large impact along with the environmental and economic effects on global climate and the marine ecosystem, it is of vital importance that LUC mitigation policies are not only limited to direct terrestrial greenhouse gas emissions, but also incorporate the aquatic and marine CO_2 emissions as well as the invisible carbon footprint.

7.5 Discussion

- In terms of global relevance, this study shows that the effects of land use change reach beyond the terrestrial realm and also affect the estuaries and coastal ocean in terms of CO_2 emissions, but also carbonate dissolution through the invisible carbon footprint.
- The findings of this study show that Southeast Asia is not such a hotspot for tropical river outgassing as previously thought. However, it appears that the short residence time of rivers creates relatively modest CO_2 emissions in the rivers, but in fact shifts this process of CO_2 emission to the estuaries and coastal ocean where the majority of the exported organic carbon is respired.
- With respect to the development of climate change mitigation strategies as one of the overarching goals of SPICE and CISKA, the advice is to develop measures for an additional 60% of CO_2 uptake in addition to terrestrial LUC carbon losses, in order to

compensate for carbon losses due to indirect LUC emissions from the rivers, estuaries and coastal ocean, as well as the invisible carbon footprint. This may be best achieved by starting at the source of the problem, which would mean to reduce soil carbon leaching and fluvial carbon export.

- In contrast to endemic tropical peat plants, leaves of secondary vegetation are relatively labile and therefore more DOC is leached from secondary leaf litter. For restoration purposes, it is therefore important to aim to restore the original circumstances with respect to groundwater table, as well as endemic plant species in order to avoid additional soil carbon leaching.

References

Alin, S.R. et al., 2011. Physical controls on carbon dioxide transfer velocity and flux in low-gradient river systems and implications for regional carbon budgets. *Journal of Geophysical Research: Biogeosciences*, 116(G1). Available at: http://dx.doi.org/10.1029/2010JG001398.

Alkhatib, M., Jennerjahn, T.C. & Samiaji, J., 2007. Biogeochemistry of the Dumai River estuary, Sumatra, Indonesia, a tropical black-water river. *Limnology and Oceanography*, 52(6), pp.2410–2417.

Andersson, A.J., 2013. The Oceanic CaCO3 Cycle. *Treatise on Geochemistry: Second Edition*, 8, pp.519–542.

Andersson, A.J., MacKenzie, F.T. & Lerman, A., 2005. Coastal ocean and carbonate systems in the high CO2 world of the anthropocene. *American Journal of Science*, 305(9), pp.875–918.

Anon, 2015. DWD Global Precipitation Climatology Centre (GPCC). Available at: http://kunden.dwd.de/GPCC/Visualizer.

Anthony, K.R.N. et al., 2008. Ocean acidification causes bleaching and productivity loss in coral reef builders. *Proceedings of the National Academy of Sciences of the United States of America*, 105(45), pp.17442–17446. Available at: http://www.pubmedcentral.nih.gov/articlerender.fcgi?artid=2580748&tool=pmcentrez&rendertype=abstract%5Cnhttp://www.ncbi.nlm.nih.gov/pubmed/18988740.

Archer, D., Kheshgi, H. & Maier-Reimer, E., 1998. Dynamics of fossil fuel CO2 neutralization by marine CaCO3. *Global Biogeochemical Cycles*, 12(2), pp.259–276.

Battin, T.J. et al., 2009. The boundless carbon cycle. *Nature Geoscience*, 2(9), pp.598–600. Available at: http://www.nature.com/doifinder/10.1038/ngeo618 [Accessed April 28, 2014].

Bauer, J.E. et al., 2013. The changing carbon cycle of the coastal ocean. *Nature*, 504(7478), pp.61–70. Available at: http://www.ncbi.nlm.nih.gov/pubmed/24305149.

Baum, A., 2008. *Tropical blackwater biogeochemistry: The Siak River in Central Sumatra, Indonesia*.

Baum, A., Rixen, T. & Samiaji, J., 2007. Relevance of peat draining rivers in central Sumatra for the riverine input of dissolved organic carbon into the ocean. *Estuarine, Coastal and Shelf Science*, 73(3–4), pp.563–570. Available at:

http://linkinghub.elsevier.com/retrieve/pii/S0272771407000637.

Bennett, A.S., 1976. Conversion of in situ measurements of conductivity to salinity. *Deep Sea Research and Oceanographic Abstracts*, 23(2), pp.157–165. Available at: http://dx.doi.org/10.1016/S0011-7471(76)80024-1.

Blair, N.E. & Aller, R.C., 2012. The Fate of Terrestrial Organic Carbon in the Marine Environment. *Annual review of marine science*, 4, pp.401–423.

Boden, T., Andres, B. & Marland, G., 2016. CDIAC: Carbon Dioxide Information Analysis Center. Available at: http://cdiac.ornl.gov/CO2_Emission/timeseries/global.

Borges, A. V. et al., 2015. Globally significant greenhouse-gas emissions from African inland waters. *Nature Geoscience*, 8(July), pp.637–642. Available at: http://www.nature.com/doifinder/10.1038/ngeo2486.

Borges, A. V, Delille, B. & Frankignoulle, M., 2005. Budgeting sinks and sources of CO2 in the coastal ocean: Diversity of ecosystems counts. *Geophysical Research Letters*, 32(March), pp.1–6.

Bunkley-Williams, L. & Williams, E.H., 1990. Global Assault on Coral Reefs. *Natural History*, 4(90), pp.46–54.

Butman, D. & Raymond, P.A., 2011. Significant efflux of carbon dioxide from streams and rivers in the United States. *Nature Geoscience*, 4(12), pp.839–842. Available at: http://www.nature.com/doifinder/10.1038/ngeo1294.

Cai, W., 2011. Estuarine and Coastal Ocean Carbon Paradox: CO2 Sinks or Sites of Terrestrial Carbon Incineration? *Annual review of marine science*, 3, pp.123–145.

Castillo, M.M., Kling, G.W. & Allan, J.D., 2003. Bottom-up controls on bacterial production in tropical lowland rivers. *Limnology and Oceanography*, 48(4), pp.1466–1475.

Chen, C.A. et al., 2013. Air – sea exchanges of CO2 in the world's coastal seas. *Biogeosciences*, 10, pp.6509–6544.

Ciais, P. et al., 2013. Carbon and Other Biogeochemical Cycles. In: Climate Change 2013: The Physical Science Basis. Contribution of Working Group I to the Fifth Assessment Report of the Intergovernmental Panel on Climate Change.

Ciais, P. et al., 2013. *Carbon and Other Biogeochemical Cycles. In: Climate Change 2013: The Physical Science Basis. Contribution of Working Group I to the Fifth Assessment Report of the Intergovernmental Panel on Climate Change*, Cambridge, United Kingdom and New York, NY, USA.

Cinner, J.E. et al., 2016. Bright spots among the world's coral reefs. *Nature*, 535(7612),

pp.416–432. Available at: http://www.nature.com/doifinder/10.1038/nature18607.

Clark, J.M. et al., 2007. Export of dissolved organic carbon from an upland peatland during storm events: Implications for flux estimates. *Journal of Hydrology*, 347(3–4), pp.438–447.

Clark, J.M. et al., 2008. Link between DOC in near surface peat and stream water in an upland catchment. *Science of the Total Environment*, 404(2–3), pp.308–315.

Cole, J.J. et al., 2007. Plumbing the Global Carbon Cycle: Integrating Inland Waters into the Terrestrial Carbon Budget. *Ecosystems*, 10(1), pp.172–185. Available at: http://link.springer.com/10.1007/s10021-006-9013-8 [Accessed April 28, 2014].

Couwenberg, J., Dommain, R. & Joosten, H., 2010. Greenhouse gas fluxes from tropical peatlands in south-east Asia. *Global Change Biology*, 16(6), pp.1715–1732.

Doctor, D.H. et al., 2008. Carbon isotope fractionation of dissolved inorganic carbon (DIC) due to outgassing of carbon dioxide from a headwater stream. *2Hydrological Processes*, 22, pp.2410–2423.

Doney, S.C., 2010. The growing human footprint on coastal and open-ocean biogeochemistry. *Science*, 328(5985), pp.1512–1516. Available at: http://www.ncbi.nlm.nih.gov/pubmed/20558706.

Doney, S.C., 2010. The Growing Human Footprint on Coastal and Open-Ocean Biogeochemistry. *Changing Oceans*, 328.

Driessen, P. (Wageningen A.U. and I.I. for A.S. and E.S. et al., 2001. *Lecture Notes on the Major Soils of the World*,

Ekayanti, N.W. & Rahman as-syakur, A., 2011. CO2 flux in Indonesian water determined by satellite data. *International journal of remote sensing and earth sciences*, 8, pp.1–12.

FAO/UNESCO, 2004. Digital soil map of the world and derived soil properties.

Friedlingstein, P. et al., 2010. Update on CO2 emissions. *Nature Geoscience*, 3(12), pp.811–812. Available at: http://dx.doi.org/10.1038/ngeo1022.

Gentilli, J., Smith, P.J. & Krishnamurti, T.N., 2014. Malaysian-Australian monsoon. *Encyclopaedia Britannica*. Available at: www.britannica.com/science/Malaysian-Australian-monsoon.

Griffith, D.W.T. et al., 2012. A Fourier transform infrared trace gas and isotope analyser for atmospheric applications. *Atmospheric Measurement Techniques*, 5(10), pp.2481–2498. Available at: http://www.atmos-meas-tech.net/5/2481/2012/.

Harrison, J.A., Caraco, N. & Seitzinger, S.P., 2005. Global patterns and sources of

dissolved organic matter export to the coastal zone: Results from a spatially explicit, global model. *Global Biogeochemical Cycles*, 19(4).

Hartmann, J. et al., 2011. GLORICH: Global river and estuary chemical database. *ASLO*.

Hirano, T. et al., 2007. Carbon dioxide balance of a tropical peat swamp forest in Kalimantan, Indonesia. *Global Change Biology*, 13(2), pp.412–425.

Ho, D.T., Schlosser, P. & Orton, P.M., 2011. On Factors Controlling Air-Water Gas Exchange in a Large Tidal River. *Estuaries and Coasts*, 34, pp.1103–1116.

Hooijer, A. et al., 2010. Current and future CO2 emissions from drained peatlands in Southeast Asia. *Biogeosciences*, 7(5), pp.1505–1514. Available at: http://www.biogeosciences.net/7/1505/2010/ [Accessed September 29, 2014].

Hooijer, A. et al., 2006. PEAT-CO2, Assessment of CO2 emissions from drained peatlands in SE Asia. *Delft Hydraulics report Q3943*.

Hooijer, A., Page, S., Jauhiainen, J., Lee, W.A., et al., 2012. Subsidence and carbon loss in drained tropical peatlands. *Biogeosciences*, 9(3), pp.1053–1071.

Hooijer, A., Page, S., Jauhiainen, J., Lee, W. a., et al., 2012. Subsidence and carbon loss in drained tropical peatlands. *Biogeosciences*, 9, pp.1053–1071.

Houghton, R.A. et al., 2012. Carbon emissions from land use and land-cover change. *Biogeosciences*, 9(12), pp.5125–5142.

Huang, T. et al., 2012. Fluvial carbon fluxes in tropical rivers. *Current Opinion in Environmental Sustainability*, 4(2), pp.162–169. Available at: http://dx.doi.org/10.1016/j.cosust.2012.02.004.

Huotari, J. et al., 2013. Efficient gas exchange between a boreal river and the atmosphere. *Geophysical Research Letters*, 40, pp.5683–5686.

Iglesias-Rodríguez, M.D. et al., 2002. Progress made in study of ocean's calcium carbonate budget. *Eos, Transactions American Geophysical Union*, 83(34), pp.365–375. Available at: http://doi.wiley.com/10.1029/2002EO000267%5Cnpapers3://publication/doi/10.1029/2002EO000267%5Cnhttp://doi.wiley.com/10.1029/2002EO000267.

Johnson, J.E., 1999. Evaluation of a seawater equilibrator for shipboard analysis of dissolved oceanic trace gases. *Analytica Chimica Acta*, 395(1–2), pp.119–132. Available at: http://linkinghub.elsevier.com/retrieve/pii/S000326709900361X.

Joosten, H., Tapio-Biström, M.-L. & Tol, S., 2012. Peatlands - Guidance for climate change mitigation by conservation, rehabilitation and sustainable use. Mitigation of Climate Change in Agriculture Series 5. *Proceedings of the Soil Science Conference of*

Malaysia.

Langdon, C. & Atkinson, M.J., 2005. Effect of elevated pCO2 on photosynthesis and calcification of corals and interactions with seasonal change in temperature/ irradiance and nutrient enrichment. *Journal of Geophysical Research C: Oceans*, 110(9), pp.1–16.

Laruelle, G.G. et al., 2014. Regionalized global budget of the CO2 exchange at the air-water interface in continental shelf areas. *Global Biogeochemical Cycles*, 28, pp.1199–1214.

Laruelle, G.G. et al., 2014. Seasonal response of air-water CO2 exchange along the land-ocean aquatic continuum of the North East American coast. *Biogeosciences*, pp.11985–12008.

Lauerwald, R. et al., 2015. Spatial patterns in CO2 evasion from the global river network. *Global Biogeochemical Cycles*, 29, pp.1–21.

Manzello, D.P. et al., 2008. Poorly cemented coral reefs of the eastern tropical Pacific: Possible insights into reef development in a high-CO2 world. *Pnas*, 105(30), pp.10450–10455.

Melling, L. et al., 2007. Biophysical Characteristics of Tropical Peatland. *Proceedings of the Soil Science Conference of Malaysia*, 1917, pp.1–11.

Meybeck, M., Dürr, H. & Vörösmarty, C., 2006. Global coastal segmentation and its river catchment contributors: A new look at land-ocean linkage. *Global Biogeochemical Cycles*, 20(1).

Michel, J. et al., 2015. Molluscan assemblages under the influence of peat-draining rivers off East Sumatra, Indonesia. *Molluscan Research*, 35(2), pp.81–94. Available at: http://resolver.scholarsportal.info/resolve/13235818/v35i0002/81_mautioproesi.

Miettinen, J. et al., 2012. Historical Analysis and Projection of Oil Palm Plantation Expansion on Peatland in Southeast Asia. *International Council on Clean Transportation*, 22.

Miettinen, J. & Liew, S.C., 2010. Degradation and development of peatlands in Peninsular Malaysia and in the islands of Sumatra and Borneo since 1990. *Land Degradation and Development*, 21(February), pp.285–296.

Miettinen, J., Shi, C. & Liew, S.C., 2016. Land cover distribution in the peatlands of Peninsular Malaysia, Sumatra and Borneo in 2015 with changes since 1990. *Global Ecology and Conservation*, 6, pp.67–78. Available at: http://dx.doi.org/10.1016/j.gecco.2016.02.004.

Milliman, J.D. & Farnsworth, K.L., 2011. *River discharge to the coastal ocean: a global synthesis*, Cambridge University Press.

Moore, S. et al., 2013. Deep instability of deforested tropical peatlands revealed by fluvial organic carbon fluxes. *Nature*, 493(7434), pp.660–3. Available at: http://www.ncbi.nlm.nih.gov/pubmed/23364745.

Moore, T.R. & Jackson, R.J., 1989. Dynamics of dissolved organic carbon in forested and disturbed catchments, Westland, New Zealand: 2. Larry River. *Water Resources Research*, 25(6), p.1331.

Müller, D. et al., 2015. *Fate of peat-derived carbon and associated CO2 and CO emissions from two Southeast Asian estuaries*, Available at: http://www.biogeosciences-discuss.net/12/8299/2015/.

Müller, D., 2015. *Water-atmosphere greenhouse gas exchange measurements using FTIR spectrometry*.

Myers, E.C., 2007. Policies to Reduce Deforestation and. *Bat conservation international*, (December), p.80.

Nachtergaele, F., Velthuizen, H. Van & Verelst, L., 2009. *Harmonized world soil database*,

Nightingale, P.D. et al., 2000. In situ evaluation of air-sea gas exchange parameterizations using novel conservative and volatile tracers. *Global Biogeochemical Cycles*, 14(1), pp.373–387.

Noriega, C. & Araujo, M., 2014. Carbon dioxide emissions from estuaries of northern and northeastern Brazil. *Scientific reports*, 4(6164), pp.1–9.

Page, S.E., Rieley, J.O. & Banks, C.J., 2011. Global and regional importance of the tropical peatland carbon pool. *Global Change Biology*, 17(2), pp.798–818.

Page, S.E., Rieley, J.O. & Banks, C.J., 2010. Global and regional importance of the tropical peatland carbon pool. *Global Change Biology*, 17(2).

Polsenaere, P. & Abril, G., 2012. Modelling CO2 degassing from small acidic rivers using water pCO2, DIC and δ13C-DIC data. *Geochimica et Cosmochimica Acta*, 91, pp.220–239.

Raymond, P.A. et al., 2013. Global carbon dioxide emissions from inland waters. *Nature*, 503(7476), pp.355–9. Available at: http://www.ncbi.nlm.nih.gov/pubmed/24256802.

Raymond, P.A. & Cole, J.J., 2001. Technical Notes and Comments Gas Exchange in Rivers and Estuaries: Choosing a Gas Transfer Velocity. *Estuaries*, 24(2), pp.312–317.

Raymond, P. a. et al., 2012. Scaling the gas transfer velocity and hydraulic geometry in streams and small rivers. *Limnology & Oceanography: Fluids & Environments*, 2,

pp.41–53. Available at: http://lofe.dukejournals.org/cgi/doi/10.1215/21573689-1597669.

Regnier, P. et al., 2013. Anthropogenic perturbation of the carbon fluxes from land to ocean. *Nature Geoscience*, 6(8), pp.597–607. Available at: http://www.nature.com/doifinder/10.1038/ngeo1830.

Reuter, H.I., Nelson, A. & Jarvis, A., 2009. *An evaluation of void filling interpolation methods for SRTM data*, Available at: http://dx.doi.org/10.1080/13658810601169899.

Ricciardulli, L., Wentz, F.J. & Smith, D.K., 2011. Remote Sensing Systems QuikSCAT Ku-2011 Monthly Ocean Vector Winds on 0.25 deg grid, Version 4. *Remote Sensing Systems, Santa Rosa, CA*. Available at: www.remss.com/missions/qscat.

Richey, J.E. et al., 2002. Outgassing from Amazonian rivers and wetlands as a large tropical source of atmospheric CO2. *Nature*, 416(6881), pp.617–20. Available at: http://www.ncbi.nlm.nih.gov/pubmed/11948346.

Rixen, T. et al., 2016. Carbon Leaching from Tropical Peat Soils and Consequences for Carbon Balances. *Frontiers in Earth Science*, 4(July). Available at: http://journal.frontiersin.org/article/10.3389/feart.2016.00074.

Rixen, T. et al., 2008. The Siak, a tropical black water river in central Sumatra on the verge of anoxia. *Biogeochemistry*, 90(2), pp.129–140. Available at: http://link.springer.com/10.1007/s10533-008-9239-y.

van Rossum, G., 2007. Python language reference, version 2.7.

Sarma, V.V.S.S. et al., 2012. Carbon dioxide emissions from Indian monsoonal estuaries. *Geophysical Research Letters*, 39(3), pp.1–5.

Sarmiento, J.L. & Gruber, N., 2005. *Ocean Biogeochemical Dynamics*,

Schiff, S. et al., 1998. Precambrian shield wetlands: Hydrologic control of the sources and export of dissolved organic matter. *Climatic Change*, 40(2), pp.167–188.

Schindlbacher, A. et al., 2015. Contribution of carbonate weathering to the CO2 efflux from temperate forest soils. *Biogeochemistry*, 124, pp.273–290.

Schlünz, B. & Schneider, R.R., 2000. Transport of terrestrial organic carbon to the oceans by rivers: re-estimating flux and burial rates. *International Journal of Earth Sciences*, 88, pp.599–606.

Schneider, U. et al., 2015. Global Precipitation Analysis Products of the GPCC. *Internet Publication*, (May), pp.1–13. Available at: ftp://ftp-anon.dwd.de/pub/data/gpcc/PDF/GPCC_intro_products_2008.pdf.

Schneider, U. et al., 2011. GPCC Monitoring Product: Near Real-Time Monthly Land-

Surface Precipitation from Rain-Gauges based on SYNOP and CLIMAT data. Available at: http://dx.doi.org/10.5676/DWD_GPCC/MP_M_V4_100.

Schwarz, T., 2014. *Climate-Data*, Available at: en.climate-data.org.

Smith P. et al., 2014. *Agriculture, Forestry and Other Land Use (AFOLU). In: Climate Change 2014: Mitigation of Climate Change. Contribution of Working Group III to the Fifth Assessment Report of the Intergovernmental Panel on Climate Change [Edenhofer, O., R. Pichs-Madruga, Y.*, Cambridge, United Kingdom and New York, NY, USA.

Sonnerup, R.E. & Quay, P.D., 2012. 13C constraints on ocean carbon cycle models. *Global Biogeochemical Cycles*, 26(2), pp.1–16.

Sorensen, K.W., 1993. Indonesian peat swamp forests and their role as a carbon sink. *Chemosphere*, 27(6), pp.1065–1082.

Striegl, R.G. et al., 2012. Carbon dioxide and methane emissions from the Yukon River system. *Global Biogeochemical Cycles*, 26(4), p.GB0E05. Available at: http://dx.doi.org/10.1029/2012GB004306.

Takahashi, T. et al., 2009. Climatological mean and decadal change in surface ocean pCO2, and net sea–air CO2 flux over the global oceans. *Deep Sea Research Part II: Topical Studies in Oceanography*, 56(8–10), pp.554–577. Available at: http://linkinghub.elsevier.com/retrieve/pii/S0967064508004311.

Tranvik, L.J. et al., 2009. Lakes and reservoirs as regulators of carbon cycling and climate. *Limnology and Oceanography*, 54(1), pp.2298–2314.

Turetsky, M.R. et al., 2015. Global vulnerability of peatlands to fire and carbon loss. *Nature Geosci*, 8(1), pp.11–14. Available at: http://dx.doi.org/10.1038/ngeo2325.

UN, 2017. Development Goal 14. Available at: http://www.un.org/sustainabledevelopment/oceans/.

UNESCO, 2017. Implement Urgent Actions to Mitigate and Adapt to Ocean Acidification. Available at: http://www.unesco.org/new/en/natural-sciences/ioc-oceans/focus-areas/rio-20-ocean/10-proposals-for-the-ocean/1a-ocean-acidification/.

UNFCCC, 2017. FOCUS: Mitigation - Action on mitigation: Reducing emissions and enhancing sinks.

UNFCCC, 2008. Report of the Conference of the Parties on its thirteenth session, held in Bali from 3 to 15 December 2007. *Http://Unfccc.Int/Resource/Docs/2007/Cop13/Eng/06a01.Pdf*, pp.1–60. Available at: http://unfccc.int/resource/docs/2007/cop13/eng/06a01.pdf.

Wanninkhof, R., 1992. Relationship between wind speed and gas exchange over the ocean. *Journal of Geophysical Research: Oceans*, 97(C5), pp.7373–7382. Available at: http://dx.doi.org/10.1029/92JC00188.

Warren, M.W. et al., 2012. A cost-efficient method to assess carbon stocks in tropical peat soil. *Biogeosciences*, 9(11), pp.4477–4485.

Weiss, R.F., 1974. Carbon dioxide in water and seawater: the solubility of a non-ideal gas. *Marine Chemistry*, 2, pp.203–215.

van der Werf, G.R. et al., 2008. Climate regulation of fire emissions and deforestation in equatorial Asia. *Proceedings of the National Academy of Sciences of the United States of America*, 105(51), pp.20350–5. Available at: http://www.pnas.org/content/105/51/20350.short%5Cnpapers2://publication/uuid/C21236BF-F287-4A75-BC10-C71DD759AAEA.

van der Werf, G.R. et al., 2009. CO2 emissions from forest loss. *Nature Geosci*, 2(11), pp.737–738. Available at: http://dx.doi.org/10.1038/ngeo671.

Wessel, P. & Smith, W.H.F., 1998. New, improved version of the Generic Mapping Tools released. *EOS Trans. AGU*, 79, p.579.

Wit, F. et al., 2015. The impact of disturbed peatlands on river outgassing in Southeast Asia. *Nature Communications*, 6:10155, pp.1–9.

Worrall, F., Burt, T.P. & Adamson, J., 2006. The rate of and controls upon DOC loss in a peat catchment. *Journal of Hydrology*, 321(1–4), pp.311–325.

Wösten, J.H.M., Ismail, A.B. & Wijk, A.L.M. van, 1997. Peat subsidence and its practical implications: a case study in Malaysia. , 78, pp.25–36. Available at: http://edepot.wur.nl/147654.

Zeebe, R.E. & Wolf-Gladrow, D. a., 2001. Ch1: CO2 dynamics. In *CO2 in Seawater: Equilibrium, kinetics, isotopes*.

Acknowledgements

First of all, I would like to express my sincere gratitude to my supervisor Dr. Tim Rixen for giving me the opportunity to do this PhD and his overwhelming guidance, inspiration and knowledge throughout my research. I could not have imagined a better supervisor for my PhD study. In addition, I would like to thank Prof. Ulrich Saint-Paul for being part of my PhD panel and the insightful discussions during meetings.

With gratitude I want to acknowledge the support of the German Federal Ministry of Education and Research (BMBF) for providing the funds that made this PhD project possible in the framework of the project SPICE III.

I also wish to thank the other members of SPICE III subproject 1, Dr. Herbert Siegel, Iris Stottmeister, Dr. Dominik Kneer, Dr. Harald Asmus, Dr. Julien Michel, Dr. Bernhard Mayer and Dr. Thomas Pohlmann, for the enjoyable collaboration and field expeditions. Many thanks as well to the crew and scientific staff of the field expeditions on board the Matahari Ku vessel.

My PhD study would not have been possible without the valuable work of the lab technicians Dieter Peterke, Matthias Birkicht, Dorothee Dasbach, Achim Meyer and Christina Staschok. Moreover, I would like to thank the other ZMT staff members who assisted my PhD research in terms of logistical, administrative and technical support, particularly Ulrich Pint, Christoph Lutz and Kai Schrader for readily assisting with any technical issue, Olaf Thormann who went beyond his duties in teaching me the basics of Python, and Petra Käpnick and Gabriele Böhme who helped in all sort of matters.

Furthermore, I would like to give special thanks to Dr. Antje Baum for the translation of this thesis summary to German.

I want to give many, many thanks to all my friends and colleagues, who made my PhD time an absolute pleasure, with special thanks to my colleagues/friends/housemates Astrid Contreras, Huang Min Ge and Dieuwke Hoeijmakers for the marvelous company and chats over dinner and tea; and Maryam Shahraki, Alejandra Sepúlveda, Anita Flohr, Swati Sappal, Kim Vane, Debora Pestana, Celeste Sánchez, Marianna Audfroid, Lucy Gilles and Aline Quadros for all the fun and unforgettable moments we shared.

In addition, I would like to thank my friends at the Bremer-Badminton-Club, for welcoming me so warmly into their midst and for all the challenging matches and fun outings.

I also want to give biggest and greatest thanks to my family for their inexhaustible love and supporting me spiritually throughout this PhD study and my life in general: specifically, my parents Dirk-Jan and Elizabeth who provided me with the best academic education as possible; and my brother and sisters who have encouraged me and provided moral support every step of the way. With deepest gratitude and love, I wish to thank my boyfriend Rens for his infinite support, understanding, encouragement, love and care. Finally, I wish to thank my dearest friends Linda and Tamara, for their love and friendship over so many years and for sharing our stories with equal interest.

Ort, Datum: Alkmaar, 27 October 2017

Versicherung an Eides Statt

Ich, Francisca Maria Constance Wit, Kennemerstraatweg 37, 1814 GB Alkmaar, the Netherlands,

.

versichere an Eides Statt durch meine Unterschrift, dass ich die vorstehende Arbeit selbständig und ohne fremde Hilfe angefertigt und alle Stellen, die ich wörtlich dem Sinne nach aus Veröffentlichungen entnommen habe, als solche kenntlich gemacht habe, mich auch keiner anderen als der angegebenen Literatur oder sonstiger Hilfsmittel bedient habe.
Ich versichere an Eides Statt, dass ich die vorgenannten Angaben nach bestem Wissen und Gewissen gemacht habe und dass die Angaben der Wahrheit entsprechen und ich nichts verschwiegen habe.
Die Strafbarkeit einer falschen eidesstattlichen Versicherung ist mir bekannt, namentlich die Strafandrohung gemäß § 156 StGB bis zu drei Jahren Freiheitsstrafe oder Geldstrafe bei vorsätzlicher Begehung der Tat bzw. gemäß § 161 Abs. 1 StGB bis zu einem Jahr Freiheitsstrafe oder Geldstrafe bei fahrlässiger Begehung.

_____

Unterschrift